Modeling of Machining Characteristics and Tool Shape in Electrical Discharge Machining using Composite Tool Tip

A Thesis Submitted in Fulfillment of the Requirement for the Award of the Degree of

MASTER OF ENGINEERING

in

Production Engineering

Submitted By

MAYANK GARG

801685012

Under Supervision of

Dr. Vineet Srivastava

Assistant Professor, MED

MECHANICAL ENGINEERING DEPARTMENT

THAPAR INSTITUTE OF ENGINEERING & TECHNOLOGY

(A DEEMED TO BE UNIVERSITY), PATIALA, PUNJAB

JUNE, 2018

CERTIFICATE

I Mayank Garg hereby certify that the work presented in this thesis entitled **"Modeling of machining characteristics and tool shape in Electrical Discharge Machining using Composite tool tip"** in fulfilment of the requirement for the award of degree of **Master of Engineering (Production Engineering)** submitted at Thapar Institute of Engineering & Technology (Deemed to be University), Patiala is authentic record of work carried out under supervision of **Dr. Vineet Srivastava,** Assistant Professor, Mechanical Engineering Department, TIET, Patiala from July 2017 to June 2018. The matter presented in this has not been submitted either in part or full to any other university or institute for the award of any other degree.

Date: 27.07.2018

Mayank Garg

801685012

It is certified that the above statement made by the student is correct to the best of our knowledge and belief.

Dr. Vineet Srivastava

Assistant Professor

Mechanical Engineering Department

Thapar Institute of Engineering & Technology

(Deemed to be University), Patiala, Punjab

Date: 27/07/2018

ACKNOWLEDGEMENT

I would like to thank all the people who contributed in many ways to describe the work in thesis. First and foremost, I thank my thesis supervisor **Dr. Vineet Srivastava, Assistant Professor Mechanical Engineering Department, Thapar Institute of Engineering & Technology, Patiala** for his guidance, support, inspiring and the development of thesis at every step. He took keen interest in my report and helped me to access facilities of Mechanical Engineering Department Laboratories.

I would also like to thank **Dr. S.K. Mohapatra, Head & Senior Professor, Mechanical Engineering Department, Thapar Institute of Engineering & Technology, Patiala** for providing permission to avail all facilities for completion of the research work.

A special thank to my big brother Mr. Arminder Singh Walia, Research Scholar MED for his help and support during thesis work.

In the end, I wish to express my deep sense of gratitude to my family, for supporting and encouraging me at every step of my work. It is the power of their blessings, which has given me the courage, confidence and zeal for hard work.

ABSTRACT

Electrical Discharge Machining (EDM) is a non-conventional and non-contact type of machining process in which metal is eroded by thermo-electrical properties of tool and workpiece when sparks are applied in between tool and workpiece under the dielectric medium. Apart from all benefits, it can't be said that EDM process is free from limitations. Tool wear rate is the critical problem among all other problems which ultimately impacts the shape of tool. In the current research, the surface morphology and the machining characteristics such as tool wear rate, material removal rate, out of roundness and surface roughness have been studied by creating the semi-empirical model with help of dimensional analysis and process parameters i.e. discharge current, pulse-on time, pulse-off time. Here, there is use of ceramic tool tip of copper titanium carbide which is fabricated by following powder mixing, compacting and sintering, in comparison with simple copper tool for machining H13 tool steel workpiece. The experiments have been performed by both the tools i.e. copper and copper-titanium carbide. Then, the semi-empirical model for the Cu-TiC tool machining is evaluated which is compared with its statistical model. The surface morphology has been done for studying the surface integrity of workpiece material after machining by both the electrode tools. The deformities like cracks, debris, pores, white cast and recast layer are found to be less in workpiece surface machining by simple copper tool as compared to the machining by Cu-TiC ceramic tool. The less TWR and high MRR are found with use of Cu-TiC ceramic tool as compared to simple Cu tool.

Keywords: Electrical Discharge Machining, Tool Wear Rate, Material Removal Rate, Surface Roughness, Out of Roundness, Tool Shape.

Table of Contents

List of Figures

List of Tables

NOMENCLATURE AND ABBREVIATIONS

A	Ampere
ANOVA	Analysis of Variance
CCD	Central Composite Design
CCRD	Central Composite Rotatable Design
CNC	Computer Numerical Control
Cu-W	Copper-Tungsten
DF	Degree of Freedom
DOE	Design of Experiment
EDM	Electrical Discharge Machining
EDS	Energy Dispersive X-Ray Spectroscopy
EWR	Electrode Wear Rate (mm^3/min,g/min), Electrode Wear Ratio (%)
HV	Vickers Hardness
I_p	Discharge Current
K	Thermal Conductivity
LT	Layer Thickness
MRR	Material Removal Rate (mm^3/min, g/min)
MS	Mean Square
N	Total Number of Experiments
OA	Orthogonal Array
OOR	Out of Roundness
PVC	Polyvinyl Chloride
R	Electrical Resistivity
R^2	Multiple Correlation Coefficient
R_a	Actual Surface Roughness (µm)
ROC	Radial Overcut
RSM	Response Surface Methodology
SEM	Scanning Electron Microscopy
SS	Sum of Squares
SR	Surface Roughness
T	*t*-distribution
T_{on}	Pulse-on Time (µs)
T_{off}	Pulse-off Time (µs)

TiC	Titanium Carbide
Ti-B_4C	Titanium Boron Chloride
TWR	Tool Wear Rate
V	Voltage
WC	Tungsten Carbide
WEDM	Wire Electrical Discharge Machining
XRD	X-Ray Diffraction
Z	Machining Response
ZTA	Zirconia Toughened Alumina
A	Level of Confidence Interval
μm	Microns
μs	Micro Second
ρ	Density (Kg/m^3)

CHAPTER 1

INTRODUCTION

1.1 BACKGROUND OF EDM

The substantial rise in developments of the different innovative fields demands the utilization of new materials, which could survive in high temperatures with other constraints. The development in non-traditional techniques with the utilization of thermal and electrical energy has enormously helped in accomplishment of economical machining of materials with low machininability and complex shapes. Electrical Discharge Machining (EDM) is one of those processes in which machining is based upon these principles.

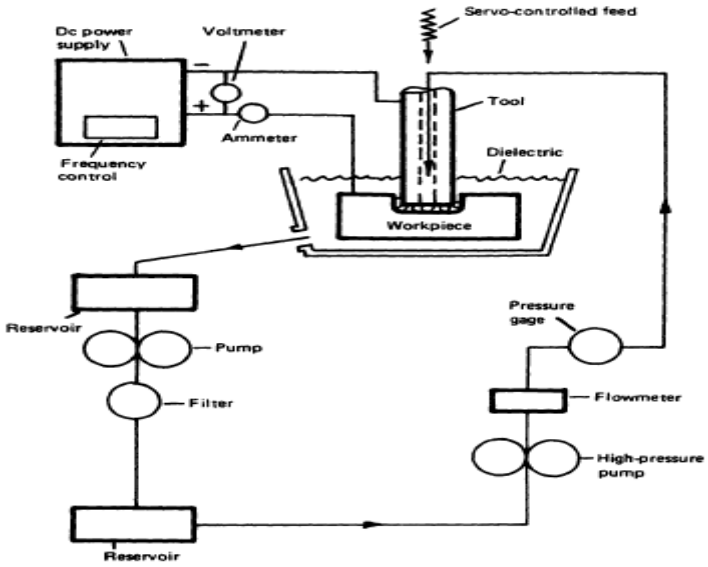

Figure 1.1 Electrical Discharge Machining [1]

The basic phenomenon behind the EDM process is the expulsion of the material from the surface of the metal workpiece which results due to immediate striking of beam of electrons on the surface of metal workpiece in the medium of dielectric fluid as shown in figure 1.1. The dielectric fluid is continuously supplied by the help of feed pump which collect the fluid from machining dielectric tub and feed the fluid from the reservoir after filtration. To maintain the ionization process, the gap between the electrode tool and workpiece material is kept within a limit of 10 - 100 μm by moving the cathode tool towards the workpiece by the help of servo controller [1]. Short duration of discharge is produced in a gap of fluid dielectric which leads to increase the temperature of medium in order of millions of degree per second. The material is eroded from electrode tool and workpiece by the shock wave impact produced due to the explosion of the plasma channel created by the electrical

discharge. The removed material is carried away by the flow of dielectric fluid to the reservoir.

1.1.1 Mechanism

When high pulsed voltage is applied to the electrodes, dielectric breakdown occurs. In the presence of electric field, there is liberation of electrons from the electrodes inside the medium where the ions of electrode and the dielectric fluid start to collide with each other, which grow up and multiplies leading to formation of an avalanche of electrons due to which the temperature of machining zone grows up too high. The thermal energy produces a plasma channel between the electrode tool and workpiece at a temperature within limits between 8000°C and 20000°C instating a considerable measure of heating and melting of material at the each electrode surface [2]. After shutdown of discharge current, a sudden decrease in the temperature and pressure enables the dielectric liquid to explode the plasma channel, which creates a shock wave impact and flushes the liquid material coming out from the electrode surfaces as tiny particles as shown in figure 1.2.

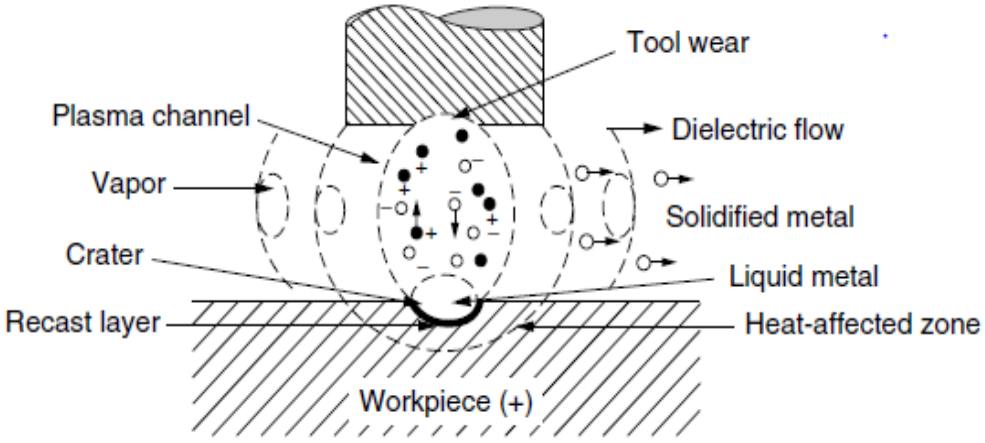

Figure 2.2 EDM Mechanisms [3]

In EDM, there is no physical contact between the cathode tool and the workpiece, hence the problems of mechanical stresses, vibration and chatter issues can be avoided which is generated during the conventional machining process. In spite of the fact that this does not imply that metallurgical consequences and induced stresses for the workpiece are fundamentally absent [4]. This process reduces machining time as compared to the other conventional machining process. The rapid heating and cooling during machining leads to case-hardening of workpiece surface which is good advantage of this process. EDM machining has huge application in many industries of metal cutting where high strength, heat treated alloys and carbides are used for machining process because it is capable of machining

ultra hard materials like various hard diamonds, cemented carbides and conducting ceramics. The advancement of various present day composite materials in the most recent decade has prompted an extension of EDM applications. This process has a unique ability to utilize the thermal energy for machining of electrically conductive materials regardless of their hard character which is advantageous in the manufacturing of automotive, mould, aerospace, die and surgical components. The two most broadly utilized sorts of EDM are die sinking EDM and wire EDM (WEDM). Die sinking EDM is broadly utilized as a part of the mould making ventures. The approach of computer numerical control (CNC) in EDM got colossal advances enhancing the productivity of the machining activity.

1.1.2 Theories of Metal Removal Mechanism

There are three types of material removal mechanism have been planned based on experimental outcomes: high pressure theory, static field theory (electromechanical component) and high temperature theory (thermal, electro-thermal system).

a) High Pressure Theory - The immediate impact of electrodynamics waves with high impulse pressure results in the erosion of metal from the electrode surface. Here the pressure is less than the value which was reported because the area of the discharge pressure acting is assumed to be wider than the crater area. The duration of pressure acting is found to be longer than the electric discharge periods. Discharge current is not alone sufficient, other factor like heat should be considered as well.

b) Static Field Theory – Electrostatic forces developed between electrode tool and workpiece due to which high stress is produced that may cross the value of ultimate stress limit which leads to tensile fracture. Erosion of metal is developed because of the forces in tensile fracture due to extremely high current density which creates a strong electric field gradient. When this force reaches the value of tensile strength, the tensile fracture occurs which results in the removal of particles.

c) High Temperature Theory – The electrons of high energy bombard on the electrode surface which create high temperature at the machining area leads to the material erosion after leaving crater on workpiece surface. The bombardment of electrons has the contribution of not only the development of high current but also the development of high current density. The wear of electrode decreases as the erosion rate increases.

Hence, the theory of high temperature is broadly adequate in clarifying the significant segment of the phenomenon of the metal removal. Alternate hypotheses can't be completely

ignored as they might be contributing towards the unaccountable material removal through thermal model. [5]

1.1.3 Benefits and Problem Areas of EDM

The characteristics of EDM have been studied in the course of the most recent five decades. By going through the literatures, it explored that EDM of steels has been taken maximum consideration. The producers of EDM machining tool have additionally been giving machining information of steels in accordance with their house of experimentation. Such collected information are based upon the qualitative and quantitative connection between the innovative parameters like surface integrity and erosion rate and input factors like machining parameters and materials properties of tool and workpiece, for example, pulse duration, discharge current, duty cycle, gap voltage and so on [6]. The following advantages of EDM as given below:-

1. Difficult and complicated geometries are possible.
2. EDM process is burr-free process.
3. Cavities with fine features with thin walls can be produced.
4. Hardness of material can't affect the EDM machining process.
5. There is no direct contact between tool and workpiece.

Despite all the advantages, the EDM process is not free from drawbacks. One of the major drawbacks is the high rate of electrode wear. Other drawbacks include difficulty in reproducing sharp corners on the workpiece due to electrode wear, surface and subsurface damage, creation of thin and brittle heat-affected zone and slow rate of material removal. Among from these problems, high electrode wear rate is the prominent issue because it raises the cost of input in the production process due to the increase in use of number of tools which leads to the decrement of productivity. So, for overcoming this problem, many researchers have tried to reduce the tool wear rate by applying various fabrication process of manufacturing. For complex three-dimensional shapes, machining, casting, electro-forming, sintering, spark plasma sintering or metal spraying may produce electrodes. Fabrication of electrodes using rapid prototyping technology can also reduce the cost of producing electrodes with complex geometry.

1.1.4 Electrode Material

In the EDM process, electrode tool is basically the mode of the generation of electrical energy for the metal removal of the workpiece material. It may have the surface profile which

can be the reverse of the profile of workpiece. The surface condition of the workpiece is mostly depends on the tool stability under the conditions of flushing and electrical stress. The heat energy received by the electrode tool from the plasma channel should be dissipated faster towards the workpiece so that the melting and evaporation of the tool material can be minimised. That is why the material used in the manufacturing of the electrode tool should be of highly thermal and electrically conductive. The selection of the electrode tool material should be decided on the following factors as given below:-

- The material removal should be as high as possible.
- Electrode wear ratio should be less.
- Easy to fabricate according to desired shape required.
- Cost should be as low as possible

The electrode tool material can be categories into the following groups given below:-

(i) Metallic electrode: Copper and copper alloys, Brass, Aluminium and its alloys, tungsten, steel, etc. Copper is the commonly used electrode tool for EDM process due to its excellent thermal and electrical properties. It is difficult to cast due to the easily reactive towards the oxygen from other oxides.

(ii) Non-metallic electrod**e:** Graphite is the most important electrode among this group. It is available in various types and grades. Graphite electrodes high value of electrical conductivity and can be capable of withstanding extremely high heat.

(iii) Combined metallic and non-metallic electrode**:** Copper-Graphite. These types of electrodes are the combination of the metal and non-metal material which is manufactured according to the desired properties. This combination is used for controlling the drawback of individual material.

(iv) Ceramics: Copper-Tungsten, copper silicon, etc. Ceramic materials are hard, brittle, and weak in shear and tension, strong in compression. They sustain very high temperature and chemical erosion which generally occurs in some materials subjected to the environment of acidic or caustic.

(v) Metallic coating as insulators: Copper on ceramic and copper on mould plastic. These types of electrodes are manufactured by firstly simple electrode is made followed by electroforming bath which gain again the electrical properties but it can't be called as electrolytic process. These mainly manufactured by aiming of making moulds and dies [5].

1.2 MOTIVATION

It has been found that huge amount of heat and thus electrode tool wear are the most imperative factors influencing execution and profitability of machining operations. In machining tasks, electrode tool wear is an unavoidable issue and in the end prompts failure of tool. Conventional cooling techniques are inadequate as well as pollute the workplace by delivering dangerous gasses and smokes. The rate of electrode tool wear is noteworthy on account of an electrode tool of small diameter and this problem generates difficulty in machining very hard materials like composites as ceramics. The lessening in electrode tool wear is compulsory for enhancing the efficiency of EDM.

The nature of the machined surface plays a significant factor in assessing the efficiency of the machining operation. Surface roughness is an important design factor which impacts properties like strength, fatigue, and wears resistance. It is a standout amongst the most vital measures in machining and in addition completing finishing operation. That is why; it is difficult to accomplish a decent surface finish [7] and exactness through better shape maintenance of the electrode tool. The quick electrode tool wear can be lessened by using composite like ceramics which has the high strength and hardness. In perspective of these factors, the present work explores the impact of EDM parameters on the machinability and surface integrity of H13 tool steel utilizing very hard ceramic material.

1.3 ORGANISATION OF THESIS

The work of research has been categorized as given below:-

Chapter 1 exhibits a prologue to Electrical Discharge Machining (EDM) process. It gives outline of various techniques of material erosion, coordination of different advances with EDM, advantages and drawbacks of EDM process. This part additionally gives a review of the research issue, procedure and proposition association.

Chapter 2 gives a basic review of past literature on different aspects of EDM with an accentuation on elective strategies to manufactured EDM electrode tool, surface topography of workpiece and creating a semi-empirical model on various response parameters. Research gaps have been recognized and the explanation for present research work into endeavour is featured. This part additionally gives a review of the research gap, objectives and methodology plan.

Chapter 3 is concentrated around the trial examination on EDM of H13 tool steel utilizing simple conventional electrode tool and other is ceramic composite electrode tool, utilizing statistically composed investigations. Impacts of process parameters on execution

measure are MRR, TWR, SR and OOR have been considered. The experimental models have been created to forecast reactions and significant parameters are set up. The subtle elements of optimization and reaction surfaces are given. A basic correlation of the EDM forms with conventional electrode tool and ceramic composite tool has been displayed.

Chapter 4 exhibits the impact of process parameters on surface morphology of H13 tool steel utilizing Conventional EDM process using Cu & Cu-TiC as tool electrode. An evaluation of the impact of process parameters at topography of surface and in addition subsurface microstructure has been exhibited. Trial comes out have been studied and included to comprehend mechanism of material expulsion amid EDM of H13 tool steel. Hence, the examination has been introduced in light of surface uprightness between Cu & Cu-TiC as tool for EDM process.

Chapter 5 concentrated over the evaluation of the semi-empirical model of various response parameters are MRR, TWR, SR and OOR has been developed by the help of dimensional analysis, the physical and thermal properties of machined materials are density, thermal conductivity, linear coefficient of expansion, electrical resistivity and hardness were considered. The process parameter of machining are discharge current, pulse-on time and pulse-off time were also taken to be in consideration with material properties. The comparison has also been shown between statistical and theoretical values of models.

Chapter 6 outlines the significant discoveries of the exploration work did and the headings without bounds inquire about have been featured.

CHAPTER 2

LITERATURE REVIEW

2.1 INTRODUCTION

As per discussion in the previous chapter, the main concerns are low material removal rate, high tool wear rate, less surface finish and distortion of the tool shape have come out from among various researches in EDM. So, for improving the efficiency or performance of EDM machine, various alternatives were suggested and analyzed. Some researchers used the various combinations of the compositions of tool material for machining hard materials in order to get low tool wear rate with maximum material removal rate. Here also some efforts have been made to get good performance in EDM machining process with particular ceramic composite tool over a hard workpiece and further, semi-empirical analysis has been done along with the study of surface morphology. So, various past studies which were done by researchers in the particular field are discussed in this chapter.

As it is a thermal machining process, the main unavoidable factor of high electrode wear which leads to the manufacturing of more number of electrodes for machining various job. In EDM, the cost of machining increases as the number of tool are manufactured which are very costly and contribute upto 70% of the total processing cost [8]. EDM is widely used in the manufacturing of various types of dies and machining of various hardened materials. The cost and time are the main factors for the manufacturing of electrodes and these factors are generally determined by what type of accuracy and complexity of geometry is demanded. And these electrodes are generally manufactured by unconventional machining methods. This chapter has been introduced to discuss the past researches which were in the direction of complex electrode fabrication using various methods in order to get better performance of EDM machining process.

2.1.1 Types of Electrodes & Workpieces

Li et al. [8] studied over the effect of mixing Titanium Carbide (TiC) varying from 5% to 45% with Copper-Tungsten (Cu-W) and with simply Copper (Cu) in order to the fabrication of electrode tool for using Electrical Discharge Machining (EDM) process. In order to densification of tool system, 3.5% of nickel had been added to the total composition of tool which shows the good solubility. Particle size distribution was shown less spread due to the increment of TiC, which leaded to the better performance of surface finish. 15% of TiC

has shown much better performance highest MRR, lowest TWR and best surface finishing but in TiC/Cu, 25% of TiC has shown satisfactory results.

Kumar et al. [9] assessed the Electrical Discharge Machining performance of TiCN–20wt. % Ni cermets containing 10wt. % of various additional carbides: WC, NbC and TaC. The results for highest MRR came out without any addition of carbide to TiCN-20wt% Ni cermet. When it came to the addition of carbides, lowest TWR and moderate MRR along with good surface finish came with TiCN-20wt% Ni-10wt.% TaC. Melting and evaporation occurs during EDM was revealed by SEM which show the transferring of workpiece material to cermet and the formation of recast layer retards the material removal.

Monzon et al. [10] experimented for the validation of EDM electrodes which were manufactured by rapid tooling technologies followed by electroforming technologies. By this tool manufacturing method, tool was made with high dimensional precision. In this paper, electrodes manufactured by different methods had been tested in EDM machine and its performance was compared with conventionally manufactured electrolytic copper electrodes. By this research, three problems have been resolved i.e., conventional electrode with excessive weight, copper geometries which are difficult to machine and graphite milling tool which are dust generated. Hence these electroformed electrodes have shown good result in comparison to conventional copper electrode.

Harpuneet Singh [11] studied over the effect of using Brass and Copper Chromium electrode while Electric Discharge machining of EN-31 Die Steel with using Positive polarity. Investigation had been done over machining parameters like material removal rate, tool wear, depth of cut and hardness while varying pulsed current. He had taken the range of current from 6A-12A. Depth of cut, over cut, Hardness and Material removal rate were found better for copper chromium as compared to brass electrode. Electrode wear rate was less for copper chromium electrode in comparison to brass electrode.

Satyarthi and Pandey [12] investigated over the surface characteristics while machining the conductive ceramic of alumina (Al_2O_3-SiC_w-TiC) in a processing set up containing Electric Discharge machining (EDM) and electric discharge grinding (EDG). The input parameters were taken into considers are wheel speed, discharge current, table speed, duty cycle and pulse on time. After, it was found that surface produced by processing with EDG is better as compared to EDM which was investigated by scanning electron microscope (SEM) at 1000X and 500 X resolutions for EDG and EDM respectively in where alteration of material composition, pits formation, cracks were seen over the workpiece.

Islak et al. [13] studied the effect of varying the sintering temperature on microstructure and electrical properties of Hot Pressed CU-TiC composites for 4 min under a pressure of 50MPa. In Cu matrix, it had been seen that TiC particles were uniformly distributed. No formation of copper oxide which was shown by XRD. Relative density was decreased while increasing the hardness of the composites. But both were increased when the sintering temperature was increased. It also had been seen that inclusion of TiC in composites decreased the electrical conductivity but highest was shown while sintering at 800 ^{o}C.

Afzaal Ahmed [14] investigated over Ti-B_4C powder metallurgy tool with the deposition of aluminum coating in EDM process. This EDM process was carried out with some different tool parameters like composition and compaction pressure of electrode tool material and process variables like pulse duration and peak current for observing some response parameters like tool wear rate, material deposition rate and average layer thickness The outcomes of this experiment comes out is that the higher values taken of compaction pressure, peak current and pulse duration leads to non-uniform deposition on workpiece surface. Average hardness recorded was 640 HV at cross-section. The most impacting parameter for reactions MDR, TWR and LT was found to be crest current (Ip) with a rate commitment of 60.72%, 59.52% and 42.09%, respectively.

Younis et al. [15] conducted an analysis over the effect of electrode material during electrical discharge machining (EDM) for avoiding results of cracks generating, residual stress and surface roughness in which two types of electrodes were used i.e., Dura graphite 11 and Poco graphite EDMC-3 for machining the two types of tool steel materials I.e., DIN 1.2080 and DIN 1.2379. Dura graphite 11 has shown more cracks on the surface of DIN 1.2379 as compared to DIN 1.2080 while this has shown the higher surface roughness. It was later studied that the higher residual stresses were resulted by POCO Graphite EDMC-3 electrode as compared to Dura graphite 11 electrode.

Gadow et al. [16] studied the electrical and mechanical properties along with the machining processes characteristics which had an influence over the workpiece. In experiment, the alumina based ceramics was used which was of high hardness and reasonable cost and its fracture resistance was improved by addition of ZTA materials (Zirconia toughened alumina). Further titanium carbide (TiC) was added to increase its hardness and good machinability. Machining experiment was performed with two different machines followed by wear test. From the ceramic manufacturing point of view, for the production of higher item numbers, various forming process are only the economical processes.

Liu et al. [17] investigated the densification and mechanical properties of Boron carbide-Titanium dibromide (B_4C-TiB_2) composites which is fabricated by the help of pulsed electric current sintering with the powder mixture of TiC and amorphous B powder which use for the removal of carbon comes generated due to chemical reaction. After all, Boron carbide-Titanium dibromide (B_4C-TiB_2) composites were densified and synthesized under pressure of 50 MPa at 1900^oC and the effects generated were investigated. The high strength was associated to fine microstructure and distribution was homogenous which is generated by spinning effect.

Table 2.1 Major research efforts in the use of different type of tool electrode & workpiece

Investigators	Material of tool electrode	Material of work electrode	Responses
Li et al.[2001]	Titanium Carbide (TiC)(5% to 45%) with Copper Tungsten (Cu-W) and Copper (Cu)	Tool Steel (P434,P412 & P182)	15% of TiC has shown higher MRR with lowest TWR and best surface finish.
Kumar et al. [2007]	TiCN-20 wt% Ni cermets with 10 wt% of WC, NbC and TaC	High speed tool steel (HSS)	Higher MRR came out without addition to TiCN -20 wt% Ni cermets. Lowest TWR was with addition of TaC.
Monzon et al. [2008]	Copper and Copper electroformed	ABS, vacuum casting rubber silicone and PVC made by RP	Electroformed copper electrode has shown good results
Harpuneet Singh [2012]	Brass and Copper Chromium	EN-31 Die steel	Electrode wear rate was less for Copper Chromium as compared to Brass electrode
Satyarthi and Pandey [2013]	Copper	Alumina (Al_2O_3-SiC_w-TiC)	SEM represents the alteration of material, formation of pits, crack over the machined workpiece
Islak et al. [2014]	Hot pressed Cu-TiC composites	Sintering only	Highest conductivity was shown by Cu-TiC at 800^oC
Afzaal Ahmed [2015]	Ti-B_4C powder metallurgy tool with Al coating	Die-Steel	MDR, TWR, and LT were found to be crest at (I_p) at 60.72%, 59.52% and 42.09% respectively.
Younis et al. [2015]	Dura graphite 11 and Poco graphite EDMC-3	Tool steels i.e. DIN 1.2080 & DIN 1.2379	Higher residual stress were resulted by POCO Graphite EDMC-3
Gadow et al. [2016]	Alumina based with added TiC	Tool steel	Due to absence of cracks, the machined parts retain their strength.
Liu et al. [2017]	Boron carbide-Titanium dibromide (B_4C-TiB_2) composite	Sintering only	Good effects were investigated under pressure 50 MPa at 1900^OC

2.1.2 Surface Integrity

Ozgedik and Cogun [18] studied the variation occur in the tool wear characteristics, material removal rate, and surface roughness through the various setting like dielectric

flushing, pulse duration and discharge current. Experimentally, it was found that tool wear rate, material removal rate and surface roughness increased while increasing the discharge current which ultimately affects the inner and outer radii of tool. As the pulse duration increases, the material removal rate increases with tool wear rate and surface roughness but tool wear rate start to decrease with further increase in pulse duration. Increase in pulse duration also leads to decrease in inner and outer radii.

Jaharah et al. [19] studied the performance of copper electrode in Electrical Discharge machining on the workpiece of AISI Harden Steel. They considered the following parameters like pulse ON-time, pulse OFF-time and peak current for investigating the machining performance of material removal rate (MRR), electrode wear rate (EWR) and surface roughness (Ra). Time for EDM machining was kept constant for 30 minutes for seeing the better result while using the certain range of parameter values. High peak current, high pulse ON-time and low pulse OFF-time showed the high surface roughness.

Pellicer and Ciurana [20] studied over the different geometrical features of tool geometry are triangle, square, rectangle and circle and surface quality while doing electrical discharge machining of workpiece i.e., AISI H13 steel using statistical tools. A groove of 1 mm depth and 3 mm width was used as a target feature of experiment. This experiment results increment of MRR and surface roughness with discharge current. Tool geometry also showed the different machining effects are radial and axial wear ratios are presented better by rectangle and square electrodes. That means this results which is obtained presents how to select suitable process parameters values for predicting geometrical features and patterns of surface roughness and this will help in further process planning in micro machining.

Rajesha and Pradeep [21] showed the effect of using hollow tool electrode while doing electro discharge machining of Inconel 718. Response surface methodology (RSM) is used for planning the experiments. Regression analysis was done to developed mathematical models. The process parameter were used as like duty factor, flushing pressure, gap control, pulse current and sensitivity control among which high value of duty factor and pulse current shown the high MRR ranging from 14.4 to 22.6 mm^3/min. Proper flushing pressure is required while machining because very high or low settings can lead to decrement in MRR along with surface finish. Influence of the interaction among pulse current and gap control leads to decrement of surface quality. Higher value of current highly influenced the thickness of sputtered layer, tool wear and crack propagation.

Balbir and Jatinder [22] explained the effect of process parameters on MRR improvement during electrical discharge machining of AA6061/10%SiC Composites. Here,

electrolytic copper electrode of 120 mm length and 12 mm diameter for machining. Response Surface Methodology technique is used to relate the relationship between responses and input parameters. Higher MRR can be carrying out at favorable values of gap voltage and pulse OFF-time and at higher values of current and pulse ON-time. Particles of tungsten powder in dielectric had shown the intensification of MRR by 48.43% and 42.85% reduction in formation of recast layer with better surface finish.

Prakash and Rajneesh [23] studied the various effects of EDM process parameters on Material removal rate in which they used cubical form of mild steel as a workpiece and rectangular cross-section of copper piece as a tool. They used some process parameters are discharge current, pulse-on time, voltage along with straight polarity foe checking their effects on MRR. Machining time was taken 10 minutes. This experiment results that MRR increases upto certain limit with discharge current then decreases. MRR also increases along with the increasing of voltage and it is found to be affected by spark energy.

Balasubramanian and Senthilvelan [24] experimented for the optimization of machining parameters which are used in EDM machining process by the copper tool which are casted and sintered. The machining process was done over the two workpiece are EN8 & D3 steel materials in EDM machine. The important parameter were used are pulse on time, tool diameter, peak current and dielectric pressure for optimizing output responses are surface roughness (SR), tool wear rate (TWR) and Material removal rate (MRR). Response surface methodology (RSM) and Analysis of Variance (ANOVA) method were applied to do detailed analysis of process parameters. The higher MRR and low TWR for cast electrode as compared to sintered electrode. But SR was lower for Sintered electrode as compared to cast electrode.

Mandaloi et al. [25] studied the effect of using Tungsten-Thorium electrode tool on the crystalline structure of AISI M2 steel with the output responses of Surface finish, EWR and TWR with help of three process parameters and the surface topography of material were examined through some techniques like Atomic force microscopy, Optical surface profiler and Scanning electron microscopy. Tungsten based alloy tool was used to machine workpiece which is of dimension 50 x 50 x 6 mm^3. In XRD technique ,peak has been shown with the increase of current which results better properties because of homogenous dispersion of material particles in a matrix.

Niamat et al. [26] studied over the effect of using different dielectrics for evaluating effect of current and pulse on time in comparing between water and kerosene as a dielectric fluid. These dielectric performances were observed in the form of microstructure, electrode

wear rate and material removal rate. Aluminum 6061 T6 alloy was used as a workpiece for this research. Taguchi L9 Orthogonal array was used to design of experiment. Microstructures were taken by Scanning Electron Microscope (SEM) for analyzing micro-holes, globules and cracks. At last, the result was better with kerosene dielectric in the form of lower electrode wear rate and higher material removal rate. The surface was rougher in case of distilled water as compared to kerosene.

Table 2.2 Major research efforts in studying surface integrity after machined workpiece

Investigators	Materials used	Investigated factors	Response
Ozgedik and Cogun [2006]	Various tool steel workpieces	Dielectric flushing, pulse duration, discharge current	TWR, MRR, and SR were increased while increased in discharge current and pulse duration.
Jaharah et al. [2008]	AISI hardened H13 tool steel	Pulse duration and peak current	High peak current, high pulse-on time and low pulse –off time showed high SR.
Pellicer and Ciurana [2011]	H13 tool steel	Pulse current, pulse duration and open voltage.	Rectangular and square electrode have shown better wear ratio.
Rajesha and Pradeep [2012]	Inconel 718	Duty factor, flushing pressure, gap control, pulse current and sensitivity control	Higher value of current highly influenced the thickness of sputtered layer, tool wear and crack propagation.
Prakash and Rajnesh [2014]	Mild steel	Discharge current, pulse-on time and voltage	MRR increases upto certain limit with discharge current with voltage then decreases further with current only.
Balbir and Jatinder [2015]	AA6061/10%SiC Composites	Gap voltage, pulse duration and discharge current	Intensification of MRR by 48.43% & 42.85% reduction recast layer buildup was shown with better surface finish.
Balasubramanian and Senthilvelan [2014]	EN8 & D3 steel	Pulse-on time peak current, tool diameter and dielectric pressure	High MRR and low TWR was found for casted electrode as compared to sintered electrode but SR was higher.
Mondaloi et al. [2016]	AISI M2 steel	Pulse current and pulse duration	XRD results has shown the better properties with increase in current due to homogenous material dispersion.
Niamat et al. [2017]	Aluminium 6061 T6 alloy	Pulse-on time and discharge current	The result was better with kerosene dielectric in the form of lower EWR and high MRR.

2.1.3 Modeling of EDM Process

Wang and Tsai [27] developed the semi-empirical model the material removal rate and tool wear rate for various material workpieces are AISI EK2, AISI D2 and AISI H13 with tool are Cu, Gr and Ag-W by the help of Dimensional Analysis method which is based upon process parameters used in Electrical Discharge machining process. The parameters

were selected systematically are electric polarity, peak current, pulse duration and properties of materials and verified by Taguchi Method. The results show the dependency of model on the material. That is why; there can't be utilization of constant parameters. Here, non-linear methods were used for the experimental verification. The prediction of error was noticed within a range of 20% due to cathode as work and MRR is large. The equation generated for Material removal rate (MRR) or Tool wear rate (TWR) is given by:-

$$V = A_1 \left[\frac{\alpha^2}{H_v^{\frac{1}{2}}}\right] \left(\frac{I_p}{\sigma^{\frac{1}{2}}\rho^{\frac{1}{2}}\alpha^{\frac{3}{2}}}\right)^{a_1} \left(\frac{\tau_{ON}H_v}{\alpha}\right)^{b_1} \left(\frac{E}{\rho\alpha^2 H_v^{\frac{1}{2}}}\right)^{c_1} (J_a)^{d_1}$$

Tsai and Wang [28] generated the semi-empirical model the surface roughness for various material workpieces are AISI EK2, AISI D2 and AISI H13 with tool are Cu, Gr and Ag-W by the help of Dimensional Analysis method which is based upon process parameters used in Electrical Discharge machining process. The parameters were selected systematically are electric polarity, peak current, pulse duration and properties of materials and verified by Taguchi Method. The outcomes demonstrated the dependence of model on electrode and workpiece and presumed that steady measures can't be applied for diverse materials. Here, non-linear methods were used for the experimental verification. The prediction of error was noticed within a range of 12%. The equation generated for Surface finish of work is given by:-

$$R_a = A_1 \left[\frac{\alpha}{H_v^{\frac{1}{2}}}\right] \left(\frac{I_p}{\sigma^{\frac{1}{2}}\rho^{\frac{1}{2}}\alpha^{\frac{3}{2}}}\right)^{a_1} \left(\frac{\tau_{ON}H_v}{\alpha}\right)^{b_1} \left(\frac{E}{\rho\alpha^2 H_v^{\frac{1}{2}}}\right)^{c_1} (J_a)^{d_1}$$

Yahya and Manning [29] evaluated the model by the use of dimensional analysis for the investigation of effects of physical and electrical parameters for the MRR of die-sinking EDM machine. Here, the MRR is observed to be directly proportional to the properties of material and process parameters are are sparking frequency(F_s), pulse on time(t_{on}), material properties factor(α), gap voltage(U_{arc}) and gap current(I_g). The equation generated for the material removal rate (MRR) is given by:-

$$V = C\alpha U_{arc} I_g t_{on} F_s$$

where C is the dimensionless constant which was calculated by regression analysis for the prediction of erosion rate at gap current. The effect of resolidification and flushing efficiency of plasma has been taken into consideration.

Ekmekci et al. [30] explained the phenomenon of generation of high residual stresses on the machined surface of workpiece. So, for measuring its profile as depth function below

the surface, the layer removal method was used. A semi-empirical model was developed for showing the residual stress which is generated over the machined surface of workpiece at some operating conditions. DIN 1.2738 steel was used as workpiece and copper or graphite was used as tool. Machining parameters were considered are Dielectric, polarity, current and Pulse time. Measurement on machining samples of plastic mold steel had shown the dependency on pulse duration time for each electrode and dielectric. The result showed the generation of high tensile residual stress by EDM. From the surface, they start to increase and reach to the value near about the ultimate tensile strength. Then, residual stress dropped down to the low value of stress.

Poros and Zaborski [31] generated the semi-empirical model for volumetric efficiency of wire EDM for machining hard material during investigation. In this research, wires of uncoated brass, brass coated brass and zinc oxide coated brass were used as an electrode. Titanium and titanium alloys and cemented carbide were used as workpiece to be machined. The process parameters were average working voltage (U) and Pulse on time (t_{on}) for generating model for efficiency. The variation of efficiency of the WEDM for different materials and different wire electrode along with different process parameters were utilized for establishing the semi-empirical model by the help of dimensional analysis. The semi-empirical model is expressed by this given equation:-

$$Q_v = AP\sqrt{\frac{\alpha^4 k}{c_p}}\left(\frac{C_p t_{on}}{k\alpha}\right)^b \left(\sqrt{\frac{U^2\sigma k}{K}}\right)^c (T_t k)^d$$

The highest volumetric efficiency of titanium alloy Ti6AL4V material. It is found to be lower for the material having high melting point. As the discharge time increases, the volumetric efficiency increases.

Patil and Brahmankar [32] studied to determine the semi-empirical model of MRR in WEDM of a metal matrix composite by the help of dimensional analysis. This model for WED is based upon machining parameters and thermo-physical properties. The non-linear estimation technique is also used to generate the model like simplex and quasi-Newton. Prediction for the model was proposed to be more than 99%. Silicon carbide particulate which is reinforced in aluminium matrix composite is used as workpiece. RSM approach is used for the determination of relationship between process parameters. The final expression for the model is given by:-

$$V = A\sqrt{\frac{\alpha^4 \varepsilon}{C_p}}\left(\frac{C_p T_{on}}{\alpha\varepsilon}\right)^a \left(\frac{U^2\sigma\varepsilon}{K}\right)^b (T_m\varepsilon)^c \left(\frac{L_f\varepsilon}{C_p}\right)^d$$

It was found that as the ceramic reinforcement increases by 10%, MRR decreases by 12%.

Kumar et al. [33] studied over the model of tool wear rate (TWR) of powder mixed electrode which is cryogenically treated in the EDM machining with the help of Dimensional analysis. The workpiece were the three grades of titanium alloys of TITAN 31, TITAN 15 and TITAN 21 were used as workpiece to be machined. This model had been generated by the thermo-physical properties and the outcome of Taguchi model of tool material. The results showed the material transfer from the workpiece to the tool surface which was observed by SEM, XRD and EDX spectrometer. The effect of Mn powder was shown higher than W powder. It is observed by SEM that as the discharge current increases, the deformities increases. The micro-mathematical model was developed for MRR shown below:-

$$V = C\left\{\frac{I_p T_{on} V_b L_f}{k T_m}\right\}$$

Bhaumik et al. [34] studied for the generation of the semi-empirical model for Material removal rate (MRR) and radial overcut (ROC) in EDM machining by the help of Dimensional analysis. The model has been developed with the consideration of thermo-physical properties are density, coefficient of thermal expansion and thermal conductivity and machining parameters are gap voltage, peak current, duty cycle and pulse on time. AISI 304 stainless steel is used for machining in EDM machine with the help of Tungsten carbide as tool. The expression for the model of MRR is given by:-

$$MRR = A\frac{I_p^{\frac{5}{3}}\alpha^{\frac{4}{3}}V_g^{\frac{5}{3}}}{\rho^{\frac{1}{3}}k^{\frac{4}{3}}}\left(\frac{k^{\frac{5}{3}}T_{on}}{I_p^{\frac{4}{3}}\alpha^{\frac{5}{3}}V_g^{\frac{4}{3}}\rho^{\frac{1}{3}}}\right)^a(\tau)^b$$

All machining parameters and thermo-physical properties are found to be significant. The experimental results have shown good agreement with the developed model.

Table 2.3 Major research efforts in understanding modelling of responses in EDM

Investigator	Type of modeling	Responses
Wang and Tsai [2001]	Dimensional Analysis	The prediction of error was noticed within a range of 20% due to cathode as work and MRR is large.
Wang and Tsai [2001]	Dimensional Analysis	The prediction of error was noticed within a range of 12% for SR.
Yahya and Manning [2004]	Dimensional Analysis	The effect of resolidification and flushing efficiency of plasma has been taken into consideration.
Ekmekci et al. [2006]	Dimensional Analysis	Residual stress starts to increase and reach to the ultimate tensile strength and dropped down to the low value of stress.
Poros and Zaborski [2009]	Dimensional Analysis	Highest volumetric efficiency is found to be lower for the material having high melting point. As the discharge time increases, the volumetric efficiency increases.

Patil and Brahmankar [2010]	Dimensional Analysis	It was found that as the ceramic reinforcement increases by 10%, MRR decreases by 12%.
Bhaumik et al. [2016]	Dimensional Analysis	All machining parameters and thermo-physical properties are found to be significant. The experimental results have shown good agreement with the developed model.
Kumar et al. [2017]	Dimensional Analysis	It is observed by SEM that as the discharge current increases, the deformities increases.

2.2 RESEARCH GAP

From the review of the literature, it can be concluded that EDM process is convenient for machining hard material with very accurate dimensions which is not possible for conventional machining processes. Copper is the most widely used tool electrode material due to its good electrical and thermal properties. The tool wear rate is very important because when tool wears out, it directly impacts on the machining surface. Hence, reducing the tool wear rate can improve the efficiency of EDM process.

From the study of literature, it was also found that the performance of the component machined by EDM process is highly dependent on the surface integrity which consists of surface roughness and surface damage. Some important process parameters are pulse current, gap voltage, pulse duration and duty cycle have been investigated in earlier researches to understand the surface outcomes during EDM. It is apparent from the literature review that along with surface integrity, the study of material removal rate has been done which have been quite complex and depends upon process parameters and material properties.

It was also found that the shape of the tool tip gets deformed while increasing in number of pieces machined in EDM process. The application of hard electrically conductive material like composite can be used to contour this problem. An electrode tool in which various combination of materials have been used to make ceramic tool tip for increasing the hardness of the electrode can counter the problem of tool wear rate. It has been further observed from the literature that in EDM, wear of the electrode is higher and the surface finish of the part tends to be lower. The above mentioned problems can be avoided if the electrode end is replaced with hard conducting materials like cermets. Theses cermet tooltips can have the desirable properties of different combined materials. In the current work, an effort will be made to compare the performance of fabricated composite tool tip electrode with the conventional copper tool tip electrode. It was also observed that some researchers had created the semi-empirical model of machining characteristics over some tool and workpiece material.

The proposal of this dissertation is to do comprehensive study among parameters are MRR, TWR, Tool shape and Surface roughness through the variable parameters are discharge current, pulse on time and pulse off time and create a semi-empirical model of machining characteristics by considering Cu-TiC tool. Here, hard metal ceramics electrode will be used for machining.

2.3 OBJECTIVES OF THE PRESENT WORK

The major objectives of this research work for studying the EDM process are given as follows:-

- Fabrication of ceramic composite tool tip by powder metallurgy.
- Study the effect of various processes parameters on material removal rate, tool wear rate, surface roughness and out of roundness during EDM process.
- Evaluation of effect of process parameters are pulse-on time, pulse-off time and discharge current on topography and surface integrity of the machined workpiece using Cu & Cu-TiC tool.
- Determination of semi-empirical model of machining characteristics and tool shape are Tool wear rate (TWR), material removal rate (MRR), surface roughness (SR) and out of roundness (OOR) with help of dimensional analysis for copper titanium carbide (Cu-TiC) tool machining.

2.4 PLANNED METHODOLOGY

To achieve the objectives as mentioned in section 2.3 following steps were followed as given below:-

1. Selection of tool and workpiece material as per past literature survey.
2. Selection of process and machining parameters as per machine specification.
3. Fabrication of ceramic composite tool tip followed by mixing, compacting, and sintering process as per design experiment.
4. Use Minitab for generating the design of experiment according to decided level of experiment.
5. Performing machining according to the design of experiments.
6. Measure the machining characteristics are tool wear rate, material removal rate, surface roughness and out of roundness of every machined specimen after collecting the data

7. Use Analysis of Variance (ANOVA) to analyse the data for checking parameters which are significant.
8. Development of statistical and theoretical model of all the machining characteristics which are selected.
9. Comparison of statistical models between Cu & Cu-TiC tool in EDM process.
10. Comparison of statistical model and theoretical model of Cu-TiC tool in EDM process.
11. Estimation of error in the developed models.
12. Optimise the process parameters for every decided machining parameter.
13. Develop the semi-empirical model of all machining parameters.
14. Comparison of surface morphology of the workpiece machined by Cu & Cu-TiC tools.

2.5 CHAPTER SUMMARY

For overcoming the problems of higher tool wear rate, higher surface roughness and lower material removal rate, various types of techniques have been used as per seen in past literature survey. These techniques were the use of different types of electrodes, different workpieces, various modeling method for accessing the prediction of response parameters along with various setups indulged with EDM machine. Here, in current research, semi-empirical model has been tried to generate for accessing the machining characteristics and the surface integrity of H13 tool steel workpiece by ceramic tooltip.

CHAPTER 3

STATISTICAL MODELING OF EDM PROCESSES WITH COPPER AND COPPER-TITANIUM CARBIDE ELECTRODES

3.1 INRODUCTION

In Electrical Discharge Machining, the problem of tool wear is a major problem which ultimately impact upon the shape of tool and dies. When the tool wear takes place, the prescribed dimension and shape of tool gets disturbed and it directly affects the dimension of machined profile on the workpiece. As we know, the cost of machining any part is directly proportional to the cost of the tool, which includes the raw material, production cost and number of tool required. As per literature review, in EDM operations, the cost of tool has great contribution towards the overall total cost of machining operation. That is why the tool wear has major significance in EDM process. The surface quality has another major role in this process because it is directly affected by the tool wear problem, which leads to the decrement in productivity. Surface roughness is a significant factor which readily affects the properties are wear resistance, strength and fatigue that is why it is important for finishing operation. As per literature review, researchers have tried to reduce tool wear rate and obtain better surface finish of the workpiece.

Therefore, in this research work, the impact of process parameters like pulse on time, pulse off time and discharge current has been considered for studying on response parameters that is tool wear rate, material removal rate, out of roundness and surface roughness during EDM machining process. These response parameters had been used for comparing different tool variants on a single workpiece in this work.

3.2 DETAILED OF TOOL AND WORKPIECE MATERIALS

3.2.1 Tool Preparation

In this work, we have used two variants of electrode tool i.e. one is pure copper (Cu) tool and another one is Copper-Titanium Carbide (Cu-TiC) ceramic tool for EDM machining process. The tool diameter of 8 mm has been decided for the purpose of machining. First of all, pure copper rod has been cut in many pieces as per required length to be used as a tool as shown in figure 3.1.

Figure 3.1 Copper tools

Figure 3.2 Cu-TiC powder mixtures

The second tool is a ceramic of Copper-Titanium Carbide. The material composition for this ceramic tool has been decided based on the literature survey i.e. 75% is of Copper powder & 25% is of Titanium Carbide powder. A little amount of nickel powder is also added in order to prevent oxidation. Copper powder and Titanium Carbide powder had been mixed with help of ball mill machine at 25rpm for 40 minutes in order to get homogeneous mixture [13] and the mixture is shown in figure 3.2. Now after getting this homogenous mixture, it was required to make small pallets of this mixture. So, the tungsten carbide (WC) dies has been taken which is shown in figure 3.3 with its complete set.

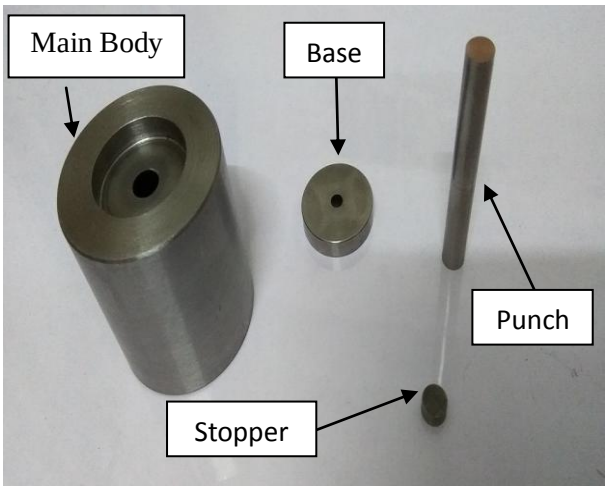

Figure 3.3 Tungsten carbide dies set.

Figure 3.4 Hydraulic press machine

The base has been put inside the big hole area of main body along with stopper in small hole. The powder mixture has been filled inside hole and closed the hole by put the punch inside. The complete set has been put inside the hydraulic press machine as shown in figure 3.4 and compacting has been done at the pressure of around 10 kg/mm^2 for 15 minutes holding time for each samples. The resulting samples are shown in figure 3.5.

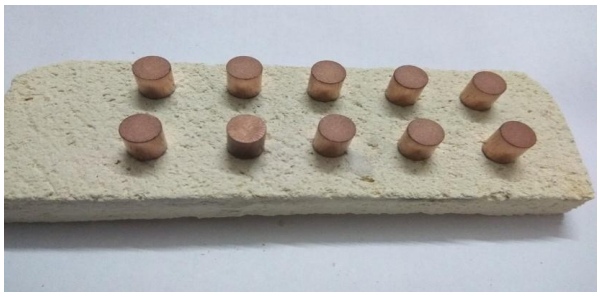

Figure 3.5 Cu-TiC samples after compacting

Further these samples were sintered to obtain better strength of the Cu-TiC pallets so that bonding of the ceramics become strong. The sintering process has been conducted in three stages i.e. 450 ^{o}C, 700 ^{o}C and 900 ^{o}C with 45 minutes holding time at rate of 3^{o}C/min in hot tabular furnace as shown in figure 3.6.

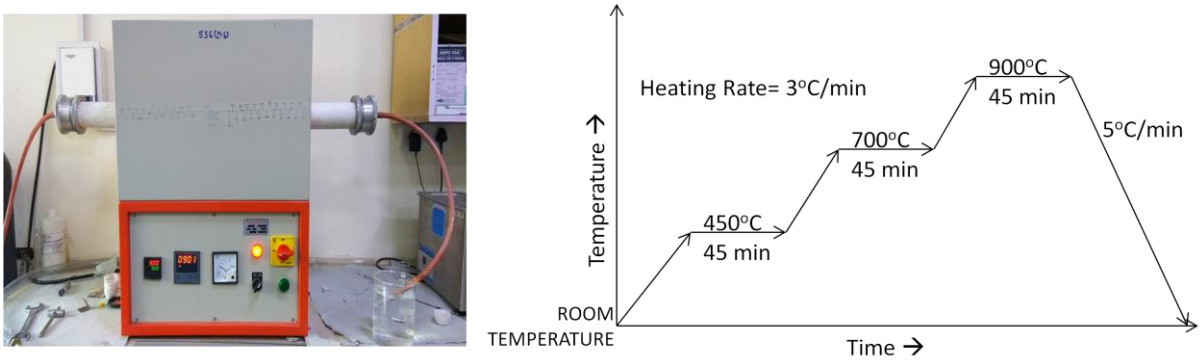

Figure 3.6 (a) Hot tabular furnace (b) Sintering cycle used in this study

Figure 3.7 (a) Sintered Cu-TiC pallets (b) Final Cu-TiC tools

The sintered pallets are shown in figure 3.7 (a). Then pallets are brazed to copper rod to make it convenient for tool holding in EDM machine. Finally Cu-TiC ceramic tool to be used for machining process is shown in figure 3.7 (b).

3.2.2 Workpiece Preparation

In this work, H13 tool steel has been taken as the workpiece. 12 mm diameter of the rod has been cut into the required number of pieces of desired length. The surface of the

workpiece was finished manually to obtain a uniform machining surface as shown in figure 3.8.

Figure 3.8 H13 Workpiece Samples

The figure 3.9 represents Energy Dispersive X-Ray Spectroscopy (EDS) performed on non-machined workpiece for the determination of its composition. The percentage of composition has been shown in table 3.1. The material properties of both the electrodes have been shown in the table 3.2.

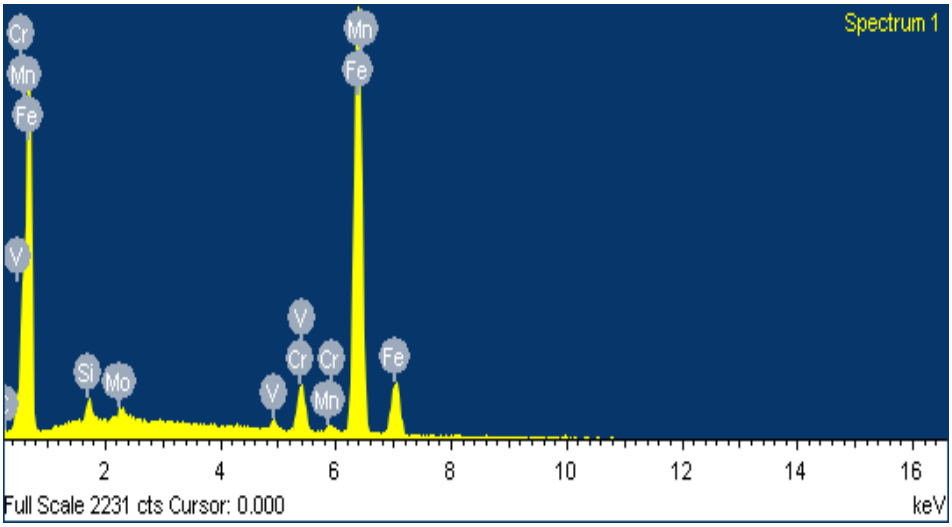

Figure 3.9 Relative intensity representing the material composition by EDS

Table 3.1 Workpiece Chemical composition (%)

C	Si	V	Cr	Mn	Mo	Fe
1.47	0.83	0.85	4.92	0.51	1.16	Rest

Table 3.2 Materials properties

Properties	Symbol	Units	Materials	
			H13 Tool Steel	Cu-TiC
Electrical Resistivity	R	Ωm	5.4E-07	9.45E-08
Thermal Expansion	A	1/K	10.4E-06	13.41E-06
Density	P	kg/cc	7800	7439.6
Thermal Conductivity	K	W/mK	28.6	75.96
Hardness	HV	HV	235	106.78

3.3. SELECTION OF PROCESS PARAMETERS

The performance of Electrical Discharge Machining of tool steel is dependent on a number of dependent variables [35]. These variables can be categorized as electrode based parameters, workpiece material based parameters electrical and non-electrical parameters. From the literature review, discharge current, pulse on time and pulse off time have been found to be the most significant parameters that influence the EDM process. Therefore, these three factors have been selected for this current research.

The experiments have been performed by considering these three factors at various levels. The ranges of values for these three factors have been decided according to the literature survey and pilot experiments. The range of values of discharge current, pulse-on time, and pulse-off time have been decided as 3 to 11 A, 100 to 500 μs and 10 to 50 μs respectively. When current was kept below 3A, it was seen that MRR was irrelevant and when it was kept above 11A, the MRR was high which leads to very high roughness on the surface of tool and workpiece. The process parameters along with its range have been shown in this given table 3.3.

Table 3.3 Ranges of process parameters

FACTORS	UNITS	RANGE
Discharge Current (Ip)	A	3,5,7,9,11
Pulse on time (Ton)	Ms	100, 200, 300, 400, 500
Pulse off Time (Toff)	Ms	10, 20, 30, 40, 50

3.4 PLANNING OF EXPERIMENTS

3.4.1 Experimental Design

A proper planned analysis can decrease the quantity of trials. In traditional strategies for experimental planning (factorial outlines, part factorial plans etc.), a substantial number of investigations must be done as the quantity of the process parameters expands, which is troublesome and time taking. In order to determine the equations of the response surface, several experimental designs exist which approximate the equation using smaller number of experiments possible. The most preferred classes of design are the orthogonal first order design and the central composite second order design.

The model of first order is admissible over a narrow range of variables. Hence, the experiments are performed for obtaining model of second order [36].

Table 3.4 Design of Experiments

Exp.No.	Discharge current (Ip)	Pulse-on Time (Ton)	Pulse-off Time (Toff)
1	0	0	0
2	0	2	0
3	0	0	0
4	1	-1	1
5	0	0	2
6	1	1	1
7	1	1	-1
8	0	0	0
9	-1	1	1
10	-2	0	0
11	0	-2	0
12	1	-1	-1
13	-1	-1	-1
14	0	0	0
15	-1	-1	1
16	-1	1	-1
17	0	0	0
18	0	0	0
19	2	0	0
20	0	0	-2

Central Composite Design (CCD) is the most attractive group of second order designs recommended by Box and Wilson [37]. Central Composite Rotatable design (CCRD) is competent of forecasting independent, quadratic and interaction effects of different parameters on the output responses. The typical experimental plan using CCRD is shown in table 3.4. An outline is rotatable if the difference of the response is consistent for all factors at a given separation from the design centre. The rotatable central composite plan would be almost orthogonal if the quantity of centre points is around five. CCRD is equipped for foreseeing autonomous, quadratic and communication impacts of various parameters on the responses. The total 20 experiments have been accomplished at five levels which have been shown in table 3.5.

Table 3.5 Levels of experiments for process parameters

FACTORS	UNITS	LEVELS				
		-2	-1	0	1	2
Discharge current	A	3	5	7	9	11
Pulse-on Time	µs	100	200	300	400	500
Pulse-off Time	µs	10	20	30	40	50

Expression generated for the second order central composite design is shown by [38].

$$z = f(y_1, y_2, \dots\dots\dots\dots, y_n) \pm \varepsilon \quad (3.1)$$

where $y_1, y_2, \dots\dots\dots\dots, y_n$ are input process parameters, z is the output of the system and ε is the error which is typically conveyed about the seen reaction z with zero mean. Here, it is accepted that the independent factors (input process parameters) are persistent and controllable by trials with very minute error. It is additionally required to locate an appropriate estimate for the genuine functional connection between independent factors and reactions. Equation 3.1 shows response surface that is why these type of designs are also known as response surface designs. In this procedure, the main goal is to optimization of response surface which is determined by different process parameters. Response Surface Methodology (RSM) clarifies the connection between input parameters and response surface [38]. Generally, a second-order regression model as shown below:-

$$z = x_0 + \sum_{i=1}^{p} x_i y_i + \sum_{i=1}^{p} x_{ii} y_i^2 + \sum_i \sum_j x_{ij} y_i y_j \pm \varepsilon \quad (3.2)$$

where all x_i's are regression coefficients controlled by least square method. The estimated coefficients or the model equation required to be approved for statistical significance.

3.4.2 Analysis of Variance

Statistical examination of the test is done by Analysis of variance (ANOVA). ANOVA is a computational strategy that empowers the evaluation of the relative involvement of every one of the controllable variable that allows the general estimation of response and communicates it as a percentage. ANOVA utilizes a mathematical method known as sum of squares to quantitatively look at the deviation of the control factor response average from the overall experimental mean response, which is referred to as the variation between the controls variables. The importance of the specific and interaction effects is evaluated by looking at the fluctuation between the control factors impacts against the difference in the experimental data because of irregular experimental error. This ratio is referred to as F-ratio and can be shaped between the control factors effect variance (the mean square because of experimental blunder). The ANOVA procedure allows picking up knowledge into which factors have fundamental impacts, cooperation impacts, less important and noise. This helps in choosing the components those are most pertinent for executing out the desired investigation consequently upgrading product robustness.

3.5 EXPERIMENTATION ON EDM WITH COPPER AS ELECTRODE

Die Sinking Electrical Discharge Machining experiments have been utilized on the EDM machine (ELECTRONICA VCP 20). In every experiment, dielectric medium was Kerosene oil. Total 20 experiments have been carried out using Central Composite Rotatable

design with independent factors at 5 separate levels. Machining time has been kept 15 minutes for each workpiece.

After EDM, H13 tool steel samples have been clear up with acetone. The weight losses of each sample have been checked out with high precision electronic weighing machine having least count of 0.01mg after each experiment. The surface roughness has been recorded by the help of surface measuring machine (Mitutoyo SJ-400, Japan). The cut-off length 0.8mm is used with a transverse length of 4 mm. The centre line average value of the surface roughness is the most widely used surface roughness parameter in industry, was selected in this study. Each sample was measured three times and the average was taken as the response [39]. Measurement of out of roundness of the tool was performed before and after machining in order to determine the actual change in the shape of the tool. This estimation was performed on Accurate Spectra 5.6.4 Coordinate Measuring Machine and Tangram software. The variation in roundness of the tool has been investigated as the response in the examination to show to the shape of the electrode tool.

TWR has been defined, as the ratio of the weight loss of tool to the machining time [40] and is given below:-

$$Tool\ Wear\ Rate = \frac{Weight\ loss\ of\ tool}{Machining\ time}$$

$$TWR(mg/min) = \frac{W_{TBM} - W_{TAM}}{T_m} \tag{3.3}$$

Where TWR is Tool wear rate, W_{TBM} is weight of tool before machining, W_{TAM} is weight of tool after machining and T_m is machining time. Similarly, MRR has been explained as the ratio of weight loss of workpiece to machining time [41].

$$Material\ Removal\ Rate = \frac{Weight\ loss\ of\ workpiece}{Machining\ time}$$

$$MRR(mg/min) = \frac{W_{WBM} - W_{WAM}}{T_m} \tag{3.4}$$

where W_{WBM} is weight of workpiece before machining, W_{WAM} is weight of workpiece after machining and T_m is machining time. Hence the measured values of TWR, MRR, SR and OOR for every experiment have been shown in given table 3.6.

Table 3.6 Experimental observations for every response of EDM process

Exp. No.	Discharge Current (Ip)	Pulse-on Time (Ton)	Pulse-off Time (Toff)	TWR	MRR	SR	OOR
	Amp	µs	µs	(mg/min)	(mg/min)	µm	Mm
1	7	300	30	6.08	119.67	4.39	0.0139
2	7	500	30	5.38	128.43	4.62	0.0123
3	7	300	30	6.12	121.87	4.41	0.0144
4	9	200	40	8.45	148.54	4.95	0.0201
5	7	300	50	5.64	125.87	4.53	0.0131
6	9	400	40	7.41	167.43	5.43	0.0186
7	9	400	20	8.31	158.43	5.15	0.0193
8	7	300	30	6.15	120.77	4.38	0.0142
9	5	400	40	3.89	85.77	4.11	0.0054
10	3	300	30	2.58	37.2	3.84	0.0018
11	7	100	30	6.45	107.71	4.29	0.0169
12	9	200	20	8.75	141.76	4.87	0.0211
13	5	200	20	4.21	70.98	3.98	0.0103
14	7	300	30	6.05	122.23	4.4	0.0138
15	5	200	40	4.15	77.43	4.03	0.0083
16	5	400	20	4.03	82.33	4.06	0.0072
17	7	300	30	6.21	119.11	4.45	0.0139
18	7	300	30	6.09	120.98	4.42	0.0141
19	11	300	30	10.49	186.32	6.02	0.0248
20	7	300	10	6.34	114.23	4.35	0.0161

3.5.1 Statistical Modelling of TWR

A statistical model for TWR has been created, by interacting the input parameters i.e. pulse-on time, pulse-off time and discharge current based on the investigation of data shown in table above 3.6, and is shown below in the form of equation given below (3.5) after neglecting all insignificant parameters.

$$\text{TWR} = -2.185 + (1.004 \times \text{I}_\text{P}) + (0.00713 \times \text{T}_\text{on}) + (0.0518 \times \text{T}_\text{off}) + (0.02804 \times \text{I}_\text{P}^2) - (0.000004 \times \text{T}_\text{on}^2) - (0.00065 \times \text{I}_\text{P} \times \text{T}_\text{on}) - (0.00625 \times \text{I}_\text{P} \times \text{T}_\text{off}) - 0.000085 \times \text{T}_\text{on} \times \text{T}_\text{off} \quad (3.5)$$

For analyzing the data of experiment, goodness of fit for the model has been checked as per requirement. So, the adequacy of the model checking consists of lack of fit test, significance on model coefficient test and regression model [38]. For fulfilling the purpose, ANOVA has been performed for checking its adequacy which is shown in table 3.7. The summary of fit prescribes that quadratic model for TWR is statistically suitable and insignificant of the lack of fit. The value of R^2 is 99.06% which represents that model of regression provide strong connection between independent factors and the response (TWR)

and gives the best justification of the interconnection between independent factors and response (TWR).

Table 3.7 ANOVA table for TWR of CU Tool

Source	DF	Adj SS	Adj MS	F-value	P-value	R^2
Model	9	68.1533	7.5726	791.32	0.000	0.9906
Ip	1	65.8532	65.8532			
Ton	1	1.0302	1.0302			
Toff	1	0.4900	0.4900			
Ip*Ip	1	0.2802	0.2802			
Ton*Ton	1	0.0614	0.0614			
Toff*Toff	1	0.0237	0.0237			
Ip*Ton	1	0.1352	0.1352			
Ip*Toff	1	0.1250	0.1250			
Ton*Toff	1	0.0578	0.0578			
Lack-of-Fit	5	0.0794	0.0159	4.86	0.054	
Pure Error	5	0.0163	0.0033			
Total	19	68.2490				

The P-value which is calculated for the lack of fit should be more than 0.05 because it justifies the insignificance of lack of fit. The percentage contribution of the model for every significant term has been represented in figure 3.10. The figure represents the most affecting parameters over the TWR in which the discharge current is resulted be in a highest significant factor with 51% contribution followed by pulse-on time and pulse-off time with 7% and 5% contribution respectively.

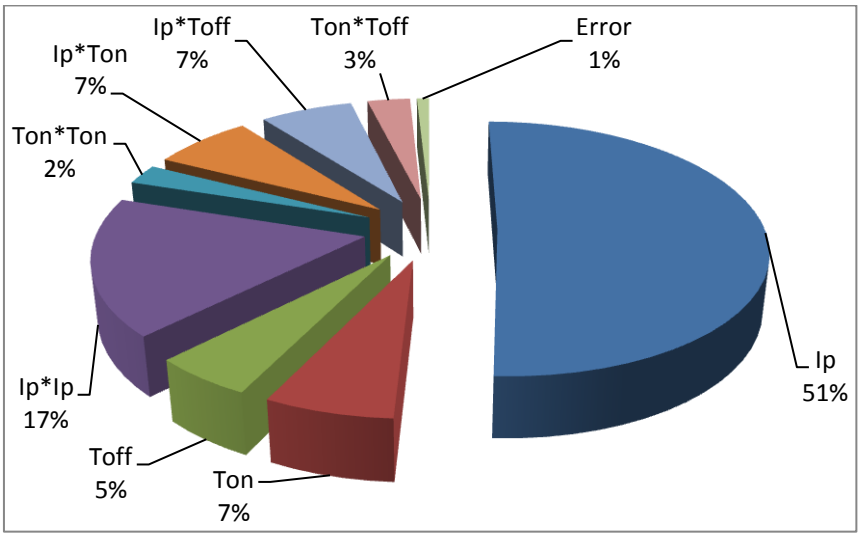

Figure 3.10: Percentage contributions of factors on TWR for EDM

3.5.2 Statistical Modelling of MRR

A statistical model has been developed for MRR by correlating of the input parameters namely pulse-on time, pulse-off time and discharge current which is based on data

represented analysis in table 3.6 and the equation given below (3.6) after neglecting insignificant parameters.

$$MRR = -51.50 + (23.73 \times I_P) + (0.0338 \times T_{on}) + (0.3059 \times T_{off}) - (0.5728 \times I_P^2) - (0.000071 \times T_{on}^2) - (0.00992 \times I_P \times T_{on}) \quad (3.6)$$

ANOVA calculation has been performed of developed model for checking its adequacy. The calculated F-Ratio for the model was compared with F-ratio tabulated value for a particular confidence interval. The ANOVA has been described by the table 3.8 and the statistical model is represented as equation 3.6. The ANOVA of model represents the significant of model as R^2 statistics is 99.24% which represents strong relationship between MRR and independent variables by regression model.

Table 3.8 ANOVA table for MRR of Cu tool

Source	DF	Adj SS	Adj MS	F-value	P-value	R^2
Model	9	23254.9	2583.9	914.54	0.000	0.9924
Ip	1	22342.0	22342.0			
Ton	1	584.3	584.3			
Toff	1	149.8	149.8			
Ip*Ip	1	139.0	139.0			
Ton*Ton	1	15.0	15.0			
Toff*Toff	1	2.0	2.0			
Ip*Ton	1	31.5	31.5			
Ip*Toff	1	4.3	4.3			
Ton*Toff	1	0.1	0.1			
Lack-of-Fit	5	20.9	4.2	2.84	0.138	
Pure Error	5	7.4	1.5			
Total	19	23283.2				

The P-value which is calculated for the lack of fit should be more than 0.05 because it justifies the insignificance of lack of fit. The percentage contribution of the model for every significant term has been represented in figure 3.11. The figure represents the most affecting parameters over the MRR in which the discharge current is resulted be in a highest significant factor with 68% contribution followed by pulse-on time and pulse-off time with approximately 0% and 14% contribution respectively.

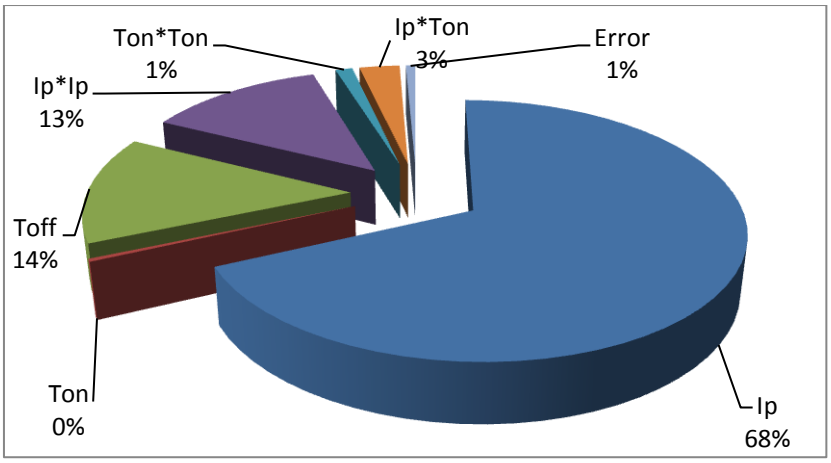

Figure 3.11: Percentage contributions of the factors on MRR for EDM

3.5.3 Statistical Modelling of SR

A statistical model has been developed for SR by correlating the input parameters that is pulse-on time, pulse-off time and discharge current which are based on data represented analysis in table 3.6 and the equation given below (3.7) after neglecting insignificant parameters.

$$SR = 4.799 - (0.3404 \times I_P) - (0.001638 \times T_{on}) - (0.00625 \times T_{off}) + (0.03195 \times I_P^2) + (0.000375 \times I_P \times T_{on}) + (0.001625 \times I_P \times T_{off}) \quad (3.7)$$

ANOVA calculation has been performed of developed model for checking its adequacy. The calculated F-Ratio for the model was compared with F-ratio tabulated value for a particular confidence interval. The ANOVA has been described by equation 3.7 for the second model which is presented in table 3.9. The ANOVA of model represents the significant of model as R^2 statistics is 98.18% which represents strong relationship between SR and independent variables by regression model.

Table 3.9 ANOVA table for SR for Cu tool

Source	DF	Adj SS	Adj MS	F-value	P-value	R^2
Model	9	5.30705	0.58967	392.22	0.000	0.9818
Ip	1	4.60102	4.60102			
Ton	1	0.15603	0.15603			
Toff	1	0.04203	0.04203			
Ip*Ip	1	0.43613	0.43613			
Ton*Ton	1	0.00422	0.00422			
Toff*Toff	1	0.00213	0.00213			
Ip*Ton	1	0.04500	0.04500			
Ip*Toff	1	0.00845	0.00845			
Ton*Toff	1	0.00500	0.00500			
Lack-of-Fit	5	0.01195	0.00239	3.88	0.082	
Pure Error	5	0.00308	0.00062			
Total	19	5.32208				

The P-value which is calculated for the lack of fit should be more than 0.05 because it justifies the insignificance of lack of fit. The percentage contribution of the model for every significant term has been represented in figure. 3.12. The figure represents the most affecting parameters over the SR in which the square of discharge current is resulted be in a highest significant factor with 71% contribution followed by pulse-on time and pulse-off time with approximately 3% and 0% contribution respectively.

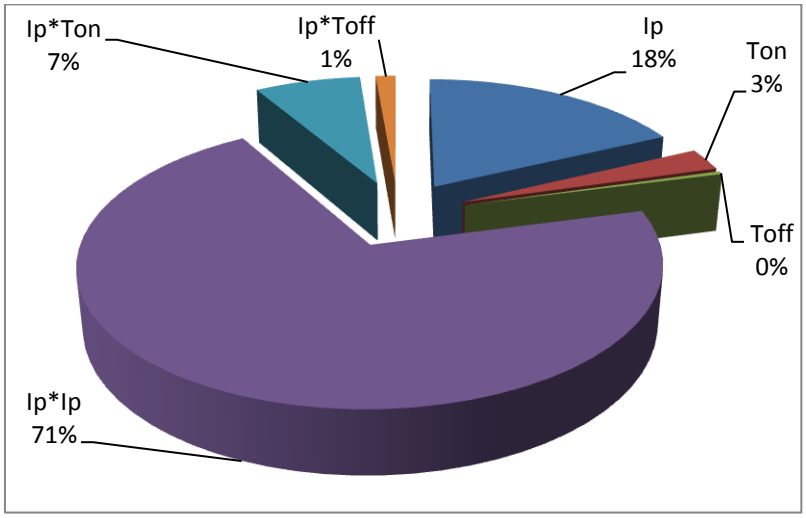

Figure 3.12 Percentage contributions of factors on SR for EDM

3.5.4 Statistical Modelling of OOR

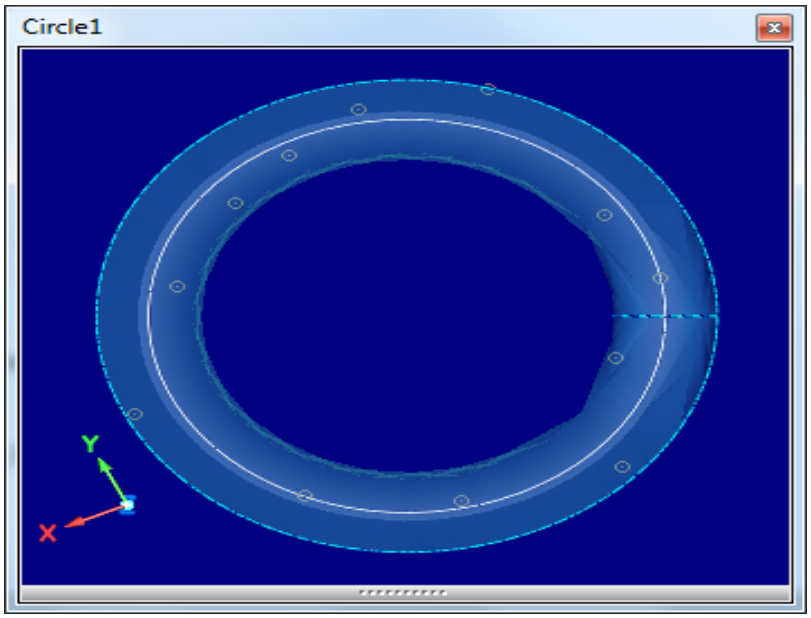

Figure 3.13 Graphs showing the out of roundness value for electrode tool

The out of roundness of the tool has been determined in copper tool to study the shape of the tool. Measurement of out of roundness of the tool has been performed, both before and after machining. The difference observed between these two measurements has been taken as

response. For each tool, twelve random points were marked on the outer periphery of tool by CMM stylus as shown in figure 3.13. Tangram software was used for the evaluation of marked points on the tool for the determination of out of roundness of tool.

A statistical model has been developed for OOR by correlating the input parameters that is pulse-on time, pulse-off time and discharge current which are based on data represented analysis in table 3.6 and the equation given below (3.8) after neglecting insignificant parameters.

$$OOR = 0.00243 + (0.002933 \times I_P) - (0.000023 \times T_{on}) - (0.000164 \times T_{off}) - (0.000064 \times I_P^2) + (0.000002 \times I_P \times T_{on}) - (0.000013 \times I_P \times T_{off}) \quad (3.8)$$

ANOVA calculation has been performed of developed model for checking its adequacy. The calculated F-Ratio for the model was compared with F-ratio tabulated value for a particular confidence interval. The ANOVA has been described by equation 3.8 for the second model which is presented in table 3.10. The ANOVA of model represents the significant of model as R^2 statistics is 98.87% which represents strong relationship between OOR and independent variables by regression model.

Table 3.10 ANOVA table for OOR for Cu tool

Source	DF	Adj SS	Adj MS	F-value	P-value	R^2
Model	9	0.000584	0.000065	628.88	0.000	0.9887
Ip	1	0.000551	0.000551			
Ton	1	0.000021	0.000021			
Toff	1	0.000008	0.000008			
Ip*Ip	1	0.000001	0.000001			
Ton*Ton	1	0.000000	0.000000			
Toff*Toff	1	0.000000	0.000000			
Ip*Ton	1	0.000001	0.000001			
Ip*Toff	1	0.000001	0.000001			
Ton*Toff	1	0.000000	0.000000			
Lack-of-Fit	5	0.000001	0.000000	3.05	0.123	
Pure Error	5	0.000000	0.000000			
Total	19	0.000586				

The P-value which is calculated for the lack of fit should be more than 0.05 because it justifies the insignificance of lack of fit. The percentage contribution of the model for every significant term has been represented in figure 3.14. The figure represents the most affecting parameters over the OOR in which the discharge current is resulted be in a highest significant factor with 47% contribution followed by pulse-on time and pulse-off time with approximately 17% and 12% contribution respectively.

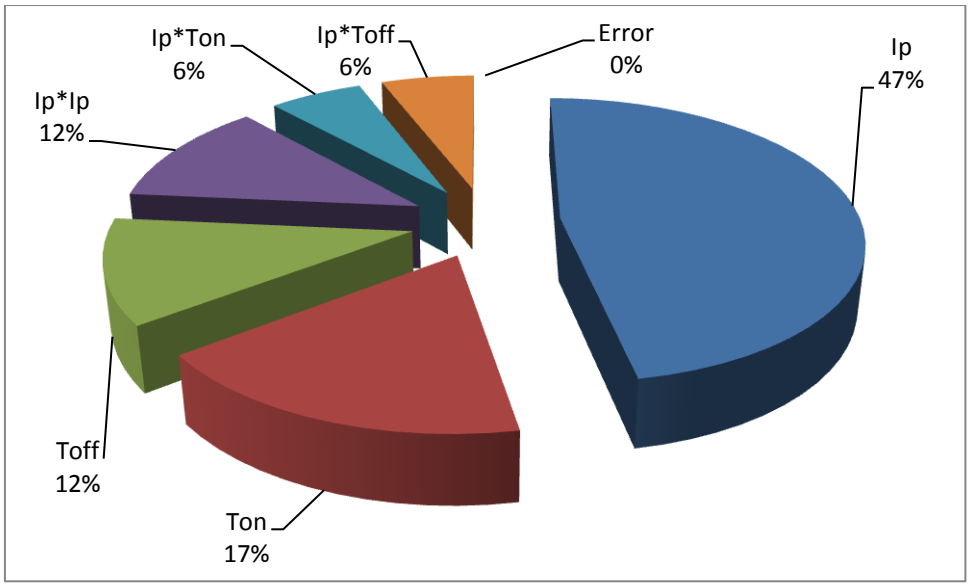

Figure 3.14 Percentage contributions of the factors on OOR for EDM

3.6 EXPERIMENTATION ON EDM WITH COPPER TITANIUM CARBIDE AS ELECTRODE

Die sinking EDM (ELECTRONICA VCP 20) have been used again for carrying out the experiment with another electrode tool i.e. Copper Titanium carbide ceramic tool. In every experiment, dielectric medium was Kerosene oil. Total 20 experiments have been carried out using CCRD with independent factors at 5 separate levels. Machining time has been kept 15 minutes for each workpiece.

After performing the experiments, the same strategies were followed for cleaning the samples and calculate the TWR, MRR, Surface Roughness of workpiece and Out of Roundness of the tool prepared as per section 3.3 and 3.5. The experimental observation of TWR, MRR, SR and OOR for every tool of Cu-TiC Tool has been shown in table 3.11.

Table 3.11 Experimental observations for every response of EDM process

Exp. No.	Discharge Current (Ip)	Pulse-on Time (Ton)	Pulse-off Time (Toff)	TWR	MRR	SR	OOR
	Amp	µs	µs	(mg/min)	(mg/min)	µm	Mm
1	7	300	30	5	143.6	7.65	0.0116
2	7	500	30	4.58	156.68	8.11	0.0103
3	7	300	30	5.03	145.03	7.55	0.0119
4	9	200	40	6.74	177.53	8.26	0.0193
5	7	300	50	4.67	148.53	7.93	0.0104
6	9	400	40	6.08	196.86	8.69	0.0164
7	9	400	20	6.64	191.7	8.43	0.0178
8	7	300	30	4.98	144.92	7.63	0.0113
9	5	400	40	2.99	104.45	6.89	0.0063
10	3	300	30	1.855	61.23	5.58	0.0034
11	7	100	30	5.22	129.2	7.33	0.0142
12	9	200	20	7.01	170.11	7.95	0.0205

13	5	200	20	3.34	91.8	6.64	0.0084
14	7	300	30	4.89	147.9	7.52	0.0117
15	5	200	40	3.31	97.54	6.75	0.0073
16	5	400	20	3.13	98.8	6.82	0.0069
17	7	300	30	4.88	142.93	7.59	0.0114
18	7	300	30	4.87	143.97	7.67	0.0121
19	11	300	30	8.41	219.88	9.14	0.0254
20	7	300	10	5.11	134.79	7.41	0.0131

3.6.1 Statistical Modelling of TWR

A statistical model for TWR has been created, by interacting the input parameters i.e. pulse-on time, pulse-off time and discharge current based on the investigation of data shown in table 3.11 and is shown below in the form of equation (3.9) after neglecting all insignificant parameters.

$$\text{TWR} = -0.357 + (0.7927 \times \text{I}_\text{P}) - (0.001775 \times \text{T}_\text{on}) + (0.0171 \times \text{T}_\text{off}) + (0.01206 \times \text{IP2} - 0.00413 \times \text{IP} \times \text{Toff} \quad (3.9)$$

For analyzing the data of experiment, goodness of fit for the model has been checked as per requirement. So, the adequacy of the model checking consists of lack of fit test, significance on model coefficient test and regression model [38]. For fulfilling the purpose, ANOVA has been performed for checking its adequacy which is shown in table 3.12. The summary of fit prescribes that quadratic model for TWR is statistically suitable and insignificant of the lack of fit. The value of R^2 is 99.08% which represents that model of regression provide strong connection between independent factors and the response (TWR) and gives the best justification of the interconnection between independent factors and response (TWR).

Table 3.12 ANOVA table for TWR of Cu-TiC tool

Source	DF	Adj SS	Adj MS	F-value	P-value	R^2
Model	9	45.8299	5.0922	705.79	0.000	0.9908
Ip	1	44.9235	44.9235			
Ton	1	0.5041	0.5041			
Toff	1	0.2209	0.2209			
Ip*Ip	1	0.0447	0.0447			
Ton*Ton	1	0.0064	0.0064			
Toff*Toff	1	0.0086	0.0086			
Ip*Ton	1	0.0313	0.0313			
Ip*Toff	1	0.0545	0.0545			
Ton*Toff	1	0.0200	0.0200			
Lack-of-Fit	5	0.0479	0.0096	1.97	0.237	
Pure Error	5	0.0243	0.0049			
Total	19	45.9020				

The P-value which is calculated for the lack of fit should be more than 0.05 because it justifies the insignificance of lack of fit. The percentage contribution of the model for every significant term has been represented in figure 3.15. The figure represents the most affecting parameters over the TWR in which the discharge current is resulted be in a highest significant factor with 56% contribution followed by pulse-on time and pulse-off time with approximately 33% and 1% contribution respectively.

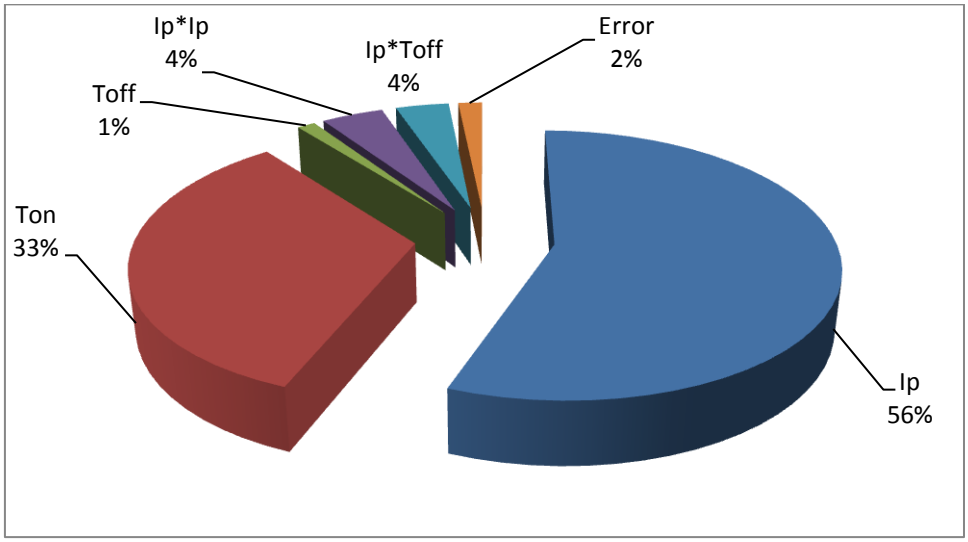

Figure 3.15 Percentage contributions of factors on TWR for EDM

3.6.2 Statistical Modelling of MRR

A statistical model has been developed for MRR correlating of the input parameters namely pulse-on time, pulse-off time and discharge current based on the investigation of data represented in table 3.11 and the equation given below (3.10) after neglecting all insignificant parameters.

$$MRR = -7.4 + (18.77 \times I_P) - (0.0495 \times T_{on}) + (0.3216 \times T_{off}) - (0.227 \times I_P^2) + (0.01688 \times I_P \times T_{on}) \quad (3.10)$$

ANOVA calculation has been performed of developed model for checking its adequacy. The calculated F-Ratio for the model was compared with F-ratio tabulated value for a particular confidence interval. The ANOVA has been described by equation 3.10 for the second model which is presented in table 3.13. The ANOVA of model represents the significant of model as R^2 statistics is 98.38% which represents strong relationship between MRR and independent variables by regression model.

Table 3.13 ANOVA table for MRR of Cu-TiC tool

Source	DF	Adj SS	Adj MS	F-value	P-value	R^2
Model	9	28357.2	3150.8	462.69	0.000	0.9838
Ip	1	27300.1	27300.1			
Ton	1	753.4	753.4			
Toff	1	165.4	165.4			
Ip*Ip	1	34.3	34.3			
Ton*Ton	1	8.2	8.2			
Toff*Toff	1	20.0	20.0			
Ip*Ton	1	91.2	91.2			
Ip*Toff	1	0.2	0.2			
Ton*Toff	1	0.7	0.7			
Lack-of-Fit	5	52.8	10.6	3.46	0.100	
Pure Error	5	15.3	3.1			
Total	19	28425.3				

The P-value which is calculated for the lack of fit should be more than 0.05 because it justifies the insignificance of lack of fit. The percentage contribution of the model for every significant term has been represented in figure 3.16. The figure represents the most affecting parameters over the MRR in which the discharge current is resulted be in a highest significant factor with 60% contribution followed by pulse-on time and pulse-off time with approximately 2% and 21% contribution respectively.

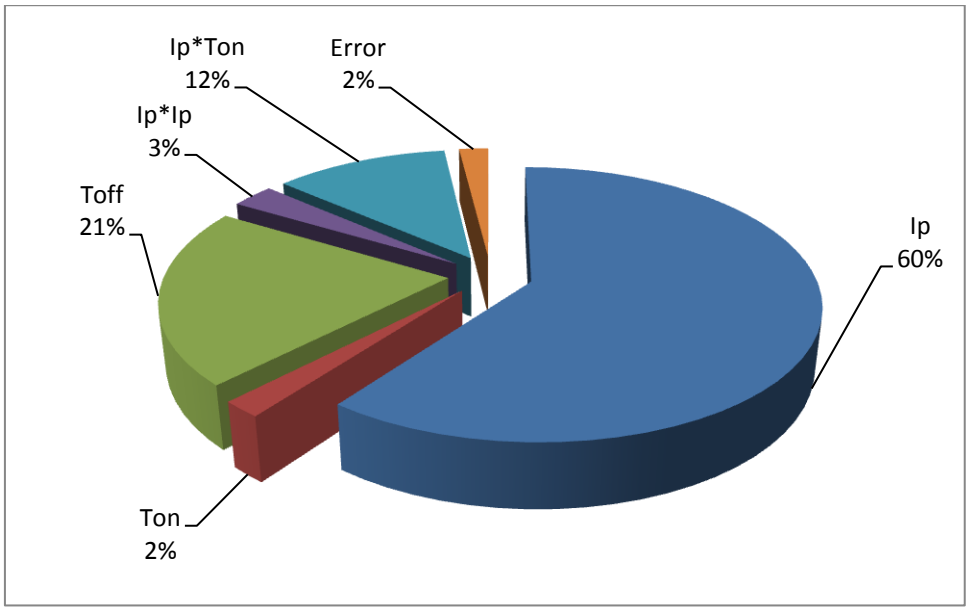

Figure 3.16 Percentage contributions of factors on MRR for EDM

3.6.3 Statistical Modelling of SR

A statistical model has been developed for SR by correlating the input parameters i.e. pulse-on time, pulse-off time and discharge current based on the investigation of data shown in table 3.11 and the equation given below (3.11) after neglecting all insignificant parameters.

$$SR = 3.763 + (0.5539 \times I_P) - (0.00084 \times T_{on}) + (0.01119 \times T_{off}) - (0.01767 \times I_P^2) + (0.000369 \times I_P \times T_{on}) \quad (3.11)$$

Table 3.14 ANOVA table for SR of Cu-TiC tool

Source	DF	Adj SS	Adj MS	F-value	P-value	R^2
Model	9	12.0445	1.3383	159.40	0.000	0.9521
Ip	1	11.1389	11.1389			
Ton	1	0.4865	0.4865			
Toff	1	0.2003	0.2003			
Ip*Ip	1	0.1015	0.1015			
Ton*Ton	1	0.0176	0.0176			
Toff*Toff	1	0.0049	0.0049			
Ip*Ton	1	0.0435	0.0435			
Ip*Toff	1	0.0190	0.0190			
Ton*Toff	1	0.0010	0.0010			
Lack-of-Fit	5	0.0667	0.0133	3.86	0.082	
Pure Error	5	0.0173	0.0035			
Total	19	12.1284				

ANOVA calculation has been performed of developed model for checking its adequacy. The calculated F-Ratio for the model was compared with F-ratio tabulated value for a particular confidence interval. The ANOVA has been described by equation 3.11 for the second model which is presented in table 3.14. The ANOVA of model represents the significant of model as R^2 statistics is 95.21% which represents strong relationship between SR and independent variables by regression model.

The P-value which is calculated for the lack of fit should be more than 0.05 because it justifies the insignificance of lack of fit. The percentage contribution of the model for every significant term has been represented in figure 3.17. The figure represents the most affecting parameters over the SR in which the discharge current is resulted be in a highest significant factor with 51% contribution followed by pulse-on time and pulse-off time with approximately 0% and 25% contribution respectively.

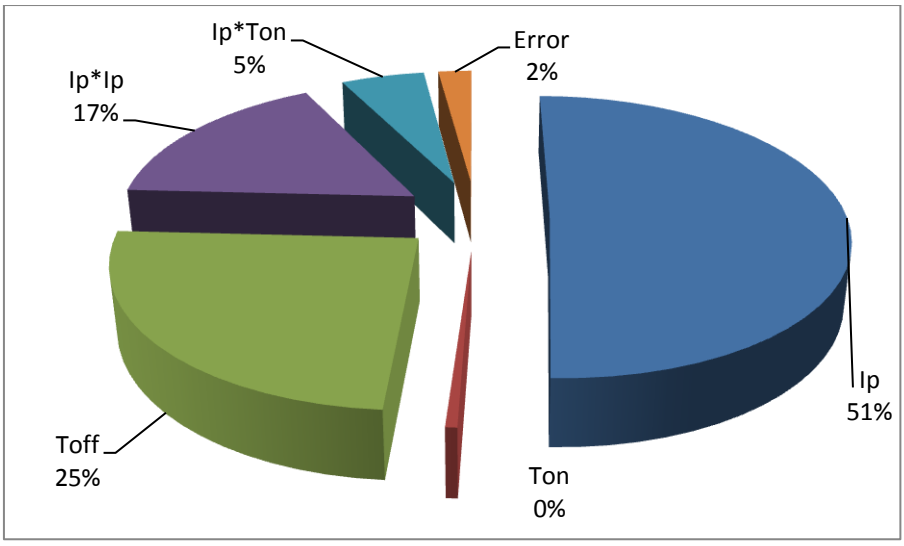

Figure 3.17 Percentage contributions of factors on SR for EDM

3.6.4 Statistical Modelling of OOR

A statistical model has been developed for OOR inter-relating of the input parameters are pulse-on time, pulse-off time and discharge current which are based on data represented analysis in table 3.11 and the equation given below (3.12) after neglecting insignificant parameters.

$$OOR = 0.00314 + (0.000903 \times I_P) - (0.000006 \times T_{on}) - (0.000061 \times T_{off}) + (0.000176 \times I_P^2) + (0.000002 \times I_P \times T_{on}) \quad (3.12)$$

The ANOVA has been described by equation 3.12 for the second model which is presented in table 3.15. The ANOVA of model represents the significant of model as R^2 statistics is 98.78% which represents strong relationship between OOR and independent variables by regression model.

Table 3.15 ANOVA table for OOR of Cu-TiC tool

Source	DF	Adj SS	Adj MS	F-value	P-value	R^2
Model	9	0.000532	0.000059	495.65	0.000	0.9878
Ip	1	0.000496	0.000496			
Ton	1	0.000016	0.000016			
Toff	1	0.000006	0.000006			
Ip*Ip	1	0.000013	0.000013			
Ton*Ton	1	0.000001	0.000001			
Toff*Toff	1	0.000000	0.000000			
Ip*Ton	1	0.000001	0.000001			
Ip*Toff	1	0.000000	0.000000			
Ton*Toff	1	0.000000	0.000000			
Lack-of-Fit	5	0.000001	0.000000	1.63	0.302	
Pure Error	5	0.000000	0.000000			
Total	19	0.000534				

The P-value which is calculated for the lack of fit should be more than 0.05 because it justifies the insignificance of lack of fit. The percentage contribution of the model for every significant term has been represented in figure 3.18. The figure represents the most affecting parameters over the OOR in which the discharge current is resulted be in a highest significant factor with 59% contribution followed by pulse-on time and pulse-off time with approximately 0% and 27% contribution respectively.

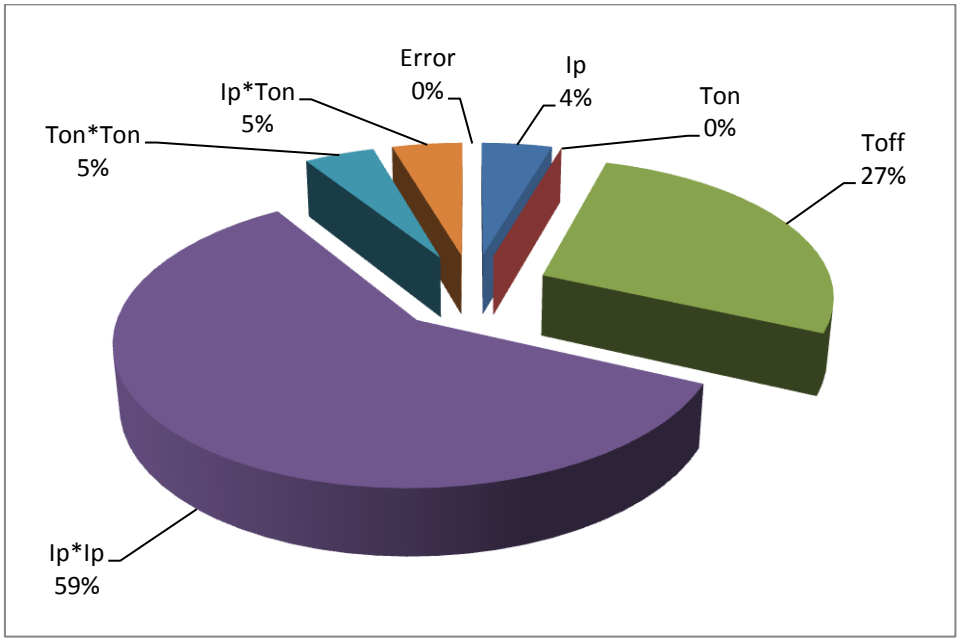

Figure 3.18 Percentage contributions of factor on OOR for EDM

3.7 RESULTS AND DISCUSSION

The work successfully estimated the functionality of EDM process using simple Cu and ceramic of Cu-TiC as a tooltip for machining H13 tool steel. Figure 3.19 and Figure 3.20 represent main effects plots of TWR for Cu and Cu-TiC tool machining where five points are taken which is obtained from the experiment data. It can be observed that as the discharge current increases, the TWR increases linearly. For the case of pulse duration, as the pulse-on time increases, the TWR decreases slightly and same trend has been shown by pulse-off time.

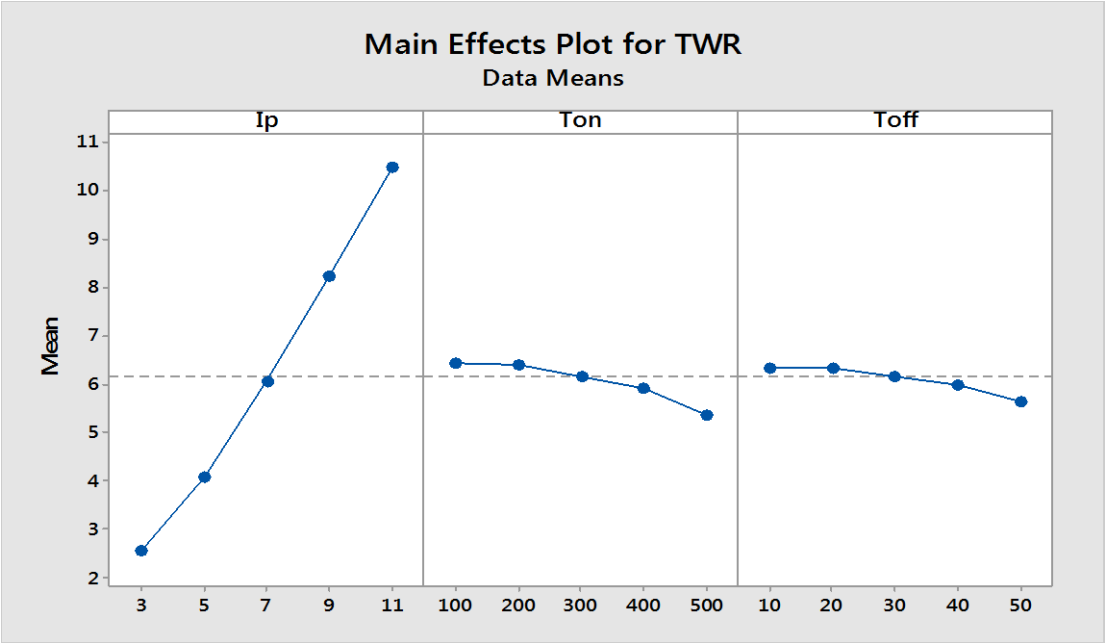

Figure 3.19 Main effects plot for TWR of EDM by Cu tool.

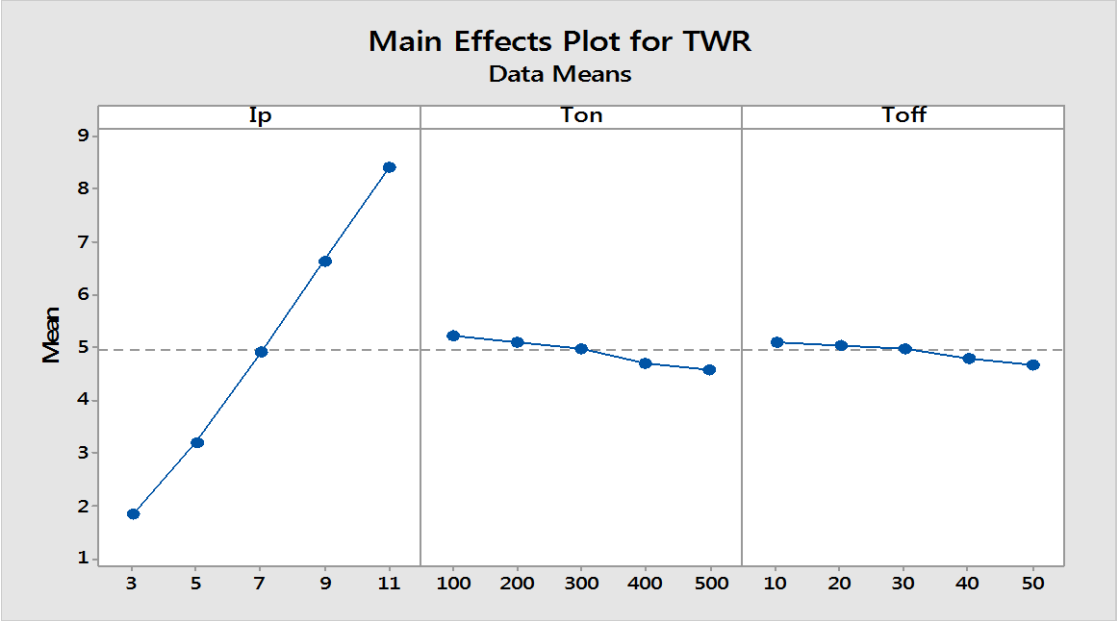

Figure 3.20 Main effects plot for TWR of EDM by Cu-TiC tool

(a)

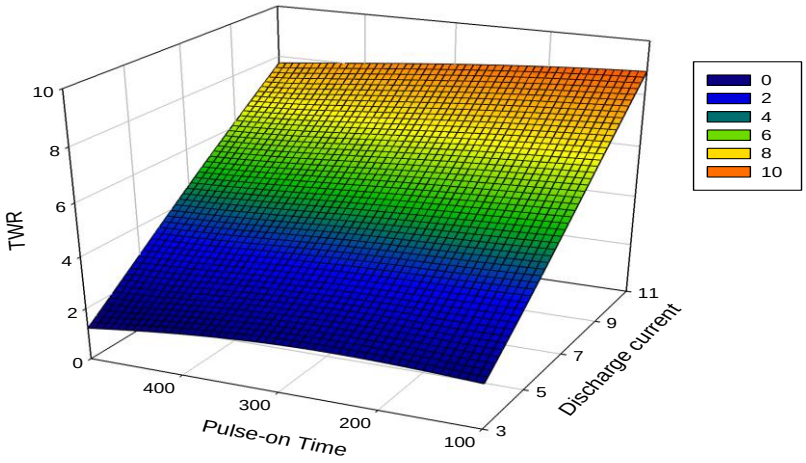

(b)

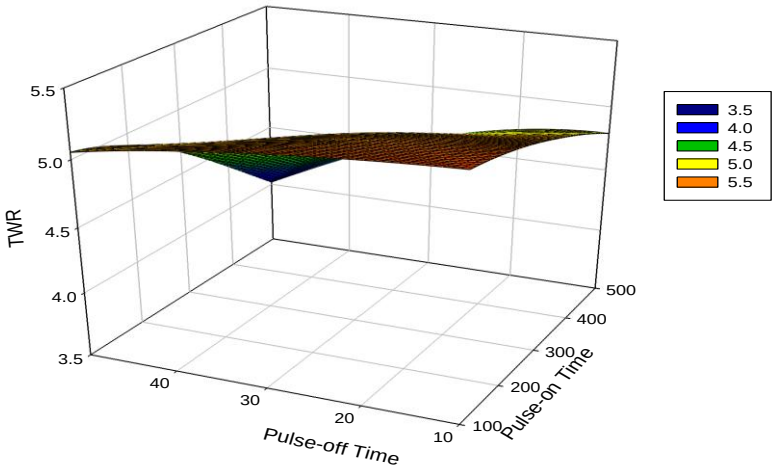

(c)

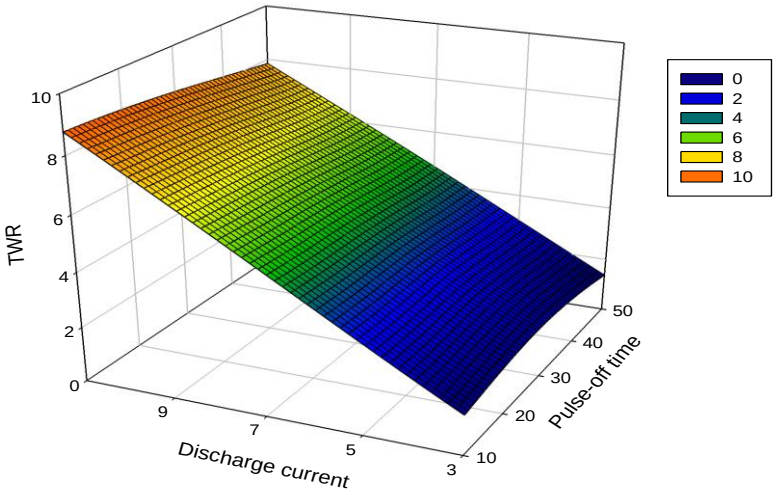

Figure 3.21 Response surface for TWR of Cu-TiC tool

Figure 3.21 represents 3D mesh plots for TWR drawn with the help of Sigma Plot [10.0] software. This plot is one of the best methods for evaluation and representation of the surface design [38, 42]. The variation of TWR with respect to discharge current can be seen in figure 3.21 (a). This graph shows that the TWR increases with increase in discharge current. This is be due to more electrical discharge energy being conducted into the machining gap with the increase in discharge current, thereby increasing the TWR It can be observed from figure 3.22 that TWR is less in Cu-TiC as compared to the copper tool. This is because the presence of titanium carbide in ceramic tool increases the wear resistance of the tooltip. This means that there is more bonding strength that avoids wearing of tool.

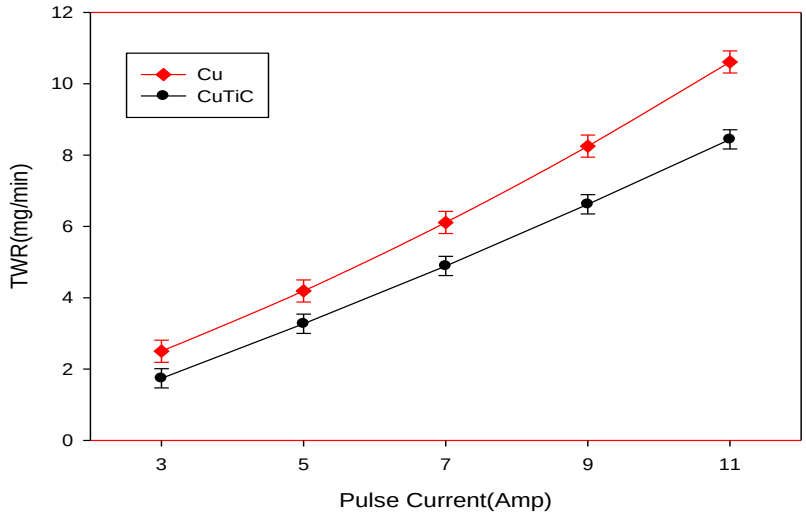

Figure 3.22 Variation of TWR with discharge current

The effect of variation of pulse-on time on the estimation of TWR is presented in figure 3.21 (b). It can be seen that an increment in pulse-on time decreases the values of TWR. This is because the discharge column's diameter increases as the pulse-on time increases which decreases the energy density present in the discharge column on the spot where the discharge has taken place [43]. Further it can be seen from the figure 3.23 that TWR in Cu-TiC tool machining process is lesser when contrasted with Cu tool machining process.

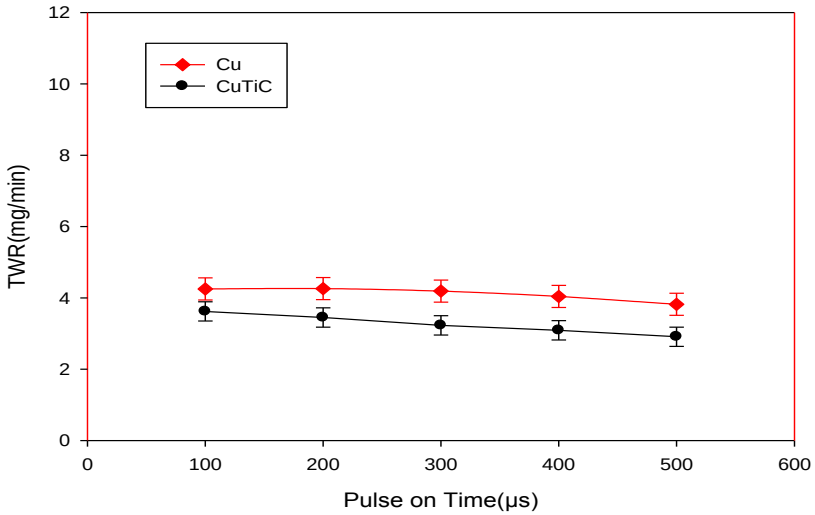

Figure 3.23 Variation of TWR with pulse-on time

The effect of variation of pulse-off time on the estimation of TWR is introduced in figure 3.21 (c). It can be seen that an increment in pulse-off time slightly decreases the values of TWR. This is because of the time duration during which the electric discharge shut off where the discharge column's diameter starts to decrease. During this time duration, the surface of the tool and workpiece starts cooling which stops wearing of tool. Further it can be seen from the figure 3.24 that TWR in Cu-TiC tool machining process is lesser when contrasted with Cu tool machining process.

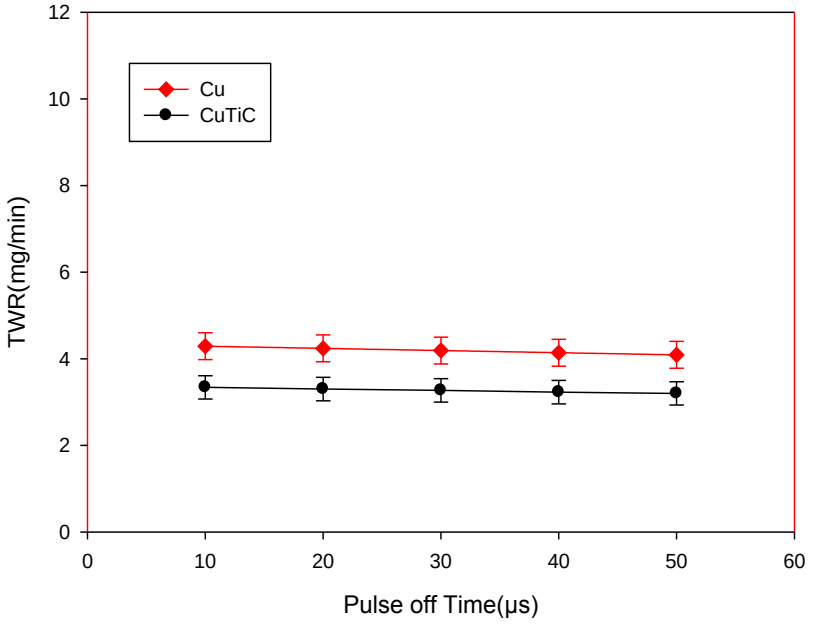

Figure 3.24 Variation of TWR with pulse-off time

Figure 3.25 and figure 3.26 represent main effects plots of MRR by Cu & Cu-TiC tool respectively where five points are taken which is obtained from the experiment data. It can be observed that as the discharge current increases, the MRR increases linearly. For the case of pulse duration, as the pulse-on time increases, the MRR increases slightly and same trend is followed by pulse-off time too.

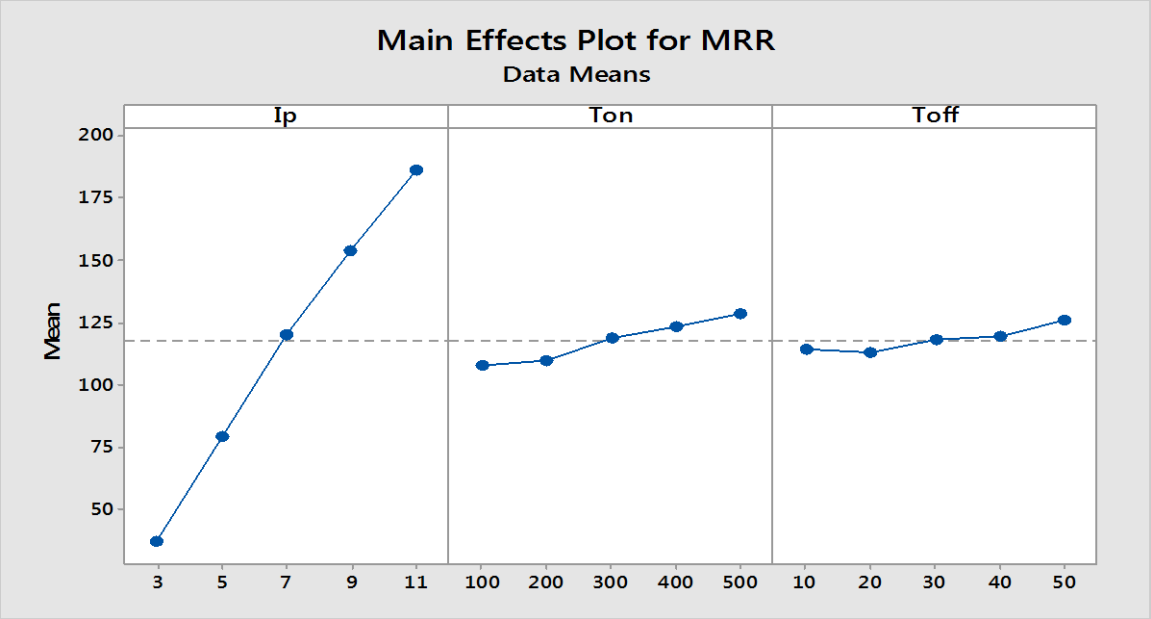

Figure 3.25: Main effects plot for MRR of EDM by Cu tool

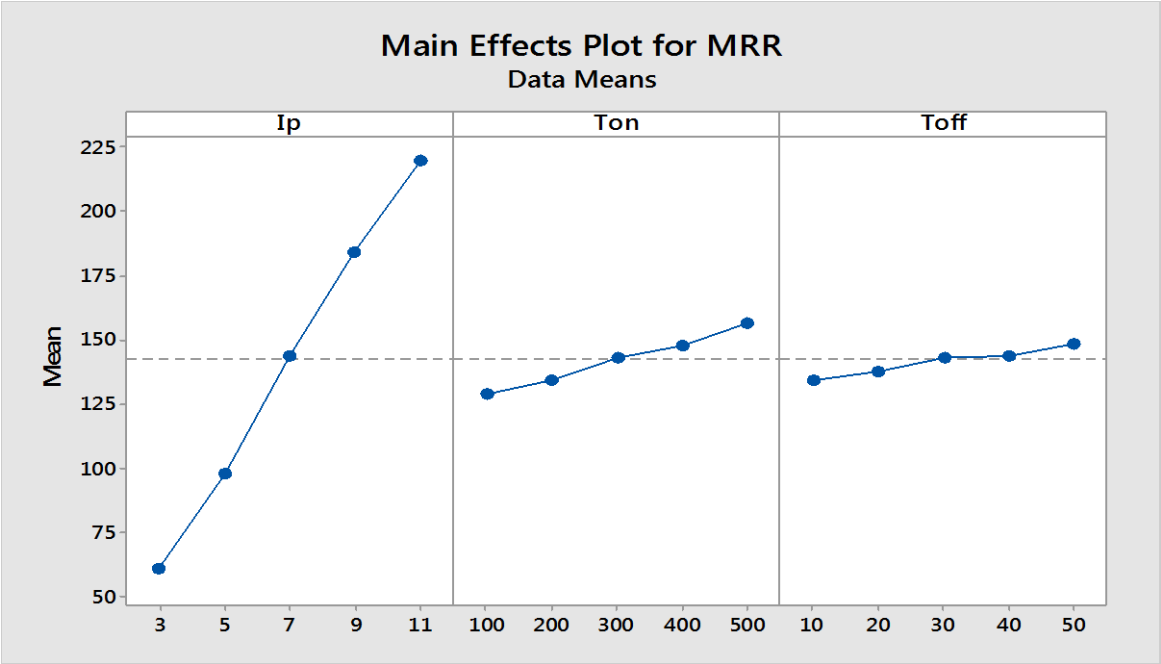

Figure 3.26 Main effects plot MRR of EDM by Cu-TiC tool

(a)

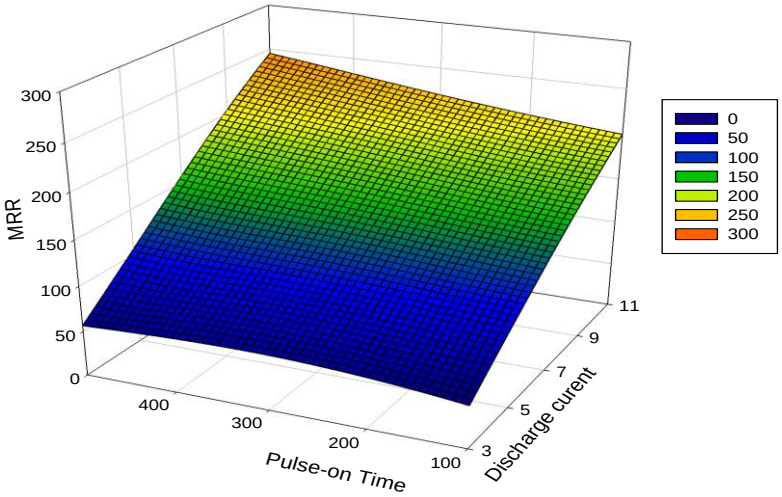

(b)

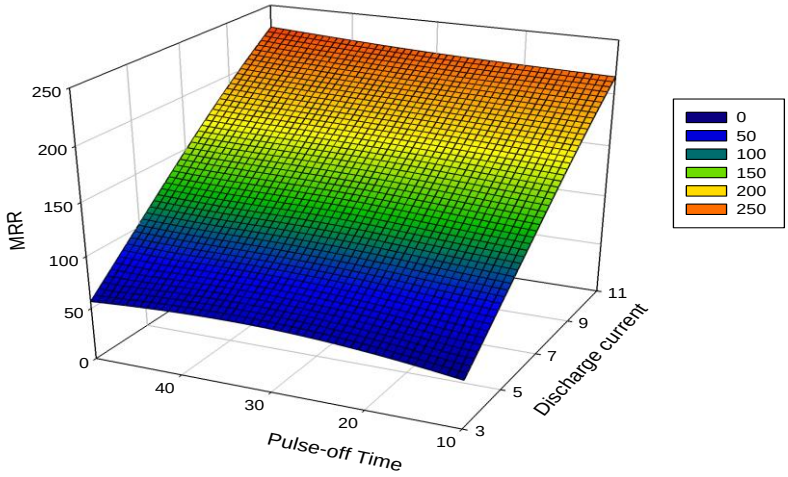

(c)

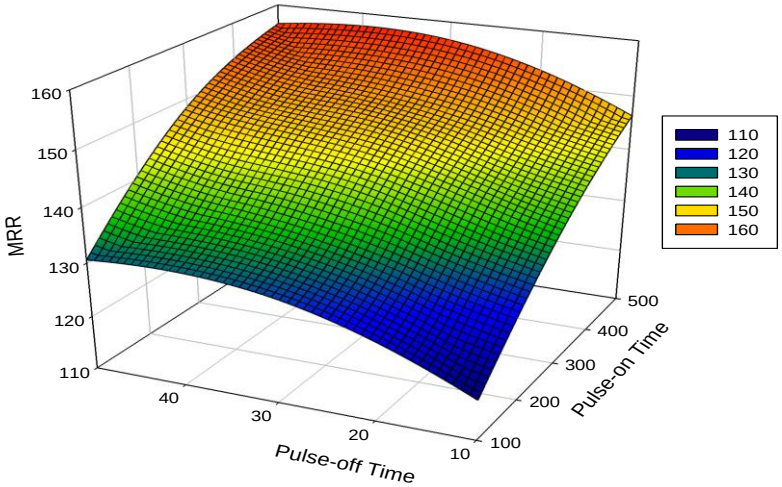

Figure 3.27 Response Surface for MRR of Cu-TiC tool

The effect of variation of MRR with respect to discharge current can be seen in figure 3.27 (a). MRR increases with discharge current because of increment of both depth and diameter of craters along with the discharge energy which results in the improvement of melting rate and evaporation. It can be estimate from figure 3.28 that MRR is more in Cu-TiC as compared to the copper tool. This is because of the involvement of TiC material powder with the copper powder results in the high electrical conductivity and hardness of the tool. This leads to increase the number of craters over the workpiece which results in more material removal of workpiece.

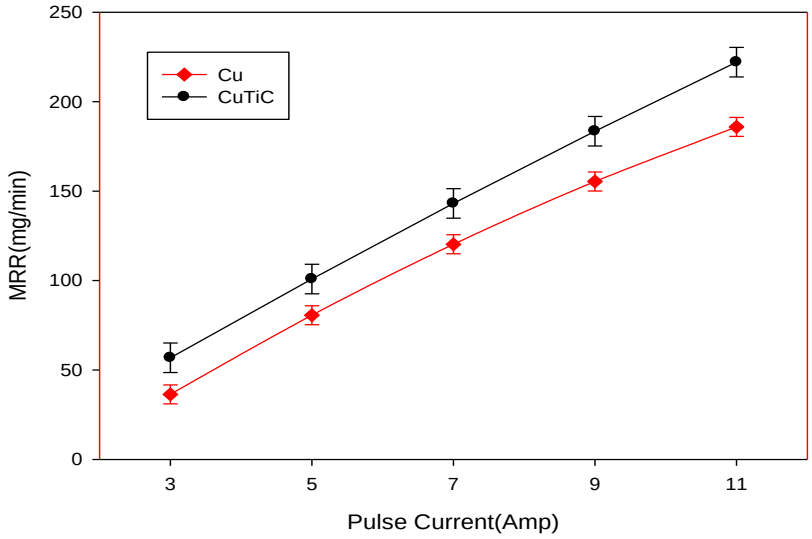

Figure 3.28 Variation of MRR with discharge current

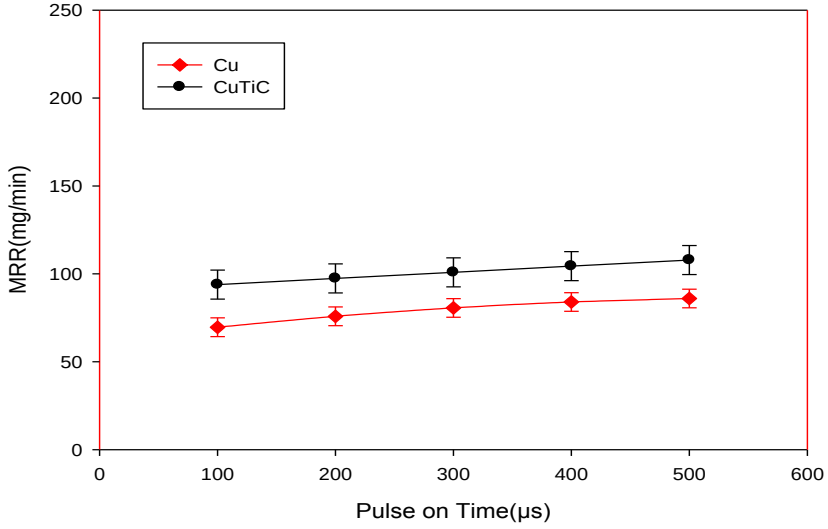

Figure 3.29 Variation of MRR with pulse-on time

The effect of variation of MRR with respect to pulse-on time can be seen in figure 3.27 (b). An increase in pulse on time causes increase in the discharge energy conducted into the machining gap within a single discharge. This increase of discharge energy causes the MRR to increase. It can be observed from figure 3.29 that MRR is more in Cu-TiC as compared to the simple copper tool.

The effect of pulse-off time on the estimation of MRR is introduced in figure 3.27 (c). It has been observed that an increment in pulse-off time slightly decreases the values of MRR. This is because of the time duration during which the electric discharge shuts off, the discharge column's diameter starts to decrease. During this time duration, the surface of the tool and workpiece starts cooling which stops wearing of tool. Further it can be seen from the figure 3.30 that MRR in Cu-TiC tool machining process is lesser when contrasted with Cu tool machining process.

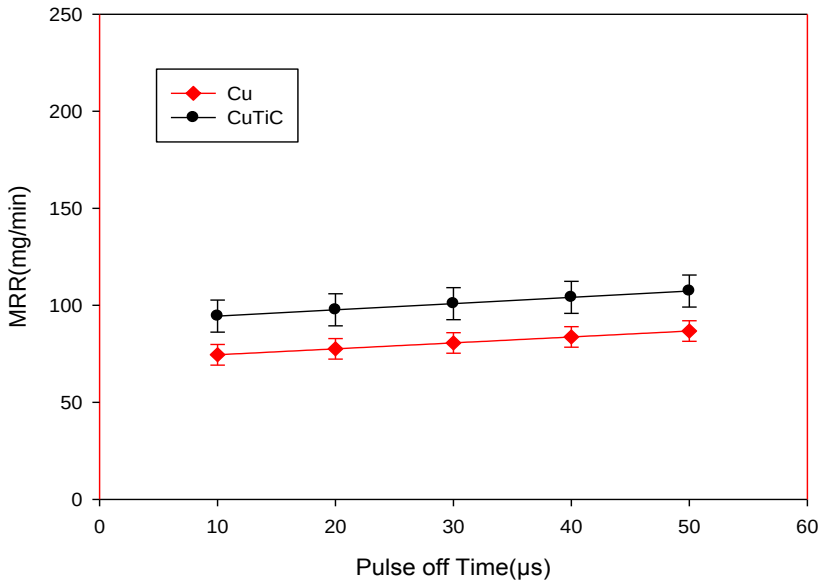

Figure 3.30 Variation of MRR with pulse-off time

Figure 3.31 and figure 3.32 represent main effects plots of SR where five points are taken which is obtained from the experiment data. It can be observed that as the discharge current increases, the SR increases linearly. For the case of pulse duration, as the pulse-on time increases, the SR increases slightly and same trend is followed by pulse-off time in case of Cu-TiC tool machining but in case of Cu tool machining, for the increment of pulse duration, SR increases slightly upto certain limit then starts to decrease.

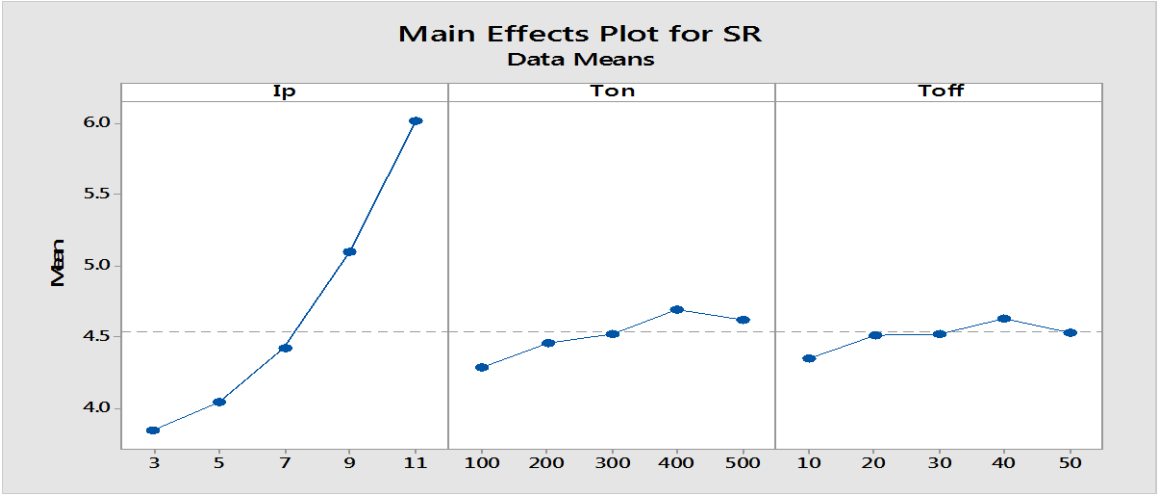

Figure 3.31 Main effects plot for SR of EDM by Cu tool

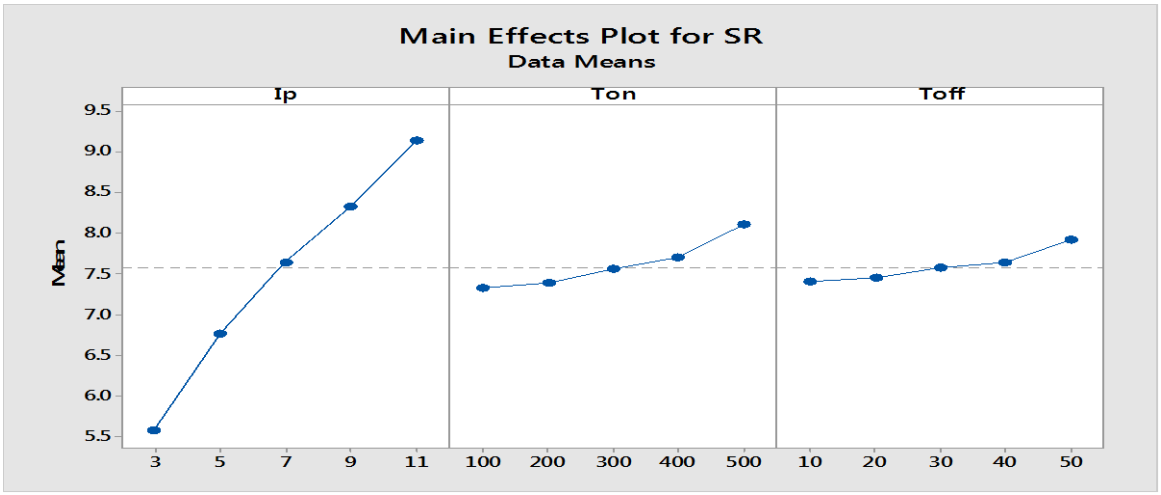

Figure 3.32 Main effects plot for SR of EDM by Cu-TiC tool

(a)

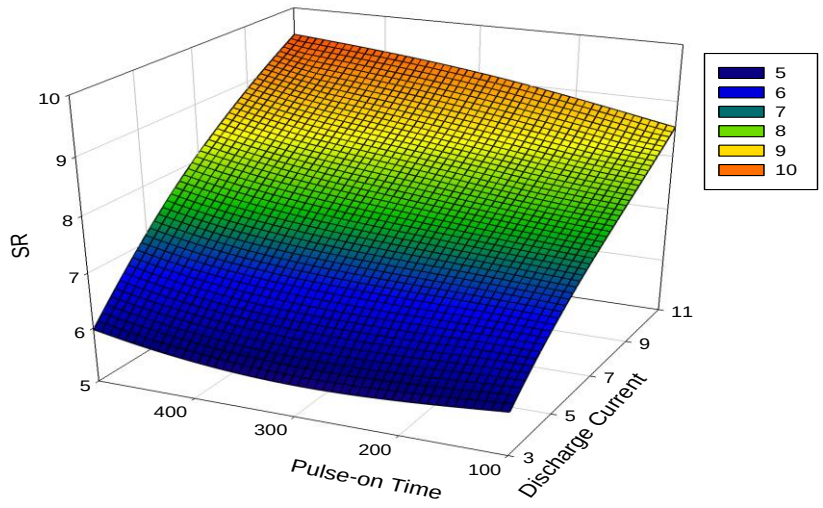

(b)

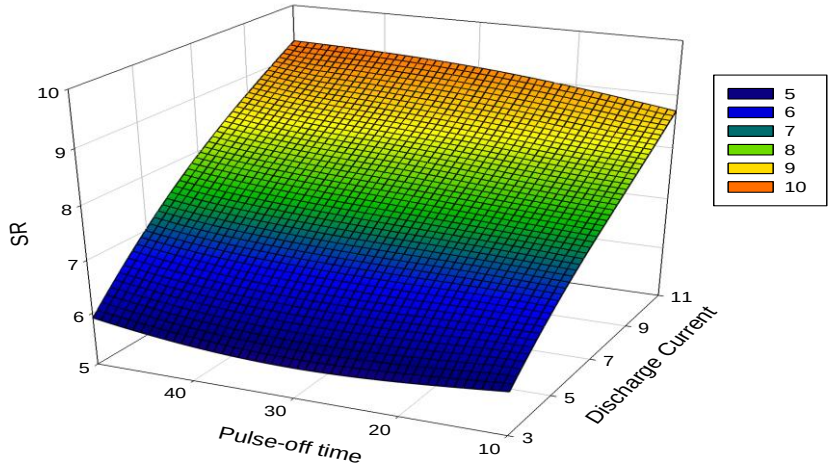

Figure 3.33 Response Surface for SR of Cu-TiC tool

The effect of variation of SR with respect to pulse-on time and discharge current which can be seen in figure 3.33(a). This plotted graph explore that SR increases with discharge current because of increasing of impulse force and discharge energy density leads to the generation of larger and deeper craters which results in increasing of SR. The graph also shows very minutely increment of SR with increase in pulse-on time. It can be estimated from figure 3.34 that SR is more in Cu-TiC as compared to the simple copper tool.

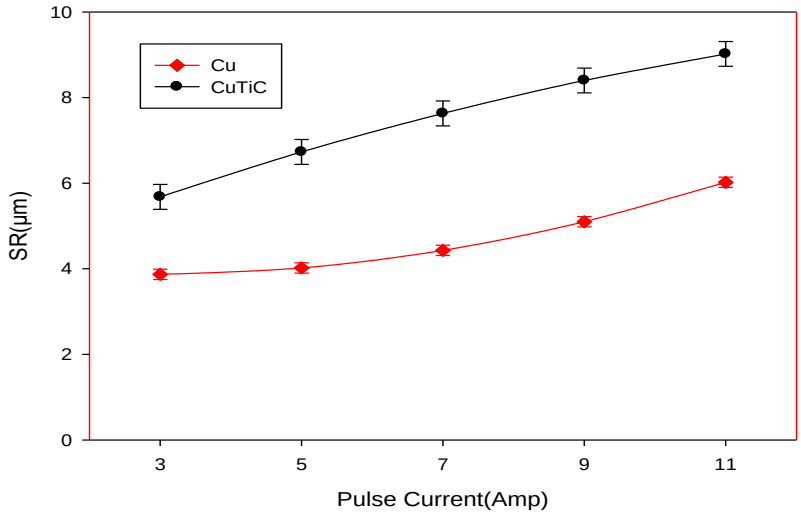

Figure 3.34 Variation of SR with discharge current

It can be further examined by the figure 3.33(b) that increase in discharge current with the increase in pulse-on time leads to increase in SR. This is because of plasma channel expansion by the increment of pulse-on time [45] which reduces both impulsive force and energy density, results in incomplete removing of melted debris and recast layer is formed

which results in increasing of SR. It can be estimate from figure 3.35 that SR is more in Cu-TiC as compared to the simple copper tool.

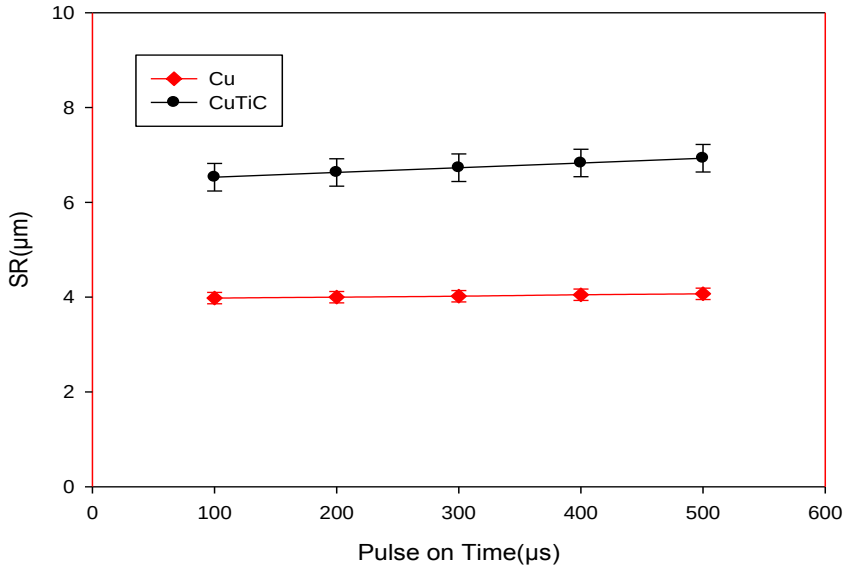

Figure 3.35 Variation of SR with pulse-on time

Figure 3.36 and figure 3.37 represent main effects plots of OOR where five points are taken which is obtained from the experiment data. It can be observed that as the discharge current increases, the OOR increases linearly. For the case of pulse duration, as the pulse-on time increases, the OOR decreases slightly and same trend is followed by pulse-off time in case of both tool but it become moderate in case of Cu tool machining at certain limit.

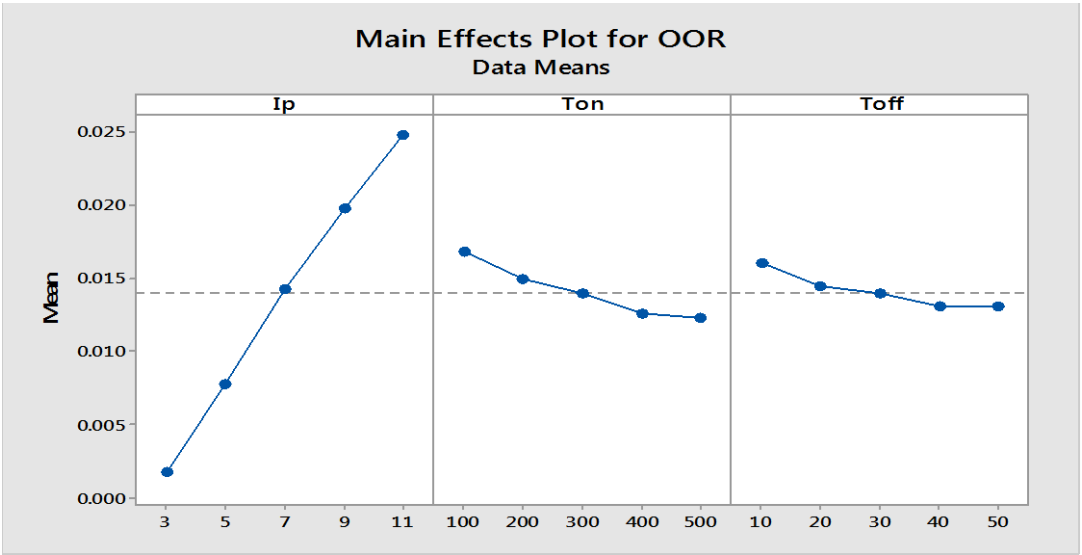

Figure 3.36 Main effects plot for OOR of EDM by Cu tool

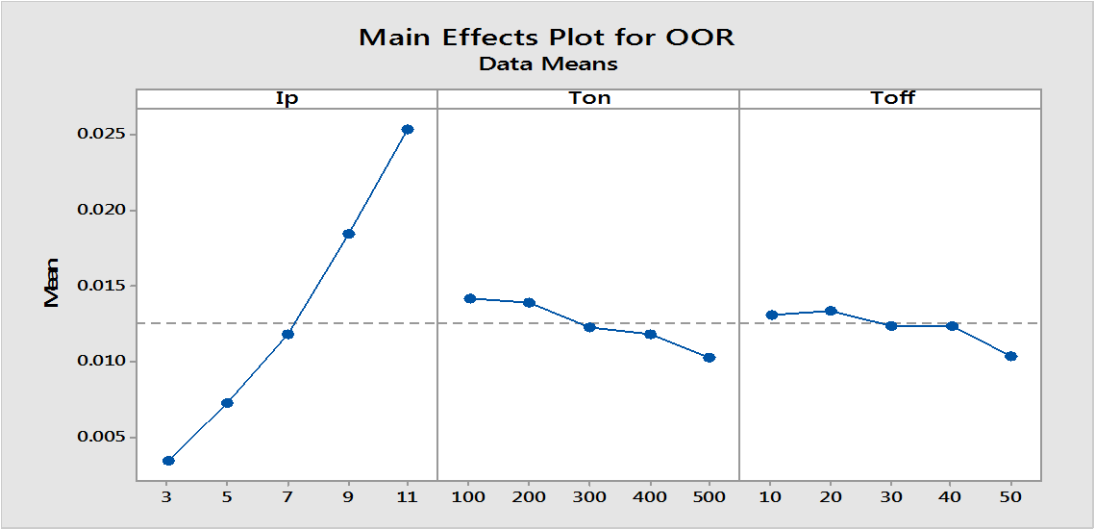

Figure 3.37 Main effects plot for OOR of EDM by Cu-TiC tool

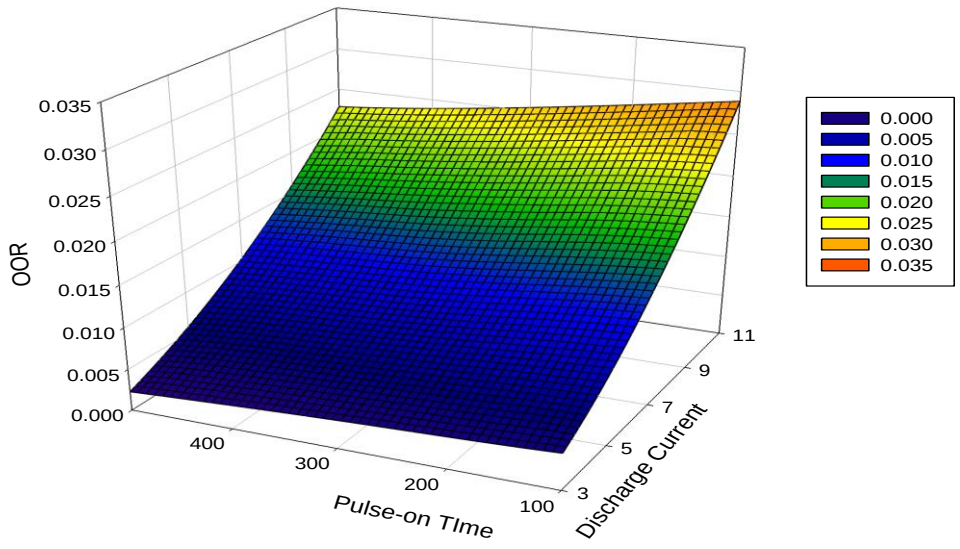

Figure 3.38: Response Surface for OOR of Cu-TiC tool

The effect of variation of OOR with respect to pulse-on time and discharge current which can be seen in figure 3.38. This plotted graph explore that OOR increases with discharge current because of increasing of impulse force and discharge energy density leads to the generation of larger and deeper craters which results in distortion of shape of tool tip [41]. The graph also shows very minutely decrement of OOR with increase in pulse-on time. It can be estimated from figure 3.39 and figure 3.40 that OOR is more in Cu-TiC as compared to the simple copper tool.

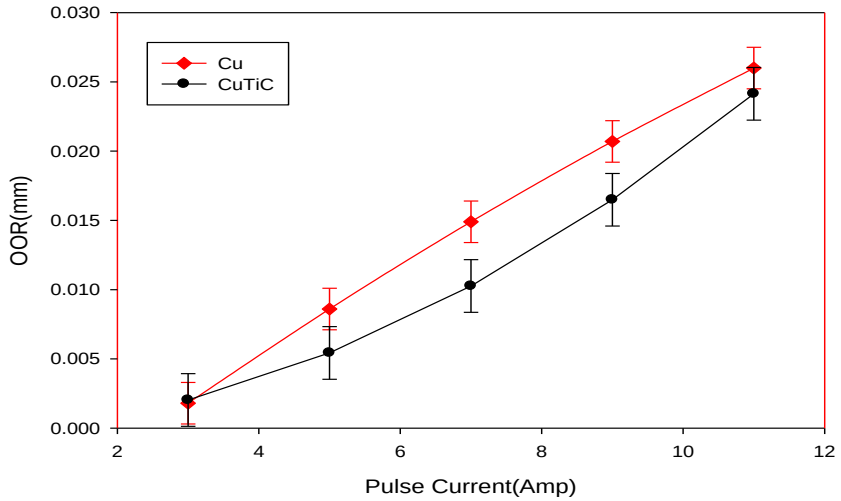

Figure 3.39: Variation of OOR with discharge current

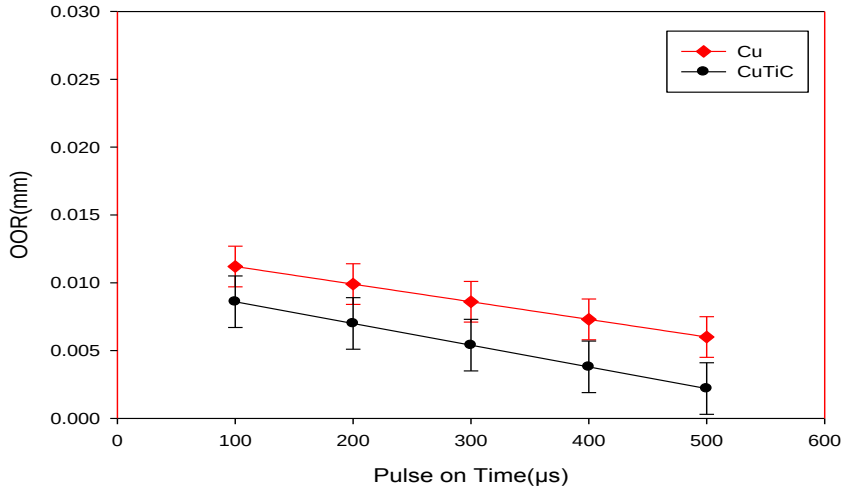

Figure 3.40 Variation of OOR with pulse-on time

3.8 CONFIRMATION EXPERIMENTS

In accordance with the experimental error, the evaluated parameters and hence the evaluated responses leads to uncertainty. The calculation of confidence interval estimated the precision of responses i.e. $\pm\Delta Z$, where ΔZ is given by

$$\Delta Z = t_{\frac{\alpha}{2},DF}\sqrt{V_e} \tag{3.13}$$

Here, Z represented as responses, namely, TWR, MRR, SR and Out of roundness where t is denoted as a value of horizontal co-ordinate on t-distribution according to justified the degree of freedom (DOF), level of confidence interval as α (which is taken as 0.01) and variance in the predicted response error as V_e. The values of ΔTWR, $\Delta MRR, \Delta SR$ and ΔOOR for TWR,

MRR, SR and OOR models for Cu as electrode tool are calculated as 0.31 mg/min, 5.3 mg/min, 0.12 µm and 0.0015 mm respectively which can be seen in table of confirmation experiment as shown in 3.16 that developed models do prediction over the TWR, MRR, SR and OOR accurately within confidence level of 99%.

Table 3.16 Confirmation Experiments (Parameters other than table 3.6)

EXP. No.	Machining Parameters			TWR(mg/min)		MRR(mg/min)		SR(µm)		OOR(mm)	
	Ip (A)	Ton (µs)	Toff (µs)	Exp.	Predicted	Exp.	Predicted	Exp.	Predicted	Exp.	Predicted
1	4	150	15	2.93	3.08 ± 0.31	46.32	48.27 ± 5.3	3.85	3.93 ± 0.12	0.01	0.0092 ± 0.0015
2	6	250	25	5.36	5.23 ± 0.31	99.56	96.79 ± 5.3	4.07	4.15 ± 0.12	0.014	0.0128 ± 0.0015
3	8	350	35	7.04	6.85 ± 0.31	148.9	143.29 ± 5.3	4.91	4.83 ± 0.12	0.018	0.0172 ± 0.0015
4	10	450	45	7.75	7.93 ± 0.31	184.3	187.76 ± 5.3	6.09	5.99 ± 0.12	0.022	0.0225 ± 0.0015
5	6	350	35	4.71	4.95 ± 0.31	100.3	104.93 ± 5.3	4.15	4.24 ± 0.12	0.011	0.0109 ± 0.0015
6	8	250	25	7.51	7.39 ± 0.31	137.5	133.18 ± 5.3	4.56	4.63 ± 0.12	0.02	0.0186 ± 0.0015
7	10	350	45	8.64	8.57 ± 0.31	178.9	180.14 ± 5.3	5.87	5.78 ± 0.12	0.022	0.0228 ± 0.0015

The values of $\Delta TWR,\ \Delta MRR, \Delta SR$ and ΔOOR for TWR, MRR, SR and OOR models for Cu-TiC as electrode tool are calculated as 0.27 mg/min, 8.26 mg/min, 0.29 µm and 0.0019 mm respectively which can be seen in table of confirmation experiment as shown in 3.17 that developed models do prediction over the TWR, MRR, SR and OOR accurately within confidence level of 99%.

Table 3.17 Confirmation Experiments (Parameters other than table 3.11)

EXP No.	Machining Parameters			TWR(mg/min)		MRR(mg/min)		SR(µm)		OOR(mm)	
	Ip (A)	Ton (µs)	Toff (µs)	Exp	Predicted	Exp.	Predicted	Exp.	Predicted	Exp.	Predicted
1	4	150	15	2.61	2.75 ± 0.27	77.65	71.58 ± 8.26	6.15	5.96 ± 0.29	0.0081	0.0066 ± 0.0019
2	6	250	25	4.31	4.19 ± 0.27	114.76	118.03 ± 8.26	6.92	7.07 ± 0.29	0.0076	0.0087 ± 0.0019
3	8	350	35	5.73	5.58 ± 0.27	164.53	169.43 ± 8.26	8.03	8.19 ± 0.29	0.0107	0.0118 ± 0.0019
4	10	450	45	6.67	6.89 ± 0.27	231.43	225.76 ± 8.26	9.57	9.32 ± 0.29	0.0168	0.0153 ± 0.0019
5	6	350	35	3.83	3.94 ± 0.27	131.78	126.43 ± 8.26	7.57	7.32 ± 0.29	0.0078	0.0065 ± 0.0019
6	8	250	25	6.11	5.91 ± 0.27	151.67	157.66 ± 8.26	7.53	7.87 ± 0.29	0.0131	0.0146 ± 0.0019
7	10	350	45	7.27	7.07 ± 0.27	211.09	213.83 ± 8.26	9.27	9.04 ± 0.29	0.0196	0.0179 ± 0.0019

3.9 OPTIMIZATION OF EDM PROCESS FOR RESPONSES

The utility of trials of EDM experiments is increased by the optimizing these response parameters with different electrodes used upto some better extent. The attempt has been made for the estimation of cutting conditions of optimum machining to get lowest TWR, high MRR and the last but not the least is the better quality surface of the electrodes within constraints. For finding of optimum levels of these machining parameters, the non-linear minimization method is utilized. MATLAB 2015a was used for performing the optimization which can be

handle at large scale. Hence, the comparison has been shown here for each machining parameter between Cu & Cu-TiC tool machining.

3.9.1 Minimization of TWR

The problem of minimization of TWR is evaluated and is shown below:-

$$Minimize(TWR)$$

$$subjected\ to$$

$$3(A) \leq I_p \leq 11(A)$$

$$100(\mu s) \leq T_{on} \leq 500(\mu s)$$

$$10(\mu s) \leq T_{off} \leq 50(\mu s)$$

The minimum value of TWR which is given by process parameters, are shown in table 3.18. Machining experiment was done at particular set of process parameters which is optimum and TWR is evaluated. It was observed that the optimum value was lying in the range of prediction.

Table 3.18 Optimum process parameters for minimizing TWR

Tools	I_p	T_{on}	T_{off}	Calculated TWR at optimum parameters (%)	Experimental TWR at optimum parameters (%)
Cu	3	100	10	1.80 ± 0.31	1.92
Cu-TiC	3	500	10	1.29 ± 0.27	1.12

3.9.2 Maximization of MRR

The problem of maximization of MRR is evaluated and is shown below:-

$$Maximize(MRR)$$

$$subjected\ to$$

$$3(A) \leq I_p \leq 11(A)$$

$$100(\mu s) \leq T_{on} \leq 500(\mu s)$$

$$10(\mu s) \leq T_{off} \leq 50(\mu s)$$

The maximum value of MRR which is given by process parameters, are shown in table 3.19. Machining experiment was done at particular set of process parameters which is optimum and MRR is evaluated. It was observed that the optimum value was lying in the range of prediction.

Table 3.19 Optimum process parameters for maximizing MRR

Tools	I_p	T_{on}	T_{off}	Calculated MRR at optimum parameters (%)	Experimental MRR at optimum parameters (%)
Cu	11	500	50	209.23 ± 5.30	212.23
Cu-TiC	11	500	50	255.77 ± 8.26	253.44

3.9.3 Minimization of SR

The problem of minimization of SR is evaluated and is shown below:-

$$Minimize(SR)$$

$$subjected\ to$$

$$3(A) \leq I_p \leq 11(A)$$

$$100(\mu s) \leq T_{on} \leq 500(\mu s)$$

$$10(\mu s) \leq T_{off} \leq 50(\mu s)$$

The minimum value of SR which is given by process parameters, are shown in table 3.20. Machining experiment was done at particular set of process parameters which is optimum and SR is evaluated. It was observed that the optimum value was lying in the range of prediction.

Table 3.20 Optimum process parameters for minimizing SR

Tools	I_p	T_{on}	T_{off}	Calculated SR at optimum parameters (%)	Experimental SR at optimum parameters (%)
Cu	3	500	50	3.74 ± 0.12	3.67
Cu-TiC	3	100	10	5.40 ± 0.29	5.57

3.9.4 Minimization of OOR

The problem of minimization of OOR is evaluated and is shown below:-

$$Minimize(OOR)$$

$$subjected\ to$$

$$3(A) \leq I_p \leq 11(A)$$

$$100(\mu s) \leq T_{on} \leq 500(\mu s)$$

$$10(\mu s) \leq T_{off} \leq 50(\mu s)$$

The minimum value of OOR which is given by process parameters, are shown in table 3.21. Machining experiment was done at particular set of process parameters which is optimum and OOR is evaluated. It was observed that the optimum value was lying in the range of prediction.

Table 3.21 Optimum process parameters for minimizing OOR

Tools	I_p	T_{on}	T_{off}	Calculated OOR at optimum parameters (%)	Experimental OOR at optimum parameters (%)
Cu	3	300	30	0.0018 ± 0.0015	0.0029
Cu-TiC	3	300	30	0.0020 ± 0.0019	0.0014

3.10 COMPARISON OF EDM PROCESS BETWEEN COPPER AND COPPER TITANIUM CARBIDE TOOL

Figure 3.41 shows the TWR for both Cu and Cu-TiC tool comparison in EDM process on H13 tool steel. TWR is found to be lower for Cu-TiC tool as compared to Cu tool

in EDM process. Due to the much hardness of the particle of Titanium carbide and their highly bonding capability made the tool harder after combining with pure copper powder. This titanium carbide powder mixing has been done with pure copper powder due to making it more conducting because copper is highly conducting material. As the tool become harder, it leads to lowering of its TWR along with the higher of MRR of workpiece material. It was observed that in case of Cu-TiC tool, the TWR reduced upto 20% as compared to machine with Cu tool.

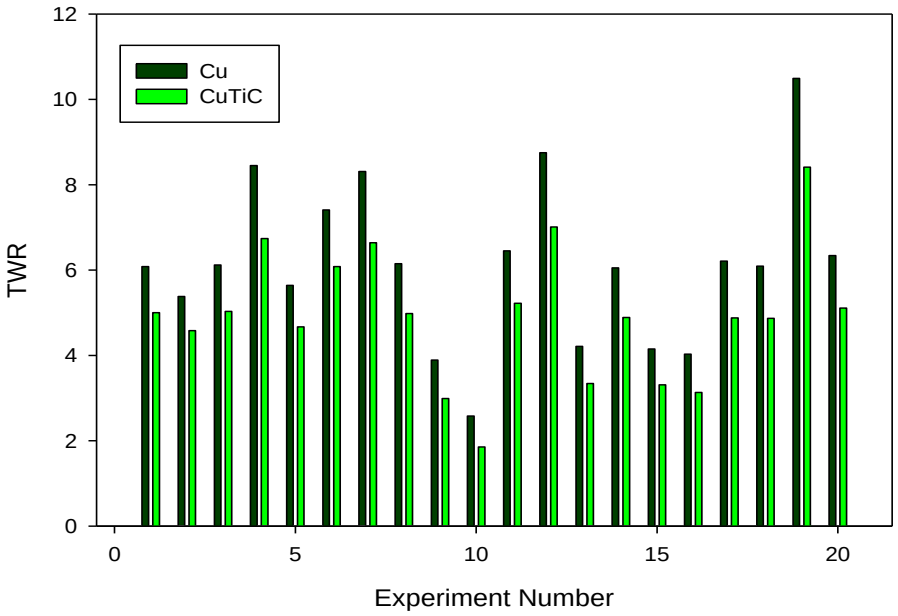

Figure 3.41 Comparison of TWR for Cu & Cu-TiC tool in EDM process

The effect on MRR for Cu & Cu-TiC tool used in EDM process has been shown in figure 3.42. The MRR is found to be higher in EDM process in which Cu-TiC tool is used as tool as compared to EDM process in which Cu is used as tool. This increment in MRR is because of high electrical conductivity of Cu-TiC tool which leads to higher of ionised zone temperature. Due to this high temperature, high heating effect generated which increase the depth of crater, resulting in more material removal of workpiece which increased upto 22% as compared to machine by Cu tool.

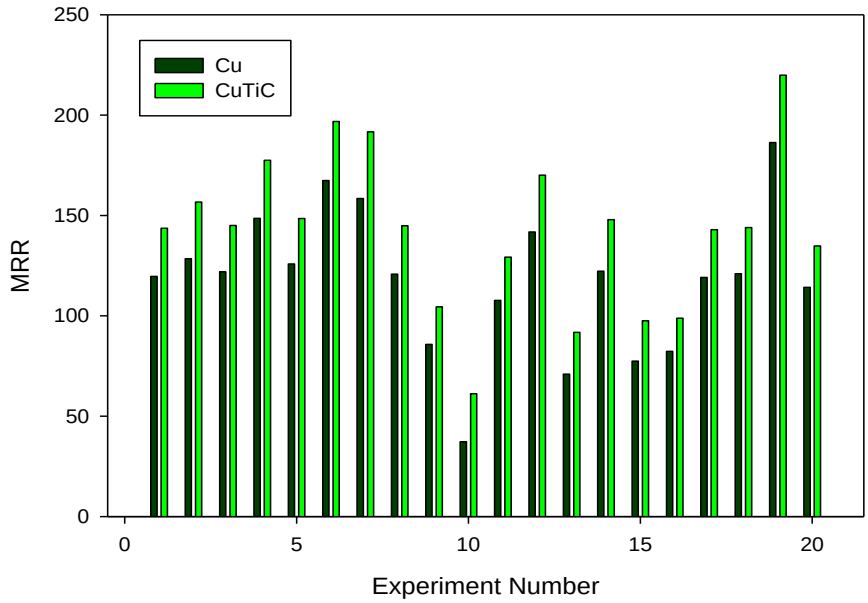

Figure 3.42 Comparison of MRR for Cu & Cu-TiC tool in EDM process

The effect on SR comparison for Cu & Cu-TiC tool used in EDM process has been shown in figure 3.43. The SR is found to be lower in EDM process in which Cu-TiC is used as tool as compared to EDM process where Cu is used as tool. The higher surface roughness of the workpiece machined by Cu-TiC tool is observed to be higher because ceramic tool made by the composition of pure copper powder and titanium carbide powder in appropriate proportion made the tool more harder and higher electrically conductivity [42]. That leads to high discharge energy in plasma channel, resulting in bigger craters on the surface of workpiece which increases the surface roughness. SR for Cu-TiC tool machining increased upto 42% as compared to Cu tool machining.

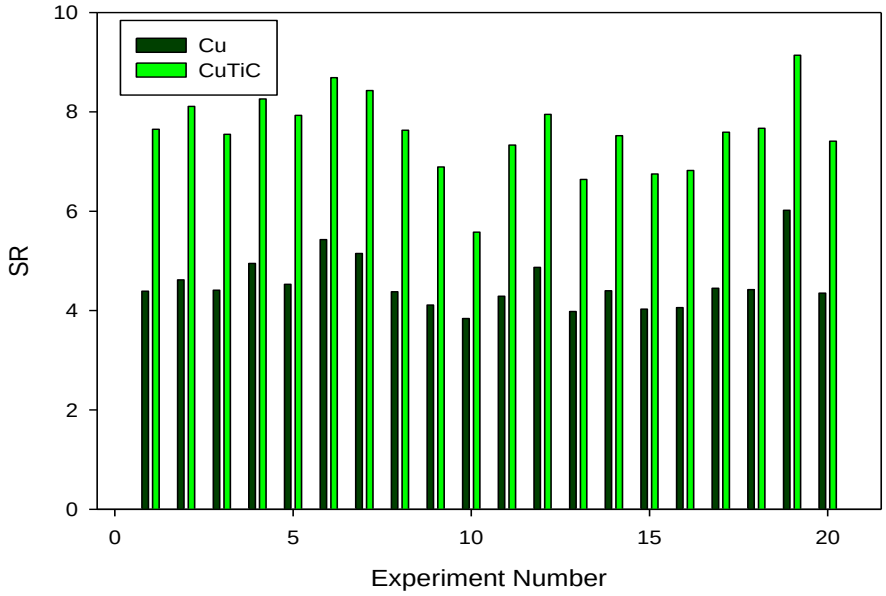

Figure 3.43 Comparison of SR for Cu & Cu-TiC tool in EDM process

The out of roundness measurement is done to study the shape of tool. The effect on OOR comparison for Cu & Cu-TiC tool used in EDM process has been shown in figure 3.44. The OOR is found to be lower in EDM process in which Cu-TiC is used as tool as compared to EDM process where Cu is used as tool. The distortion is found to be less in EDM process in which Cu-TiC is used as tool to machining process. This is because of the much tool hardness of Ceramic of Cu-TiC tool. Due to its high hardness, less tool wear occurs that is why the less distortion the tool shape occurs. OOR in case of Cu-TiC tool is reduced upto 16% as compared to Cu tool.

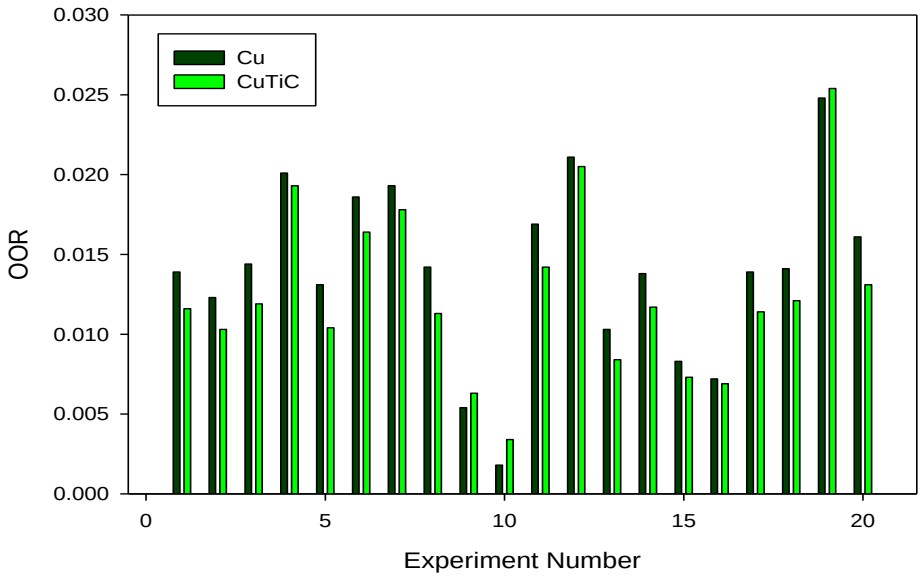

Figure 3.44 Comparison of OOR for Cu & Cu-TiC tool in EDM process

3.11 CONCLUSIONS

In this research work, EDM has been fortunately functioned on H13 tool steel workpiece material by Copper as tool. In previous section, the statistical models have been developed for the prediction of TWR, MRR, SR and OOR by inter-relating the decided input parameters, namely pulse-on time, pulse-off time and discharge current. In EDM process, identification of significant parameters has been done and for checking its adequacy of model, ANOVA was used.

The results represent that second order of TWR developed is significant. It has been examined that pulse-on time, pulse-off time and discharge current significantly affects TWR. It has been noticed that TWR increases with increases with increase in discharge current. It has also examined that TWR decreases with increase in pulse-on time and pulse-off time. Similarly, the second order model of MRR developed of MRR is statistically significant. It

has been examined that pulse-on time, pulse-off time and discharge current consequently affected the MRR. It was noticed that on increment of discharge current, MRR increases. Pulse duration also affected the MRR as on increment of pulse-on time and pulse-off time, the MRR increases slightly. The second order model of SR developed is statistically significant. It has been found that pulse-on time, pulse-off time and discharge current consequently affected the SR. It has been examined that increase in discharge current leads to increase SR. It has also been noticed that SR increases slightly upto certain limit then start to decrease as the pulse-on time and pulse-off time increase separately [40]. The second order of OOR developed is statistically significant. It has been examined that pulse-on time, pulse-off time and discharge current significantly affects OOR. It has been noticed that OOR increases with increases with increase in discharge current. It has also examined that OOR decreases with increase in pulse-on time and pulse-off time.

Further, in this research work, EDM has been fortunately functioned on H13 tool steel workpiece material by ceramic of Copper Titanium carbide as tool. In previous section, the statistical models have been developed for the prediction of TWR, MRR, SR and OOR by inter-relating the decided input parameters, namely pulse-on time, pulse-off time and discharge current. In EDM process, identification of significant parameters has been done and for checking its adequacy of model, ANOVA was used.

At last, the confirmation experiments were performed at various other values of decided parameters for showing the models which was developed for both Cu & Cu-TiC tool electrode for machining in EDM process can probably predict TWR, MRR, SR and OOR values within confidence interval of 99%. The most favourable process parameters have been examined for obtaining minimum TWR, minimum SR, maximum MRR and minimum OOR.

CHAPTER 4
SURFACE MORPHOLOGY

4.1 INTRODUCTION

The parts have to be machined by electrical discharge machining for getting the better surface finish and high dimensional accuracy. Since EDM had been created, much hypothetical and test works have been done for distinguishing the mechanism associated with material expulsion. It presently stands amongst the most valuable methods which are utilized for die production with exactness and accuracy. In spite of quick heating and cooling impacts actuated by the machining process, a thermally influenced layer creates on the part surface. The layer's structure is very not the same as the base material, and despite the fact that it is advantageous regarding the improved problem of abrasion and erosion protection. The deformities generated like induced stresses, cracks, voids and so forth cause a general distortion of the part's mechanical properties [46]. Among the surface deformities, cracks are the most noteworthy since it prompts to decrease the material protection from corrosion and fatigue, particularly under the condition of tensile loading. The extraordinary warmth created by each spark discharge brings about nearby extreme temperature gradient on the surface of a workpiece. On suspension of the discharge, the layer of surface cools rapidly and creates residual tensile stresses that are regularly adequate to deliver cracks in the machined surfaces [47].

The auxiliary changes of EDMed surfaces have been considered widely for various steels' grades and it has been demonstrated that the upper layer of the surface is an irregular or bumpy, non-etchable layer, frequently alluded to "white" layer [48]. This recast layer was formed by the liquid metal cementing after the discharge procedure. Promptly underneath the white layer is a middle layer where the warmth isn't sufficiently high to cause dissolving yet is adequately high to actuate miniaturized change in the material.

In this chapter, experiments have been performed to study the surface morphology of the work-piece and the material expulsion during machining with copper and copper-titanium carbide as tool. The degree of conceivable surface and subsurface harms due to EDM process by Cu and Cu-TiC as tool has been observed in Scanning Electron Microscopy (SEM). The perceptions of surface and subsurface harms and additionally EDX investigation of machined surface have been performed to anticipate material evacuation mechanisms.

4.2 EXPERIMENTATION

The experiments have been performed over "ELECTRONICA VCP 20" die-sinking EDM machine by Cu & Cu-TiC as an electrode tool. The electrically conductive H13 tool steel has been chosen as the work-piece. The composition percentage has been displayed in table 3.1. The work-piece's hardness has been determined as 235 HV. The investigation of work-piece has been performed at both low current limits and high current limits EDM conditions in light of the survey of past writing [49] as displayed in table 4.1. Copper has been picked as the electrode tool material in view of its lower thermal and electrical resistance. The diameter of tool tip was chosen as 8 mm. The samples of 12 mm diameter and 10 mm thickness were utilized as a part of the present examination. In every one of the trials, kerosene oil was utilized as dielectric fluid medium. A Scanning Electron Microscope (SEM) JBM-6510LV has been utilized for watching surface morphology and degree of conceivable surface damage. The samples have been cleaned with acetone chemical before performing SEM observation. EDX of machined surfaces was likewise performed. The machined surfaces' roughness has been estimated utilizing surface measuring machine (Mitutoyo SJ-400, Japan). A cut-off length of 0.8 mm along with transverse length of 4 mm has been chosen for measuring the surface roughness measurements of each experiment. The centre line normal estimation of the surface harshness (R_a) is the most broadly utilized SR parameter in industry was chosen in this examination [39].

Table 4.1 Ranges of process parameters

FACTORS	UNITS	RANGE
Discharge Current (Ip)	A	3,5,7,9,11
Pulse on time (Ton)	µs	100, 200, 300, 400, 500
Pulse off Time (Toff)	µs	10, 20, 30, 40, 50

A clamped work-pieces system has been utilized to investigate the recast layer and subsurface damage [50]. In this technique, two samples have been fixed at same measurements and one surface of every sample has been cleaned. The cleaned surfaces have been consequently clamped up face-to-face with appropriate force. Every one of the holes have been penetrated utilizing Cu & Cu-TiC tool electrode at the interface of two cleaned surfaces of workpiece as appeared in the figure 4.1. The workpiece have been isolated subsequent to machining and cleaned utilizing acetone chemical. The subsurface of the machined holes (on 12 mm diameter surface) have then been analyzed utilizing SEM.

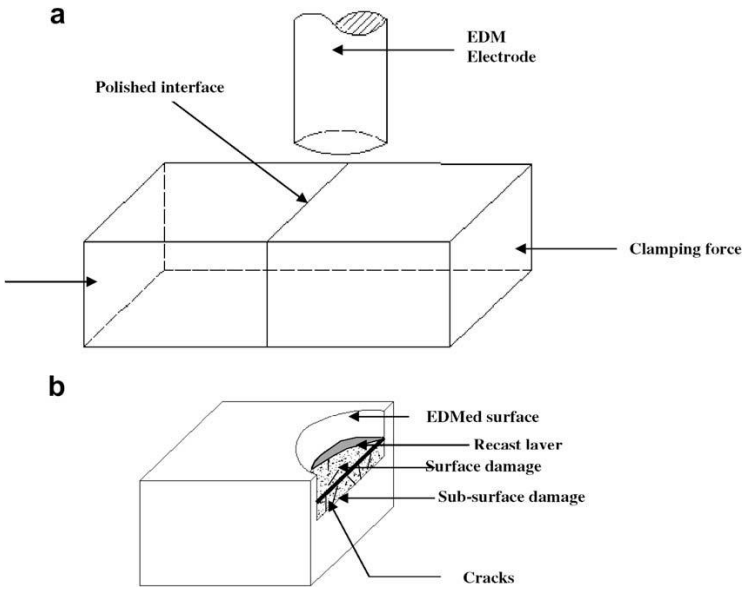

Figure 4.1 Schematic diagram of the procedure used in preparation of SEM samples to study subsurface damage (a) clamped work pieces and (b) Electro-discharge machined half-hole with recast layer and subsurface damage. [50]

4.3 RESULTS AND DISCUSSION

4.3.1 Surface Roughness and Morphology of Machined Surface

Amid the EDM procedure, because of bombardment of exceptionally high energetic electrons on the surface of the electrode tool, the machining portion accomplishes high temperature of around 10,000°C. At this high temperature, material at located portion melts out and vaporizes leaving a hole at surface of the workpiece. Be that as it may, little volume of the liquid material cools quickly under the medium of the dielectric liquid. The quick heating and cooling impact produces a profoundly extraordinary surface morphology on electrical discharge machined surfaces. Ramasawmy and Blunt [51] announced that the two EDM parameters which have the most conspicuous impact on EDM surface principle of steel are pulse-on time, pulse-off time and discharge current. Comparable perceptions have been accounted for by Puri and Bhattacharyya [52]. The variety of SR with discharge current, pulse-on time, and pulse-off time for Cu & Cu-TiC tool has been appeared in figure 4.2, figure 4.3 and figure 4.4. It can be seen from the figures that the SR increases with increment in discharge current and comparatively slightly SR increases with an increment in the pulse-on time and pulse-off time for both the procedures.

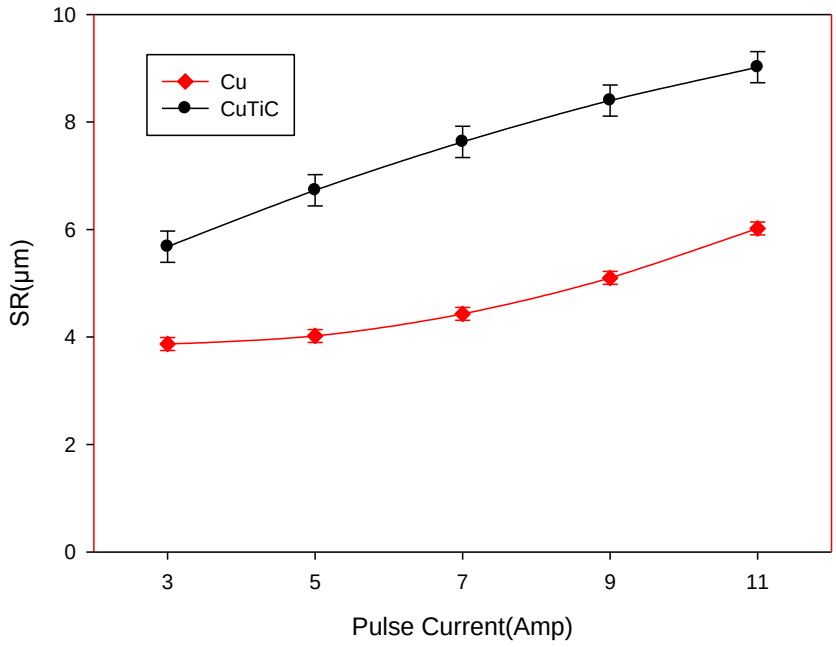

Figure 4.2 Variation of SR with discharge current for Cu & Cu-TiC tool EDM process

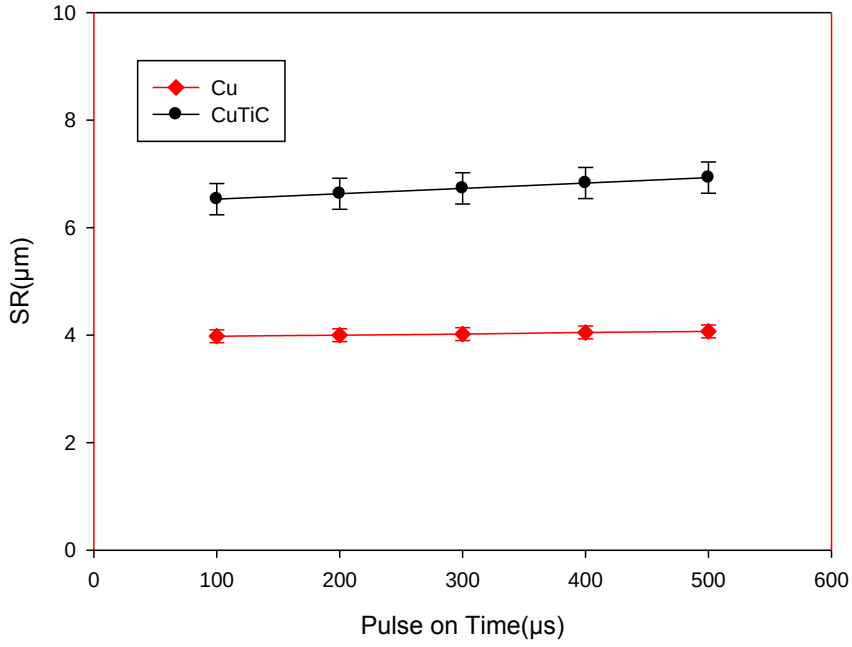

Figure 4.3 Variation of SR with pulse-on time for Cu & Cu-TiC tool EDM process

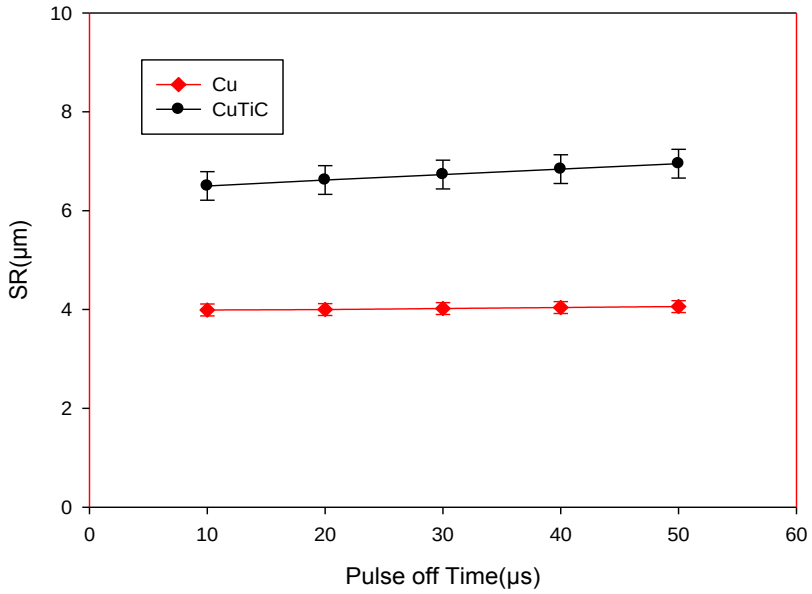

Figure 4.4 Variation of SR with pulse-off time for Cu & Cu-TiC tool EDM process

(a) (b)

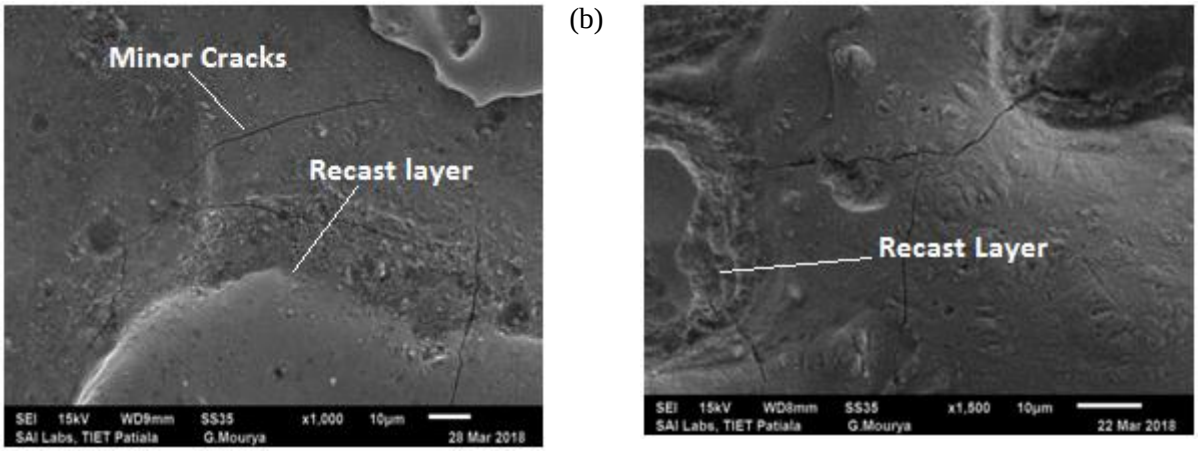

Figure 4.5 Surface characteristics of workpiece under discharge current of 3 A, pulse-on time of 300 μs, pulse-off time of 30 μs machined by tool (*a*) Cu (b) Cu-TiC

(a) (b)

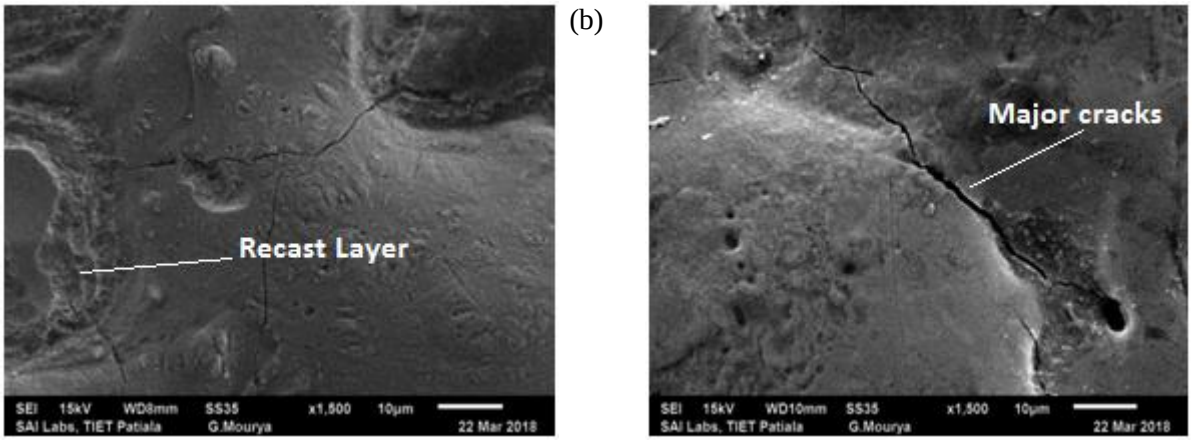

Figure 4.6 Surface characteristics of workpiece under discharge current of 7 A, pulse-on time of 300 μs, pulse-off time of 30 μs machined by tool (*a*) Cu (b) Cu-TiC

(a) (b)

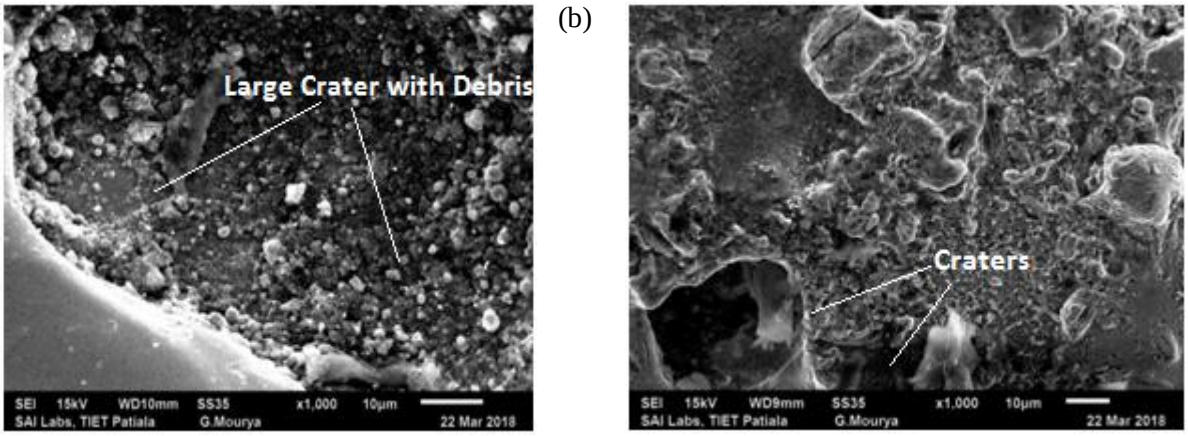

Figure 4.7 Surface characteristics of workpiece under discharge current of 11 A, pulse-on time of 300 μs, pulse-off time of 30 μs machined by tool (*a*) Cu (b) Cu-TiC

The SEM micrographs of the machined work-piece by EDM process using Cu & Cu-TiC as tool for low, mid and high value of discharge current at pulse-on time of 300 μs and pulse-off time of 30 μs are represented in figure 4.5, figure 4.6 and figure 4.7 respectively. It has been seen from the above-given figures that the surface of the machined workpiece is described by an irregular melded structure, shallow holes, globules of debris, and micro-pores. Micrographs likewise demonstrate the arrangement of recast layer on the surface of machined work-piece. The development of surface splits can be ascribed to the differentials of compression stress inside the white layer and when it exceeds the value of ultimate tensile stress of that particular material, leads to the crack formation [48]. It has been observed more from micrographs of the surface of the machined workpiece that the surface inconsistency increases with an increment in discharge current for both of the tool machining. This increment could be because of the increment in more deeper and bigger release craters which results in more damage of surface with the increment in discharge current. In advance of the higher input of power control related to increment in the discharge current leading to the more continuous splitting of dielectric, prompting more successive erosion of metal [53]. This thus offers to ascend to the higher density of globules gathered at the nearby region of machining zone along with the poor surface of a workpiece.

Further, SEM micrographs of the surface of the machined workpiece by EDM process by using Cu & Cu-TiC as tool material have been taken for a low, mid and high value of pulse-on time at a discharge current of 7 A and pulse-off time of 30 μs, represented as in figure 4.8, figure 4.9 and figure 4.10. It has been observed from the given figures that the increment of surface inconsistencies takes place with the increment in pulse-on time for both the tool machining. This might be because of the plasma channel expansion with the increment in pulse-on time [54], which has augmented the machined zone of workpiece and therefore

decreased the both impulsive force and energy density. Because of this, the melting part of debris isn't expelled totally and frames an obvious globule-like recast layer to debilitate the surface. These impacts have been seen to be more articulated as on increasing of pulse-on time. Apart from these irregularities, the micro pores and fine pit have been developed additionally credit to increment in SR.

(a) (b)

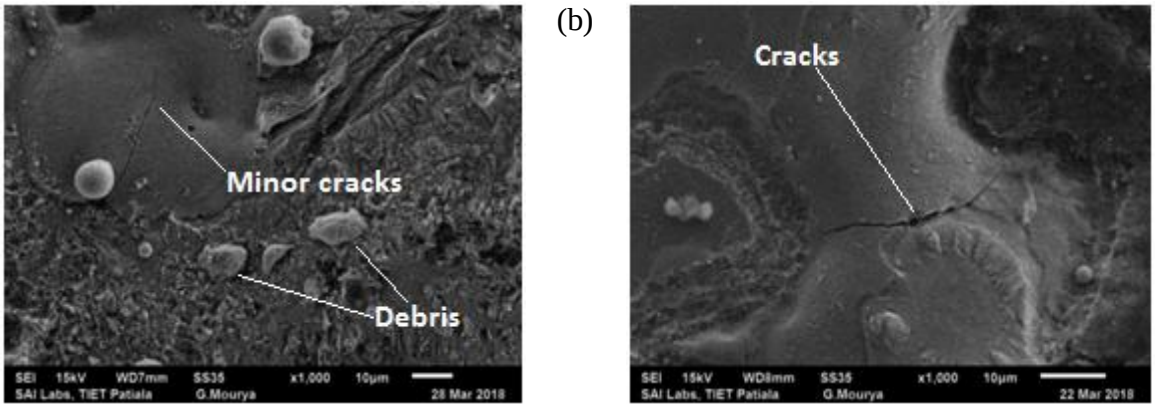

Figure 4.8 Surface characteristics of workpiece under discharge current of 7 A, pulse-on time of 100 μs, pulse-off time of 30 μs machined by tool (*a*) Cu (b) Cu-TiC

(a) (b)

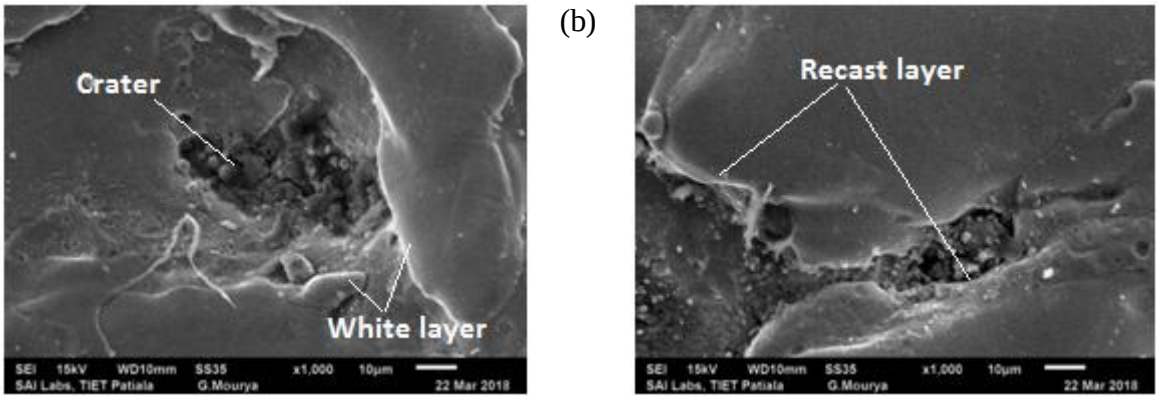

Figure 4.9 Surface characteristics of workpiece under discharge current of 7 A, pulse-on time of 300 μs, pulse-off time of 30 μs machined by tool (*a*) Cu (b) Cu-TiC

(a) (b)

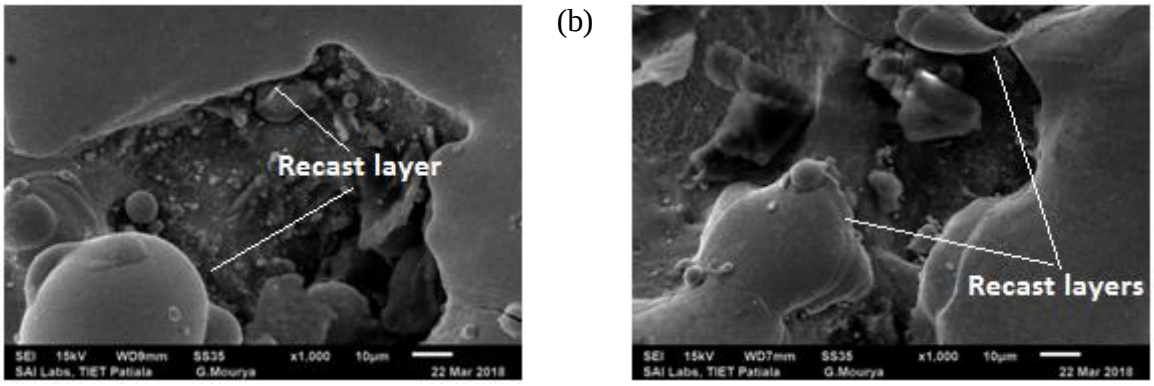

Figure 4.10 Surface characteristics of workpiece under discharge current of 7 A, pulse-on time of 500 μs, pulse-off time of 30 μs machined by tool (*a*) Cu (b) Cu-TiC

The above SEM micrographs have shown the effect of increasing of the pulse-on time while keeping the discharge current and pulse-off time constant at mid-value of the range. As discuss, on increasing of the pulse-on time, the MRR increases upto certain limit due to the expansion of discharge column, spark intensity increases and depth of the crater increases slightly. If it doesn't get enough time for the flushing out of evacuated molten material, the recast layer is formed over the surface of the workpiece material which results in the increment of SR.

Further, the subsurface harms and the formation of recast layer in EDM process by the Cu & Cu-TiC as tool electrode material have also been studied as shown in figure 4.11, figure 4.12 and figure 4.13 where pulse-off time has been varied while keeping pulse-on time and discharge current constant at mean value. The slightly increment in MRR have been observed with the increment of pulse-off time for both the tool machining. This may be because of the reason that as the pulse-off time increases; the eroded material gets time to flush away out from the surface of the workpiece. This due to the reason of de-ionisation of dielectric fluid easily occurs as it get more time when the machining process doesn't occur. As the pulse-off time is short, MRR is also less because very high arcing in short pulse-off time that is why debris remains over the surface of workpiece. Hence, the pulse-off time should be more so that better flushing of debris can take place which will lead to increase in MRR.

(a) (b)

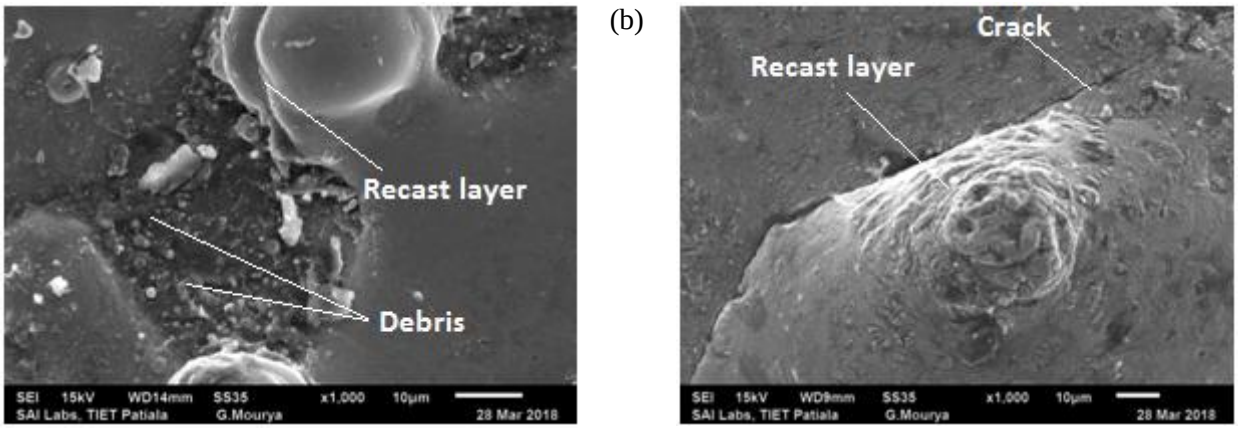

Figure 4.11 Surface characteristics of workpiece under discharge current of 7 A, pulse-on time of 300 µs, pulse-off time of 10 µs machined by tool (*a*) Cu (b) Cu-TiC

(a) (b)

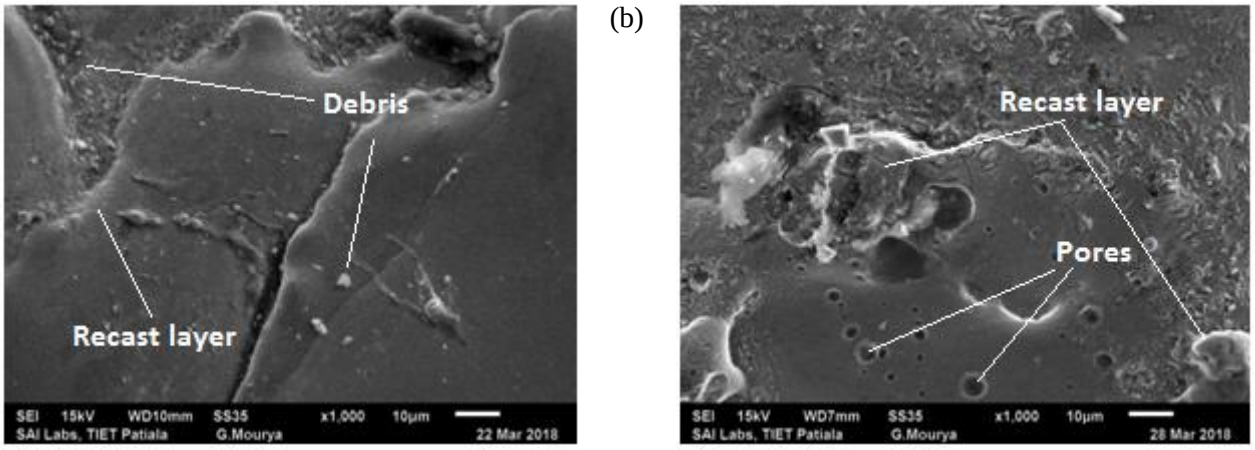

Figure 4.12 Surface characteristics of workpiece under discharge current of 7 A, pulse-on time of 300 μs, pulse-off time of 30 μs machined by tool (*a*) Cu (b) Cu-TiC

(a) (b)

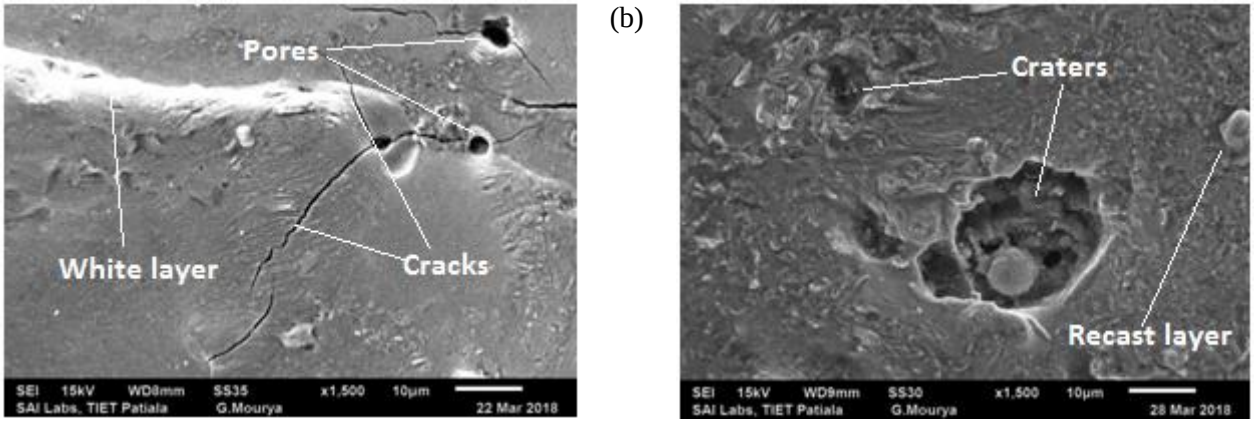

Figure 4.13 Surface characteristics of workpiece under discharge current of 7 A, pulse-on time of 300 μs, pulse-off time of 50 μs machined by tool (*a*) Cu (b) Cu-TiC

4.3.2 Material removal mechanism for EDM process

H13 tool steel has better property of electrical conductivity that is why it is effortlessly machinable by help of EDM. Roethel et al. [55] described that during EDM process; there can be the transferring of electrodes material after melting whether it is in solid, liquid or gaseous state. Fig. 4.14 represents the qualitative pattern of EDX of the layer of the surface of machined workpiece i.e. H13 tool steel which is machined by EDM with the copper an electrode tool. In this given figure, peaks have been referred to as their energy level shown in workpiece sample.

Table 4.2 Chemical composition (wt. %) of workpiece after machining by Cu tool

C	Si	V	Cr	Mo	O	Fe
30.69	0.66	0.65	3.68	0.86	5.32	Rest

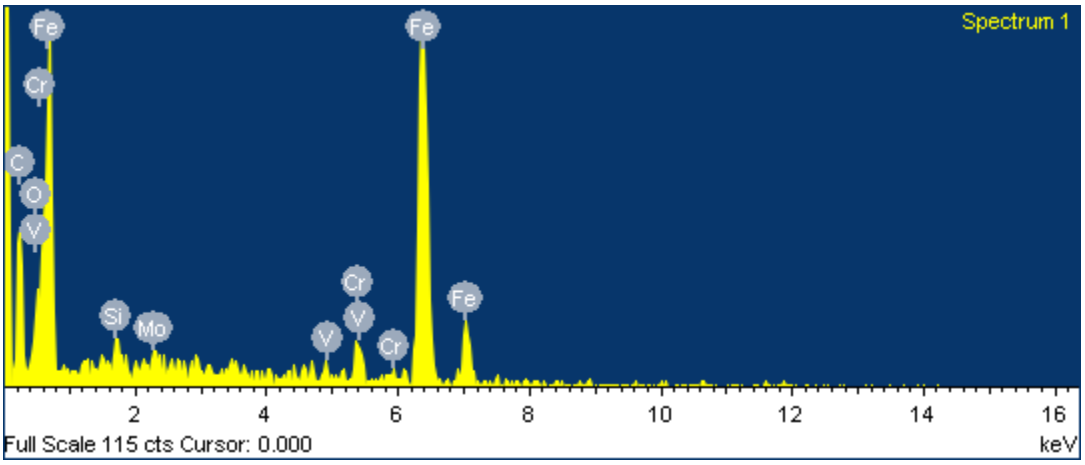

Figure 4.14 EDX showing relative intensities of different elements on surface of workpiece after EDM by Cu tool

The existence of Copper has not been seen in the recemented layer as demonstrated by EDX examination. This suggests that there is non-appearance of any noticeable electrode tool material exchange to the surface of workpiece amid the EDM process. An examination of the percentage contribution of a workpiece before machining has been shown in table 3.1 and a machined workpiece is shown in table 4.2, demonstrates that there is an extensive enhancement in carbon content in the white layer as for the parent material. The radical increment of carbon over the machined surface has been observed because of the absorption of carbon isolated from the absorbed dielectric medium kerosene oil mostly because of dielectric splitting [56]. There was an unimportant measure of oxygen found in the samples after the operation of machining. In this manner it has been inferred that some degree material expulsion is additionally because of oxidization and disintegration. Comparable perceptions have been recorded by Patel et al. [57] for EDM of ceramics and Mamalis et al. [56] for EDM of steel.

The same EDM examination has been done for sample machined by Cu-TiC tool. Here, the given Fig. 4.15, the transferring of molten material in various forms between both the electrodes has been taken place. In the sample, the existence of copper has been seen in the layer which is recemented over the surface of workpiece after machining.

Table 4.3 Chemical composition (wt. %) of workpiece after machining by Cu-TiC tool

C	Si	V	Cr	Mo	Ti	Cu	Fe
18.82	0.31	0.42	2.97	1.65	2.15	38.14	Rest

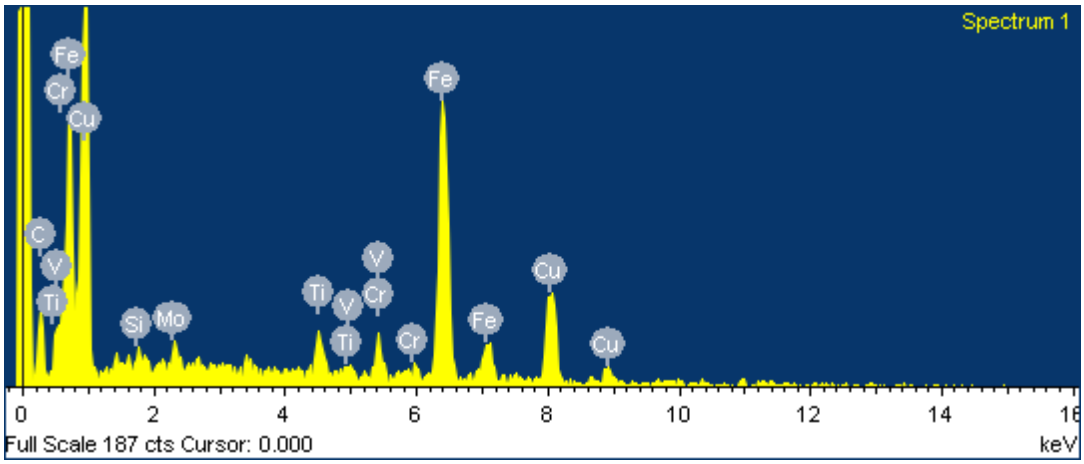

Figure 4.15 EDX showing relative intensities of different elements on surface of workpiece after EDM by Cu-TiC tool

The existence of Copper has been seen in the recemented layer as demonstrated by EDX examination. This suggests that there is appearance of noticeable electrode tool material exchange to the surface of workpiece amid the EDM process. An examination of the percentage contribution, of a workpiece before machining has been shown in table 3.1 and a machined workpiece shown in table 4.3, demonstrates that there is an extensive enhancement in carbon content which is found less in comparison to machining by Cu tool, in the white layer as for the parent material. There was an unimportant negligible measure of oxygen found in the samples after the operation of machining.

4.3.3 Comparison of Surface Integrity in EDM process by Cu & Cu-TiC tool

EDM by Cu tool

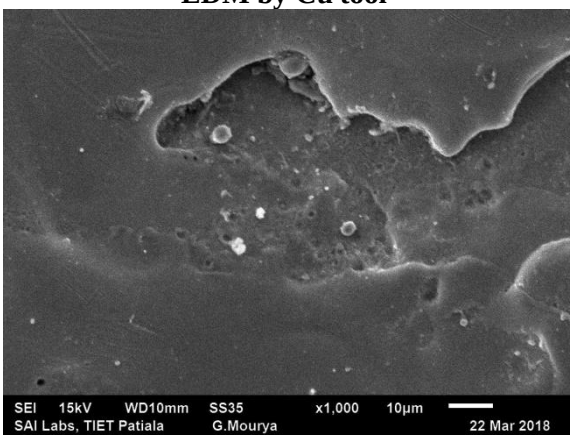

EDM by Cu-TiC tool

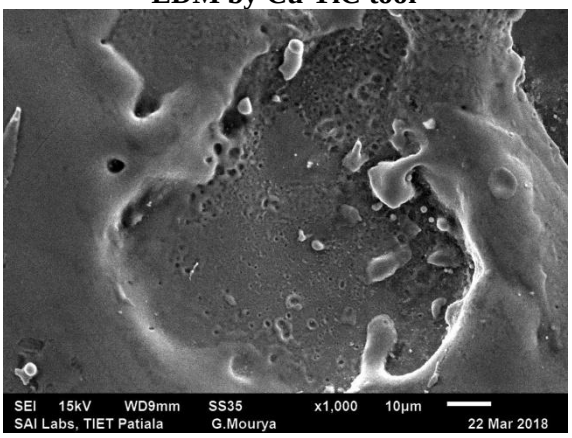

Discharge current 9A, Pulse-on time 200µs, Pulse-off time 20µs

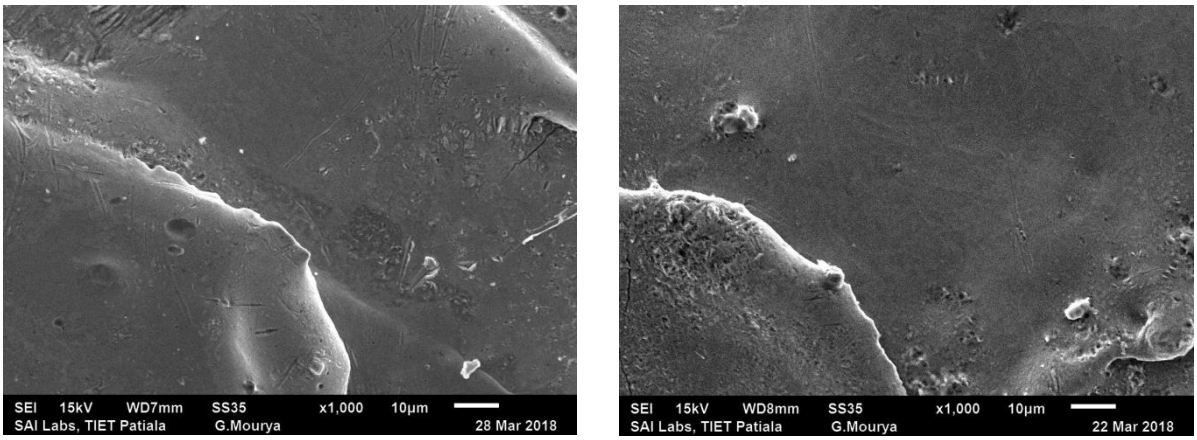

Discharge current 7A, Pulse-on time 100µs, Pulse-off time 10µs

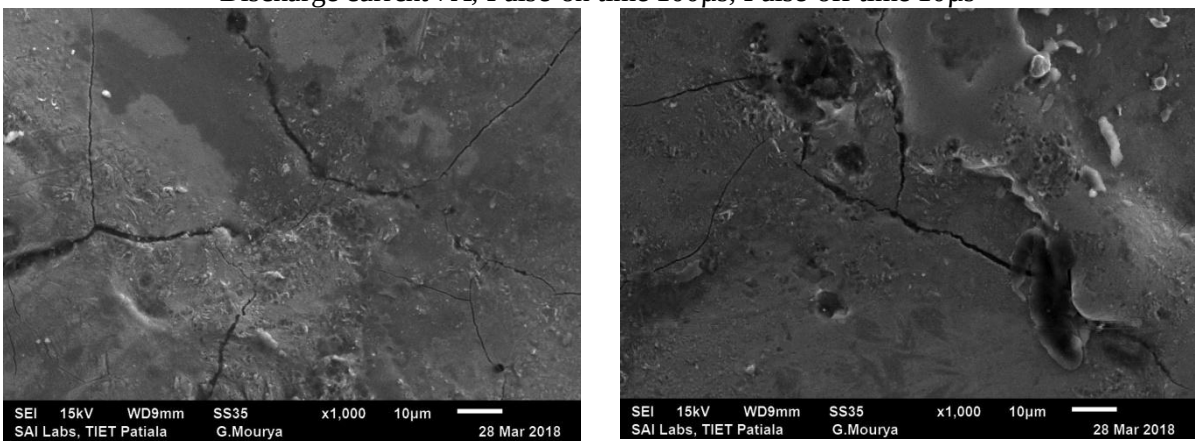

Discharge current 7A, Pulse-on time 300µs, Pulse-off time 30µs

Figure 4.16 Surface characteristics of workpiece machined at various processing conditions by Cu & Cu-TiC tool in EDM process

From above given images of SEM in figures 4.15, where many deformities have been shown during SEM investigations. However, the more number of deformities per unit area can be seen in workpiece machined by Cu-TiC tool as compared to machine by Cu tool. The debris, craters, cracks, pores and recast layers have been shown more in workpiece machined by Cu-TiC tool. The reason of origin of these deformities machined by Cu-TiC tool is the more hardness and electrical conductivity of tool material. There are maximum chances of occurring of recast layer and white layers in case of EDM by Cu-TiC tool. From the above presented SEM images. Hence, it can be concluded that the surface integrity is found to be better in machined by Cu tool.

4.4 CONCLUSION

In the current research work, it has been explored the mechanism of material removal and surface morphology of the H13 tool steel in the EDM process by Cu & Cu-TiC tool individually. It has been observed that the surface roughness is increased by the increment of discharge current. It has also been seen that on increment of pulse duration, there is slightly increment of surface roughness. This part shows surface morphology study of H13 tool steel

workpiece with decided process parameters has been efficiently machined by both the tools individually without causing noticeable loss of the surface of workpiece.

It has been observed that more deformities like debris, craters, cracks, pores, white layer and recast layers have been found when the value of discharge current and pulse duration is high. It has also been observed that the thickness of recast layer over the workpiece is increased as the pulse-on time is increased. This is because of the increment of the discharge column which leads to the decrement in discharge intensity. More the discharge current, huge material damage will occur. Further it has been said by this investigation that the more number of deformities per unit area have been seen in workpiece machined by Cu-TiC tool as compared to machine by Cu tool. The reason of origin of these deformities by Cu-TiC tool is the more hardness and electrical conductivity of tool material. Hence, the better surface integrity has been found in the machining done by Copper tool in this case.

CHAPTER 5

SEMI-EMPIRICAL MODEL OF MACHINING CHARACTERITICS OF COPPER TITANIUM CARBIDE ELECTRODE

5.1. DEVELOPMENT OF MODEL USING DIMENSIONAL ANALYSIS

It has been shown that the response parameters can be anticipated utilizing empirical models, are response surface models. Be that as it may, these models are constrained to the machining settings parameters and they don't think about the impacts of work material properties on the procedure execution. Subsequently, it was chosen to build up a model which incorporates the machining parameters and additionally material particular parameters [32].

The present work utilizes the method of dimensional analysis to build up a semi-empirical model of response parameters in EDM of H13 tool steel. Dimensional analysis is a technique by which we find data about a wonder from the single start that the circumstances can be depicted by a dimensionally rectify condition among specific factors. The hypothesis of dimensional analysis is the mathematical hypothesis which is absolutely algebraic. The utilization of dimensional analysis to a functional issue depends on the speculation that the arrangement of the issue is expressible by methods for a dimensionally homogeneous condition as far as determined factors [58]. In this model which is developed by the help of dimensional analysis, the physical and thermal properties of machined materials are density, thermal conductivity, linear coefficient of expansion, electrical resistivity and hardness were considered. The process parameters of machining are discharge current, pulse-on time and pulse-off time were also taken to be in consideration with material properties.

5.1.1 Buckingham's π Theorem

The Buckingham π theorem is a key hypothesis in dimensional examination. The hypothesis expresses that on the off chance that we have a physically significant condition including a specific number, n, of physical factors, and these factors are expressible as far as r free basic physical quantities, at that point the first articulation is proportionate to a condition including an arrangement of p = n − r dimensionless factors built from the original factors: it is a plan for non dimensionalization. This gives a technique to figuring sets of dimensionless parameters from the given factors, regardless of whether the type of the condition is as yet obscure [59]. This hypothesis is utilized to gather all factors showing up in the issue in various dimensionless items. The required relations interfacing the individual factors are resolved as the algebraic articulations relating subsequently

$$f(\pi_1, \pi_2, \pi_3 \ldots\ldots, \pi_{n-k}) = 0 \tag{5.1}$$

5.2. DIMENSIONAL ANALYSIS FOR TOOL WEAR RATE AND MATERIAL REMOVAL RATE

The material removal rate and tool wear rate are dependent upon pulse on time T_{on}, pulse off time T_{off}, discharge current I_p, electrical resistivity R, thermal conductivity κ, density of the material ρ, hardness HV and linear thermal expansion. So the equation may be written as given below:

$$V = f\left(I_p, T_{on}, T_{off}, R, \kappa, \rho, HV, \alpha\right) \tag{5.2}$$

where V is represented as wear rate which will be common for both MRR & TWR.

Table 5.1 Physical quantities, Symbols and Dimensions [27,60]

CHARACTERISTIC	FACTOR	SYMBOL	DIMENSIONS	UNITS
RESPONSE	Eroded Volume	V	M^1T^{-1}	$mg/\min$
PARAMETER	Discharge Current	I_p	$T^{-1}Q$	$Ampere$
	Pulse On Time	T_{on}	T	μs
	Pulse Off Time	T_{off}	T	μs
MATERIAL	Electrical Resistivity	R	$ML^3T^{-1}Q^{-2}$	Ω-m
	Thermal Conductivity	κ	$MLT^{-3}\theta^{-1}$	$W/m-K$
	Density of the Material	ρ	ML^{-3}	Kg/m^3
	Hardness	HV	$ML^{-1}T^{-2}$	$J/kg-K$
	Linear expansion coefficient	α	θ^{-1}	K^{-1}

In EDM, the metal is evacuated basically by melting and evaporation of little amount of liquid metal might be left staying in the crater. Some portion of the crater might be ejected out in light of the different forces acting in the region of spark established in the perceptions of the past. The measurements of the amounts given in equation (5.1) are communicated in the most broadly utilized Time (T), Mass (M), Length (L), Charge (Q) and Temperature (Θ) framework given in Table 5.1.

As per the Buckingham π theorem, the dimensional analysis formula for the equation (5.2) can be written as

$$\left[MT^{-1}\right]^{k_1}\left[T^{-1}Q\right]^{k_2}\left[T\right]^{k_3}\left[T\right]^{k_4}\left[ML^3T^{-1}Q^{-2}\right]^{k_5}\left[MLT^{-3}\theta^{-1}\right]^{k_6}\left[ML^{-3}\right]^{k_7}\left[ML^{-1}T^{-2}\right]^{k_8}\left[\theta^{-1}\right]^{k_9} = \left[M^0L^0T^0\theta^0Q^0\right] \tag{5.3}$$

By putting the forces of the fundamental units on both the sides of eq. (5.3), an arrangement of synchronous linear equations are gotten which can be later evaluated to

acquire the values of the constants. The estimations of the power records on the dimensional parameter are recorded in Table 5.2.

Table 5.2 Dimensions of the parameters

DIMENSION	INDEX (FACTOR)								
	k_1 (V)	k_2 (I_p)	k_3 (T_{on})	k_4 (T_{off})	k_5 (R)	k_6 (κ)	k_7 (ρ)	k_8 (HV)	k_9 (α)
M	1	0	0	0	1	1	1	1	0
L	0	0	0	0	3	1	-3	-1	0
T	-1	-1	1	1	-1	-3	0	-2	0
θ	0	0	0	0	0	-1	0	0	-1
Q	0	1	0	0	-2	0	0	0	0

The dimensional matrix rank can be evaluated by calculating the determinant formed by the square matrix of having five rows & columns.

$$\begin{vmatrix} 1 & 1 & 1 & 1 & 0 \\ 3 & 1 & -3 & -1 & 0 \\ -1 & -3 & 0 & -2 & 0 \\ 0 & -1 & 0 & 0 & -1 \\ -2 & 0 & 0 & 0 & 0 \end{vmatrix} = +4$$

Since this is a determinant fifth order and isn't equivalent to zero, the rank of this determinant is five. It has been demonstrated that the quantity of dimensionless items in a total set is equivalent to the distinction between the aggregate number of factors and the rank of their determinant. In this way in the present case, since there are nine factors and the determinant matrix is of rank five, there may be four dimensionless items in the entire arrangement of equations.

5.2.1. Dimensional Analysis

According to the dimensional matrix established on the homogenous linear algebraic equations, the coefficients are present in the numbers of the rows in dimensional matrix. The simultaneous equations can be formed as given below:-

$$k_1 + k_5 + k_6 + k_7 + k_8 = 0 \quad \text{.....(5.4)}$$

$$3k_5 + k_6 - 3k_7 - k_8 = 0 \quad \text{.....(5.5)}$$

$$-k_1 - k_2 + k_3 + k_4 - k_5 - 3k_6 - 2k_8 = 0 \quad \text{.....(5.6)}$$

$$k_6 + k_9 = 0 \quad \text{.....(5.7)}$$

$$k_2 - 2k_5 = 0 \quad \text{.....(5.8)}$$

Solving equations (5.4) – (5.8) for k_5, k_6, k_7, k_8, k_9, we get

$$k_5 = \frac{1}{2}k_2$$

$$k_6 = -2k_1 - \frac{3}{2}k_2 - k_3 - k_4$$

$$k_7 = -\frac{3}{2}k_1 - \frac{1}{2}k_2 - k_3 - k_4 \qquad \text{.....(5.9)}$$

$$k_8 = \frac{5}{2}k_1 + \frac{3}{2}k_2 + 2k_3 + 2k_4$$

$$k_9 = 2k_1 + \frac{3}{2}k_2 + k_3 + k_4$$

Assigning the values k_1=1, $k_2 = k_3 = k_4 = 0$ in equation (5.9) for the first solution has come out as shown below

$$k_5 = 0, k_6 = -2, k_7 = -\frac{3}{2}, k_8 = \frac{5}{2}, k_9 = 2$$

Assigning the values k_2=1, $k_1 = k_3 = k_4 = 0$ in equation (5.9) for the second solution has come out as shown below

$$k_5 = \frac{1}{2}, k_6 = -\frac{3}{2}, k_7 = -\frac{1}{2}, k_8 = \frac{3}{2}, k_9 = \frac{3}{2}$$

Assigning the values k_3=1, $k_1 = k_2 = k_4 = 0$ in equation (5.9) for the third solution has come out as shown below

$$k_5 = 0, k_6 = -1, k_7 = -1, k_8 = 2, k_9 = 1$$

Assigning the values k_4=1, $k_1 = k_2 = k_3 = 0$ in equation (5.9) for the fourth solution has come out as shown below

$$k_5 = 0, k_6 = -1, k_7 = -1, k_8 = 2, k_9 = 1$$

The solutions which are arranged in the form of matrix are represented in Table 5.3.

Table 5.3 Results of Dimensional Analysis

	k_1 (V)	k_2 (I_p)	k_3 (T_{on})	k_4 (T_{off})	k_5 (R)	k_6 (κ)	k_7 (ρ)	k_8 (HV)	k_9 (α)
π_1	1	0	0	0	0	-2	$-\frac{3}{2}$	$\frac{5}{2}$	0
π_2	0	1	0	0	$\frac{1}{2}$	$-\frac{3}{2}$	$-\frac{1}{2}$	$\frac{3}{2}$	$\frac{3}{2}$
π_3	0	0	1	0	0	-1	-1	2	1
π_4	0	0	0	1	0	-1	-1	2	1

Since the determinant matrix of arrangements contains n - r row where n = 9 is the quantity of factors and r = 5 is the rank of the determinant matrix, it comprises of fundamental arrangement of arrangements. Each row of the matrix of arrangements is a dimensionless item. Accordingly in the present investigation the accompanying complete arrangement of dimensionless items is acquired:

$$\pi_1 = \frac{MRR \times (HV)^{\frac{5}{2}} \times \alpha^2}{\kappa^2 \times \rho^{\frac{3}{2}}}, \qquad \pi_2 = \frac{I_p \times R^{\frac{1}{2}} \times (HV)^{\frac{3}{2}} \times \alpha^{\frac{3}{2}}}{\kappa^{\frac{3}{2}} \times \rho^{\frac{1}{2}}}, \qquad \pi_3 = \frac{T_{on} \times (HV)^2 \times \alpha}{\kappa \times \rho},$$

$$\pi_4 = \frac{T_{off} \times (HV)^2 \times \alpha}{\kappa \times \rho}$$

The relation between the dimensionless products can be written as $f(\pi_1, \pi_2, \pi_3, \pi_4) = 0$ or

$$\pi_1 = f(\pi_2, \pi_3, \pi_4)$$

$$\frac{MRR \times (HV)^{\frac{5}{2}} \times \alpha^2}{\kappa^2 \times \rho^{\frac{3}{2}}} = Z \times \left(\frac{I_p \times R^{\frac{1}{2}} \times (HV)^{\frac{3}{2}} \times \alpha^{\frac{3}{2}}}{\kappa^{\frac{3}{2}} \times \rho^{\frac{1}{2}}} \right)^{\alpha} \times \left(\frac{T_{on} \times (HV)^2 \times \alpha}{\kappa \times \rho} \right)^{\beta} \times \left(\frac{T_{off} \times (HV)^2 \times \alpha}{\kappa \times \rho} \right)^{\gamma}$$

$$MRR = Z \times \left(\frac{\kappa^2 \times \rho^{\frac{3}{2}}}{(HV)^{\frac{5}{2}} \times \alpha^2} \right) \times \left(\frac{I_p \times R^{\frac{1}{2}} \times (HV)^{\frac{3}{2}} \times \alpha^{\frac{3}{2}}}{\kappa^{\frac{3}{2}} \times \rho^{\frac{1}{2}}} \right)^{\alpha} \times \left(\frac{T_{on} \times (HV)^2 \times \alpha}{\kappa \times \rho} \right)^{\beta} \times \left(\frac{T_{off} \times (HV)^2 \times \alpha}{\kappa \times \rho} \right)^{\gamma} \tag{5.10}$$

Where Z is known as dimensionless constant and α, β & γ are present here as unknown exponents. The Z which is dimensionless constant and α, β & γ exponents which have evaluated by estimation of non-linear experiment data. The values of these constant Z, α, β & γ are determined to be 5.509 x 10^{-6}, 1.0271, 0.1203 and 0.0644 respectively. So, the result has been determined as equation given below:-

$$MRR = 5.509 \times 10^{-6} \times \left(\frac{\kappa^2 \times \rho^{\frac{3}{2}}}{(HV)^{\frac{5}{2}} \times \alpha^2} \right) \times \left(\frac{I_p \times R^{\frac{1}{2}} \times (HV)^{\frac{3}{2}} \times \alpha^{\frac{3}{2}}}{\kappa^{\frac{3}{2}} \times \rho^{\frac{1}{2}}} \right)^{1.0271} \times \left(\frac{T_{on} \times (HV)^2 \times \alpha}{\kappa \times \rho} \right)^{0.1203}$$

$$\times \left(\frac{T_{off} \times (HV)^2 \times \alpha}{\kappa \times \rho} \right)^{0.0644} \tag{5.11}$$

The determined equation (5.11) above, can be used for prediction of material removal rate during EDM process and the impact of different process parameters can be seen on the MRR. The above model has been validated by comparing the predicted or theoretical value which comes out from above model and the experimental or statistical value. This validation

can be observed by the graph as the theoretical values lies under the error bar of the statistical values which is shown in figure 5.1 below:-

(a)

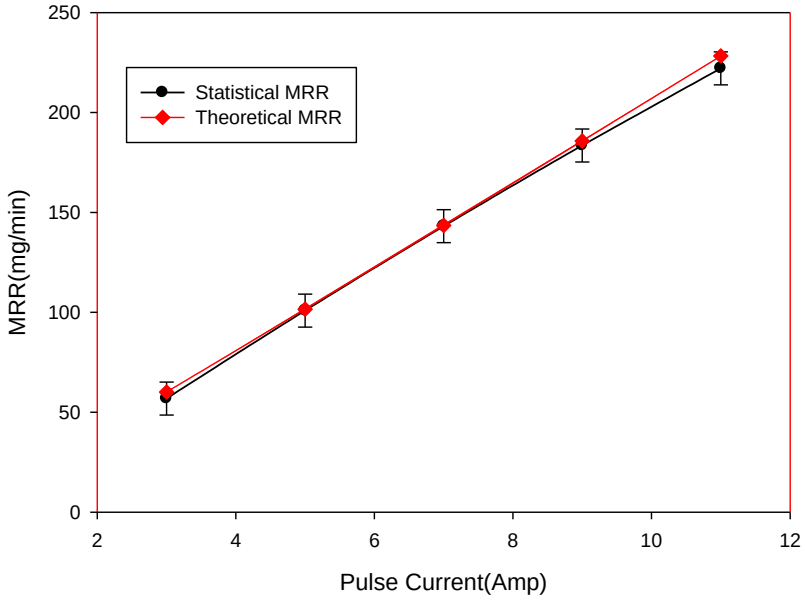

(b)

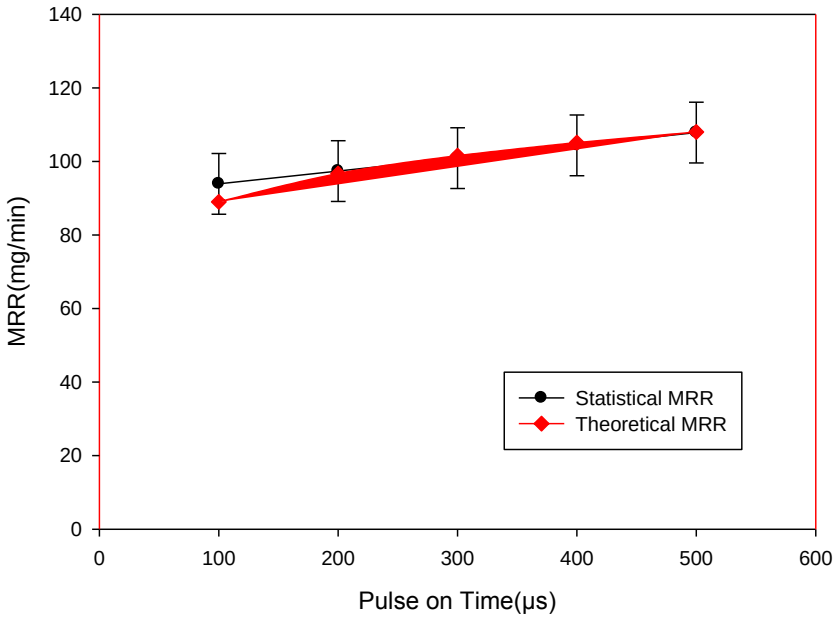

(c)

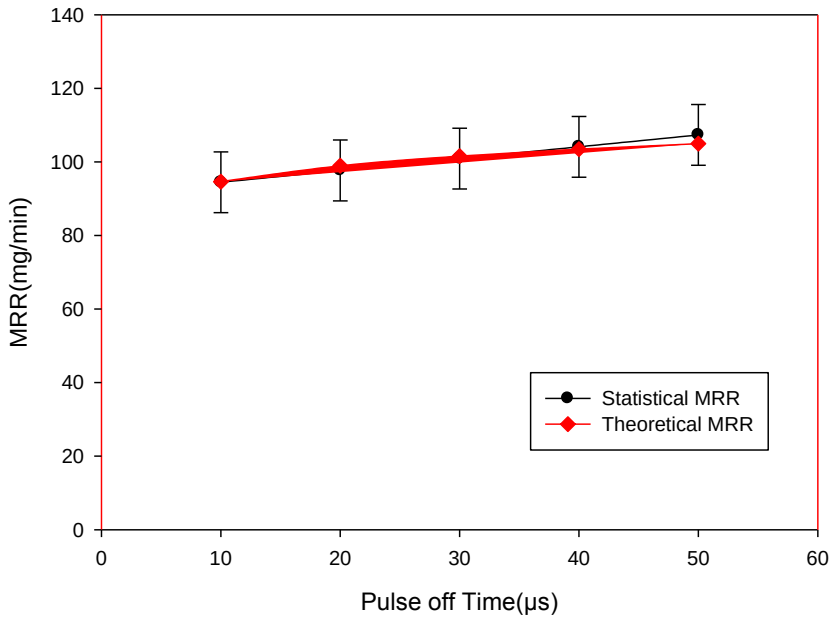

Figure 5.1 Comparison between statistical and theoretical values as

(a) MRR vs Ip, (b) MRR vs Ton, (c) MRR vs Toff

As per given above graphs, the investigations explore that MRR increases with discharge current because of increment of both depth and diameter of craters along with the discharge energy which results in the improvement of melting rate and evaporation. MRR also increases with the pulse-on time because of increment of discharge channel lowering of discharge energy, some molten material again solidify, which leads to increase MRR at low rate. It has been further watched that an increment in pulse-off time slightly decreases the values of MRR. This is because of the time duration during which the electric discharge shut off where the discharge column's diameter starts to decrease. During this time duration, the surface of the tool and workpiece starts cooling which stops wearing of tool.

Similarly, expression for the TWR model will be same as the model of MRR as per equation (5.10) because of the same dimensional units. But the values of constants are Z, α, β & γ will be different because of the different experimental data which are determined to be 5.6 x 10^{-7}, 1.1930, -0.0887 and -0.0547 respectively. So, the result has been determined as equation given below:-

$$TWR = 5.6\times10^{-7}\times\left(\frac{\kappa^2\times\rho^{\frac{3}{2}}}{(HV)^{\frac{5}{2}}\times\alpha^2}\right)\times\left(\frac{I_p\times R^{\frac{1}{2}}\times(HV)^{\frac{3}{2}}\times\alpha^{\frac{3}{2}}}{\kappa^{\frac{3}{2}}\times\rho^{\frac{1}{2}}}\right)^{1.1930}\times\left(\frac{T_{on}\times(HV)^2\times\alpha}{\kappa\times\rho}\right)^{-0.0887}$$
$$\times\left(\frac{T_{off}\times(HV)^2\times\alpha}{\kappa\times\rho}\right)^{-0.0547}$$

(5.12)

The determined equation (5.12) above, can be used for prediction of tool wear rate during EDM process and the impact of different process parameters can be seen on the TWR. The above model has been validated by comparing the predicted or theoretical value which comes out from above model and the experimental or statistical value. This validation can be observed by the graph as the theoretical values lies under the error bar of the statistical values which is shown in figure 5.2 below:-

(a)

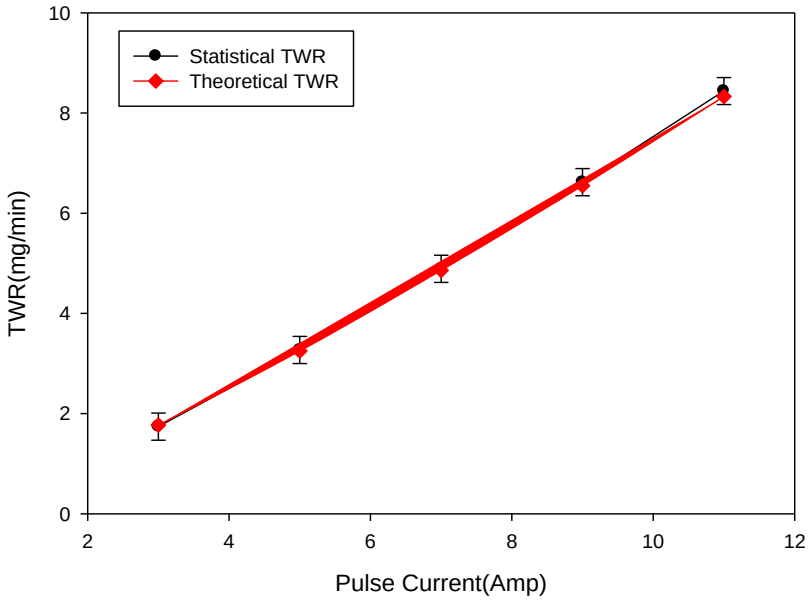

(b)

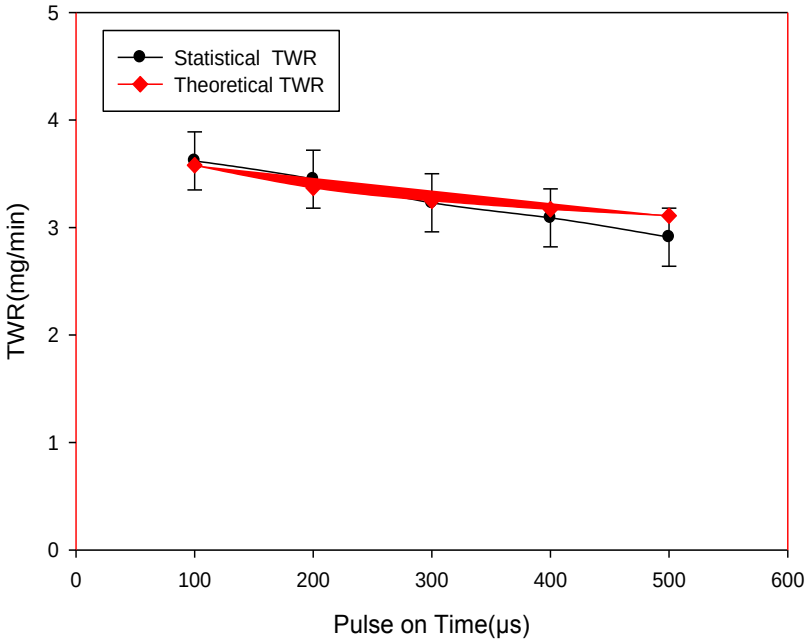

(c)

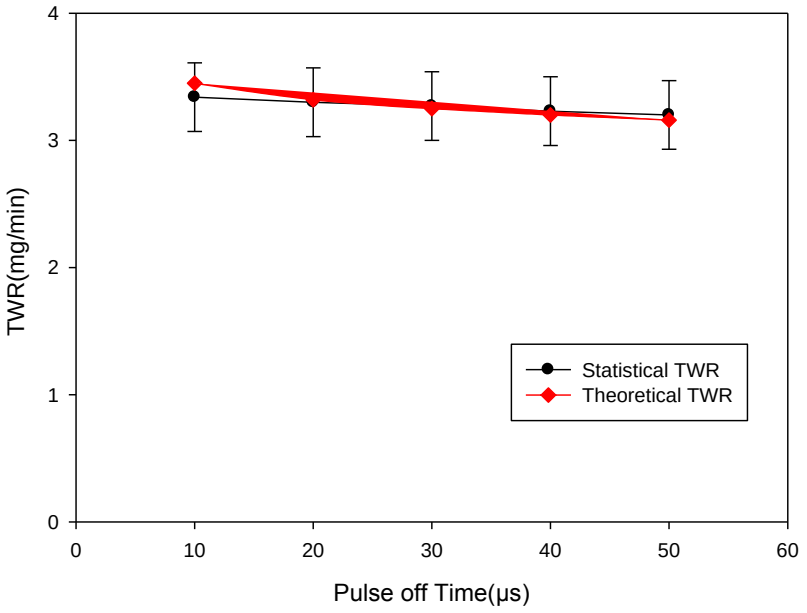

Figure 5.2 Comparison between statistical and theoretical values as
(a) TWR vs Ip, (b) TWR vs Ton, (c) TWR vs Toff

As per given above graphs, the investigations explore that TWR increases with discharge current because of the electrical discharge column in gap of electrodes during machining that wear out the surface of tool along with the unwanted material removal from workpiece. It can also be seen that an increment in pulse-on time decreases the values of TWR. This is because of the way that the discharge column's diameter increases as the pulse-on time increases which lessens the energy density present in the spark discharge column on

the spot where the discharge taken place. It has additionally been accounted for that at longer pulse-off time slightly decreases the values of TWR. This is because of the time duration during which the electric discharge shut off where the discharge column's diameter starts to decrease. During this time duration, the surface of the tool and workpiece starts cooling which stops wearing of tool.

5.3. DIMENSIONAL ANALYSIS FOR SURFACE ROUGHNESS AND OUT OF ROUNDNESS

The surface roughness and out of roundness are dependent upon pulse on time T_{on}, pulse off time T_{off}, discharge current I_p, electrical resistivity R, thermal conductivity κ, density of the material ρ, hardness HV and linear thermal expansion. So the equation may be written as given below:

$$D = f\left(I_p, T_{on}, T_{off}, R, \kappa, \rho, HV, \alpha\right) \quad \text{.....(5.13)}$$

where D is represented as dimensional unit which is common for SR & OOR.

In EDM, the metal is evacuated basically by melting and evaporation of little amount of liquid metal might be left staying in the crater which results in surface roughness. Usually, it also may happen that the some portion of outer edge of the tool periphery get distorted which results in the change of shape of the tool i.e. out of roundness. The measurements of the amounts given in equation (5.13) are communicated in the most broadly utilized Time (T), Mass (M), Length (L), Charge (Q) and Temperature (Θ) framework given in Table 5.4.

Table 5.4 Physical quantities, Symbols and Dimensions [27,60]

CHARACTERISTIC	FACTOR	SYMBOL	DIMENSIONS	UNITS
RESPONSE	Surface roughness	R_a	L	μm
PARAMETER	Discharge Current	I_p	$T^{-1}Q$	$Ampere$
	Pulse On Time	T_{on}	T	μs
	Pulse Off Time	T_{off}	T	μs
MATERIAL	Electrical Resistivity	R	$ML^3T^{-1}Q^{-2}$	Ω-m
	Thermal Conductivity	κ	$MLT^{-3}\theta^{-1}$	$W/m-K$
	Density of the Material	ρ	ML^{-3}	Kg/m^3
	Hardness	HV	$ML^{-1}T^{-2}$	$J/kg-K$
	Linear expansion coefficient	α	θ^{-1}	K^{-1}

As per the Buckingham π theorem, the dimensional analysis formula for the equation (13) can be written as

$$[L]^{k_1}[T^{-1}Q]^{k_2}[T]^{k_3}[T]^{k_4}[ML^3T^{-1}Q^{-2}]^{k_5}[MLT^{-3}\theta^{-1}]^{k_6}[ML^{-3}]^{k_7}[ML^{-1}T^{-2}]^{k_8}[\theta^{-1}]^{k_9} = [M^0L^0T^0\theta^0Q^0] \quad (5.14)$$

By putting the forces of the fundamental units on both the sides of eq. (5.14), an arrangement of synchronous linear equations are gotten which can be later evaluated to acquire the values of the constants. The estimations of the power records on the dimensional parameter are recorded in Table 5.5.

Table 5.5 Dimensions of the parameters

DIMENSION	INDEX (FACTOR)								
	k_1 (R_a)	k_2 (I_p)	k_3 (T_{on})	k_4 (T_{off})	k_5 (R)	k_6 (κ)	k_7 (ρ)	k_8 (HV)	k_9 (α)
M	0	0	0	0	1	1	1	1	0
L	1	0	0	0	3	1	-3	-1	0
T	0	-1	1	1	-1	-3	0	-2	0
θ	0	0	0	0	0	-1	0	0	-1
Q	0	1	0	0	-2	0	0	0	0

The dimensional matrix rank can be evaluated by calculating the determinant formed by the square matrix of having five rows & columns.

$$\begin{vmatrix} 1 & 1 & 1 & 1 & 0 \\ 3 & 1 & -3 & -1 & 0 \\ -1 & -3 & 0 & -2 & 0 \\ 0 & -1 & 0 & 0 & -1 \\ -2 & 0 & 0 & 0 & 0 \end{vmatrix} = +4$$

Since this is a determinant fifth order and isn't equivalent to zero, the rank of this determinant is five. It has been demonstrated that the quantity of dimensionless items in a total set is equivalent to the distinction between the aggregate number of factors and the rank of their determinant. In this way in the present case, since there are nine factors and the determinant matrix is of rank five, there may be four dimensionless items in the entire arrangement of equations.

5.3.1. Dimensional Analysis

According to the dimensional matrix established on the homogenous linear algebraic equations, the coefficients are present in the numbers of the rows in dimensional matrix. The simultaneous equations can be formed as given below:-

$$k_5 + k_6 + k_7 + k_8 = 0 \quad .....(5.15)$$

$$k_1 + 3k_5 + k_6 - 3k_7 - k_8 = 0 \quad .....(5.16)$$

$$-k_2 + k_3 + k_4 - k_5 - 3k_6 - 2k_8 = 0 \quad \text{.....(5.17)}$$

$$k_6 + k_9 = 0 \quad \text{.....(5.18)}$$

$$k_2 - 2k_5 = 0 \quad \text{.....(5.19)}$$

Solving equations (5.15) – (5.19) for k_5, k_6, k_7, k_8, k_9, we get

$$k_5 = \frac{1}{2}k_2$$

$$k_6 = -k_1 - \frac{3}{2}k_2 - k_3 - k_4$$

$$k_7 = -\frac{1}{2}k_1 - \frac{1}{2}k_2 - k_3 - k_4 \quad \text{.....(5.20)}$$

$$k_8 = \frac{3}{2}k_1 + \frac{3}{2}k_2 + 2k_3 + 2k_4$$

$$k_9 = k_1 + \frac{3}{2}k_2 + k_3 + k_4$$

Assigning the values k_1=1, $k_2 = k_3 = k_4$ = 0 in equation (5.20) for the first solution has come out as shown below

$$k_5 = 0, k_6 = -1, k_7 = -\frac{1}{2}, k_8 = \frac{3}{2}, k_9 = 1$$

Assigning the values k_2=1, $k_1 = k_3 = k_4$ = 0 in equation (5.20) for the second solution has come out as shown below

$$k_5 = \frac{1}{2}, k_6 = -\frac{3}{2}, k_7 = -\frac{1}{2}, k_8 = \frac{3}{2}, k_9 = \frac{3}{2}$$

Assigning the values k_3=1, $k_1 = k_2 = k_4$ = 0 in equation (5.20) for the third solution has come out as shown below

$$k_5 = 0, k_6 = -1, k_7 = -1, k_8 = 2, k_9 = 1$$

Assigning the values k_4=1, $k_1 = k_2 = k_3$ = 0 in equation (5.20) for the fourth solution has come out as shown below

$$k_5 = 0, k_6 = -1, k_7 = -1, k_8 = 2, k_9 = 1$$

The solutions which are arranged in the form of matrix are represented in Table 5.6.

Table 5.6 Results of Dimensional Analysis

	k_1 (R_a)	k_2 (I_p)	k_3 (T_{on})	k_4 (T_{off})	k_5 (R)	k_6 (κ)	k_7 (ρ)	k_8 (HV)	k_9 (α)
π_1	1	0	0	0	0	-1	$-\frac{1}{2}$	$\frac{3}{2}$	1

π_2	0	1	0	0	$\frac{1}{2}$	$-\frac{3}{2}$	$-\frac{1}{2}$	$\frac{3}{2}$	$\frac{3}{2}$
π_3	0	0	1	0	0	-1	-1	2	1
π_4	0	0	0	1	0	-1	-1	2	1

Since the determinant matrix of arrangements contains n - r row where n = 9 is the quantity of factors and r = 5 is the rank of the determinant matrix, it comprises of fundamental arrangement of arrangements. Each row of the matrix of arrangements is a dimensionless item. Accordingly in the present investigation the accompanying complete arrangement of dimensionless items is acquired:

$$\pi_1 = \frac{SR \times (HV)^{\frac{3}{2}} \times \alpha}{\kappa \times \rho^{\frac{1}{2}}}, \qquad \pi_2 = \frac{I_p \times R^{\frac{1}{2}} \times (HV)^{\frac{3}{2}} \times \alpha^{\frac{3}{2}}}{\kappa^{\frac{3}{2}} \times \rho^{\frac{1}{2}}}, \qquad \pi_3 = \frac{T_{on} \times (HV)^2 \times \alpha}{\kappa \times \rho},$$

$$\pi_4 = \frac{T_{off} \times (HV)^2 \times \alpha}{\kappa \times \rho}$$

The relation between the dimensionless products can be written as $f(\pi_1, \pi_2, \pi_3, \pi_4) = 0$ or

$$\pi_1 = f(\pi_2, \pi_3, \pi_4)$$

$$\frac{SR \times (HV)^{\frac{3}{2}} \times \alpha}{\kappa \times \rho^{\frac{1}{2}}} = Z \times \left(\frac{I_p \times R^{\frac{1}{2}} \times (HV)^{\frac{3}{2}} \times \alpha^{\frac{3}{2}}}{\kappa^{\frac{3}{2}} \times \rho^{\frac{1}{2}}} \right)^{\alpha} \times \left(\frac{T_{on} \times (HV)^2 \times \alpha}{\kappa \times \rho} \right)^{\beta} \times \left(\frac{T_{off} \times (HV)^2 \times \alpha}{\kappa \times \rho} \right)^{\gamma}$$

$$SR = Z \times \left(\frac{\kappa \times \rho^{\frac{1}{2}}}{(HV)^{\frac{3}{2}} \times \alpha} \right) \times \left(\frac{I_p \times R^{\frac{1}{2}} \times (HV)^{\frac{3}{2}} \times \alpha^{\frac{3}{2}}}{\kappa^{\frac{3}{2}} \times \rho^{\frac{1}{2}}} \right)^{\alpha} \times \left(\frac{T_{on} \times (HV)^2 \times \alpha}{\kappa \times \rho} \right)^{\beta} \times \left(\frac{T_{off} \times (HV)^2 \times \alpha}{\kappa \times \rho} \right)^{\gamma}$$

(5.21)

Where Z is known as dimensionless constant and $\alpha, \beta \,\&\, \gamma$ are present here as unknown exponents. The Z which is dimensionless constant and $\alpha, \beta \,\&\, \gamma$ exponents which have evaluated by estimation of non-linear experiment data. The values of these constant Z, α, β & γ are determined to be 8.6806 x 10^{-7}, 0.3670, 0.05484 and 0.03645 respectively. So, the result has been determined as equation given below:-

$$SR = 8.6806 \times 10^{-7} \times \left(\frac{\kappa \times \rho^{\frac{1}{2}}}{(HV)^{\frac{3}{2}} \times \alpha} \right) \times \left(\frac{I_p \times R^{\frac{1}{2}} \times (HV)^{\frac{3}{2}} \times \alpha^{\frac{3}{2}}}{\kappa^{\frac{3}{2}} \times \rho^{\frac{1}{2}}} \right)^{0.3670} \times \left(\frac{T_{on} \times (HV)^2 \times \alpha}{\kappa \times \rho} \right)^{0.05484}$$

$$\times \left(\frac{T_{off} \times (HV)^2 \times \alpha}{\kappa \times \rho} \right)^{0.03645}$$

(5.22)

The determined equation (5.22) above, can be used for prediction of surface roughness during EDM process and the impact of different process parameters can be seen on the SR. The above model has been validated by comparing the predicted or theoretical value which comes out from above model and the experimental or statistical value. This validation can be observed by the graph as the theoretical values lies under the error bar of the statistical values which is shown in figure 5.3 below:-

(a)

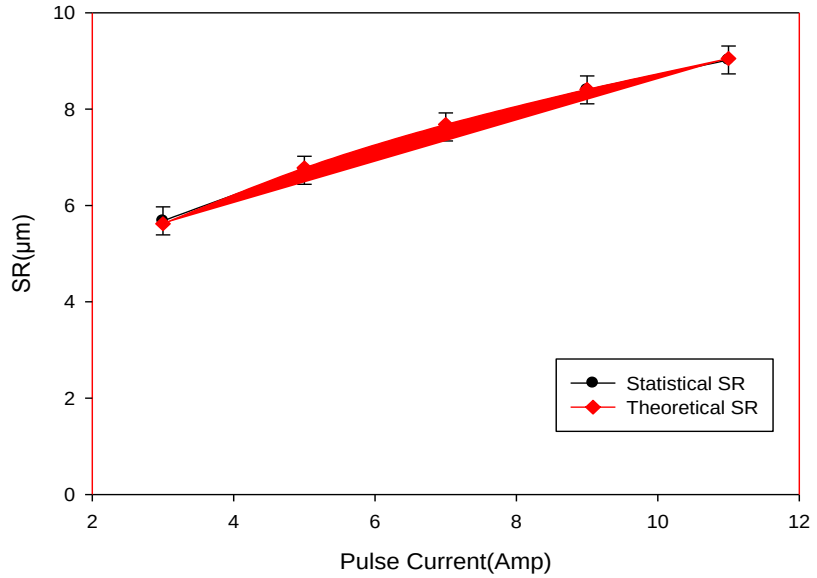

(b)

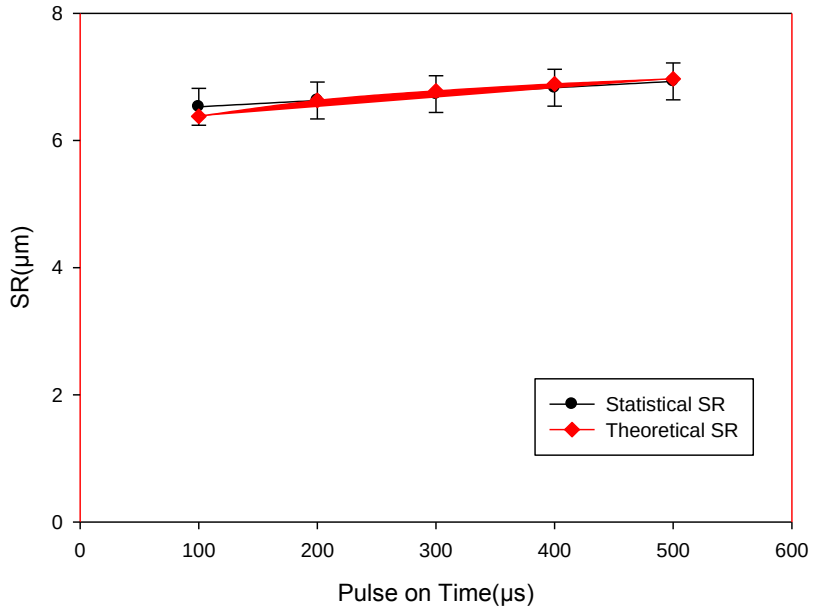

(c)

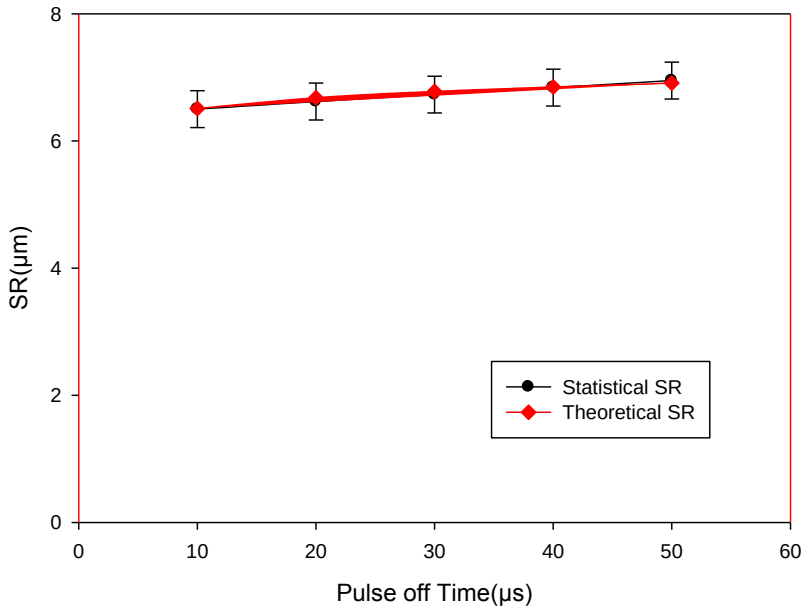

Figure 5.3 Comparison between statistical and theoretical values as
(a) SR vs Ip, (b) SR vs Ton, (c) SR vs Toff

This plotted graph explore that SR increases with discharge current because of increasing of impulse force and discharge energy density leads to the generation of larger and deeper craters which results in increasing of SR. The graph also shows very minutely increment of SR with increase in pulse-on time. This is because of plasma channel expansion by the increment of pulse-on time which reduces both impulsive force and energy density, results in incomplete removing of melted debris and recast layer is formed which results in increasing of SR. It has additionally been accounted for that at longer pulse-off time slightly increases the values of SR. This is because of the time duration during which the electric discharge shut off where the discharge column's diameter starts to decrease. During this time duration, the surface of the tool and workpiece starts cooling which stops wearing of tool.

Similarly, expression for the OOR model will be same as the model of OOR as per equation (5.21) because of the same dimensional units. But the values of constants are Z, α, β & γ will be different because of the different experimental data which are determined to be 1.144 x 10^6, 1.552, -0.2075 and -0.1298 respectively. So, the result has been determined as equation given below:-

$$OOR = 1.144\times10^{6}\times\left(\frac{\kappa\times\rho^{\frac{1}{2}}}{(HV)^{\frac{3}{2}}\times\alpha}\right)\times\left(\frac{I_p\times R^{\frac{1}{2}}\times(HV)^{\frac{3}{2}}\times\alpha^{\frac{3}{2}}}{\kappa^{\frac{3}{2}}\times\rho^{\frac{1}{2}}}\right)^{1.552}\times\left(\frac{T_{on}\times(HV)^{2}\times\alpha}{\kappa\times\rho}\right)^{-0.2075}$$
$$\times\left(\frac{T_{off}\times(HV)^{2}\times\alpha}{\kappa\times\rho}\right)^{-0.1298}$$

(5.23)

The determined equation (5.23) above, can be used for prediction of tool wear rate during EDM process and the impact of different process parameters can be seen on the TWR. The above model has been validated by comparing the predicted or theoretical value which comes out from above model and the experimental or statistical value. This validation can be observed by the graph as the theoretical values lies under the error bar of the statistical values which is shown below:-

(a)

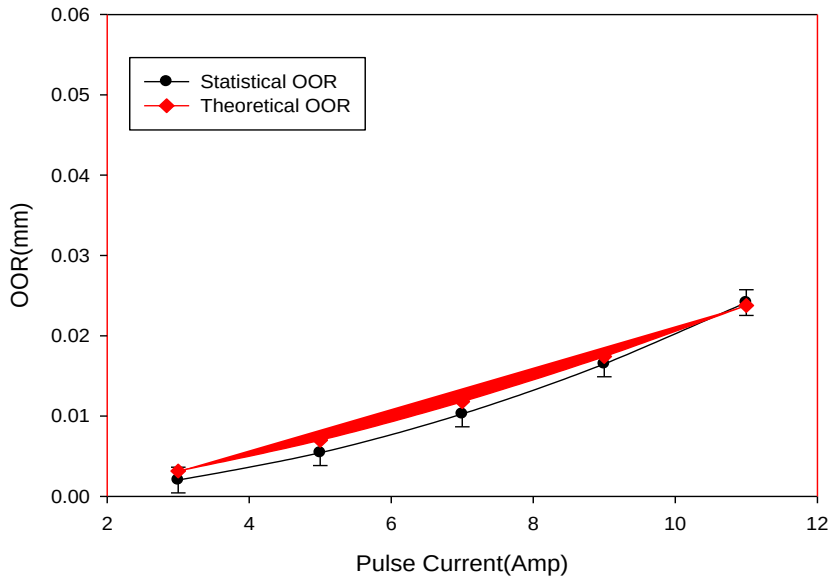

(b)

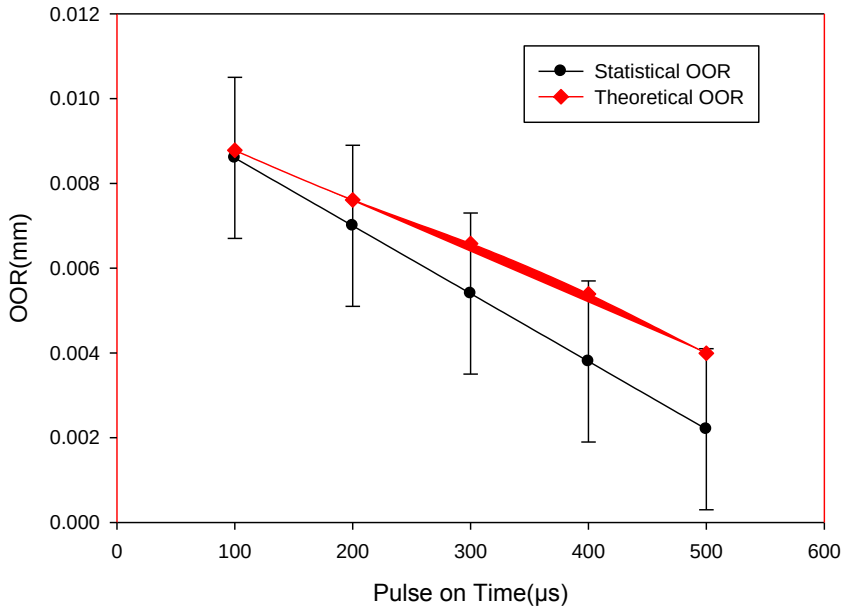

(c)

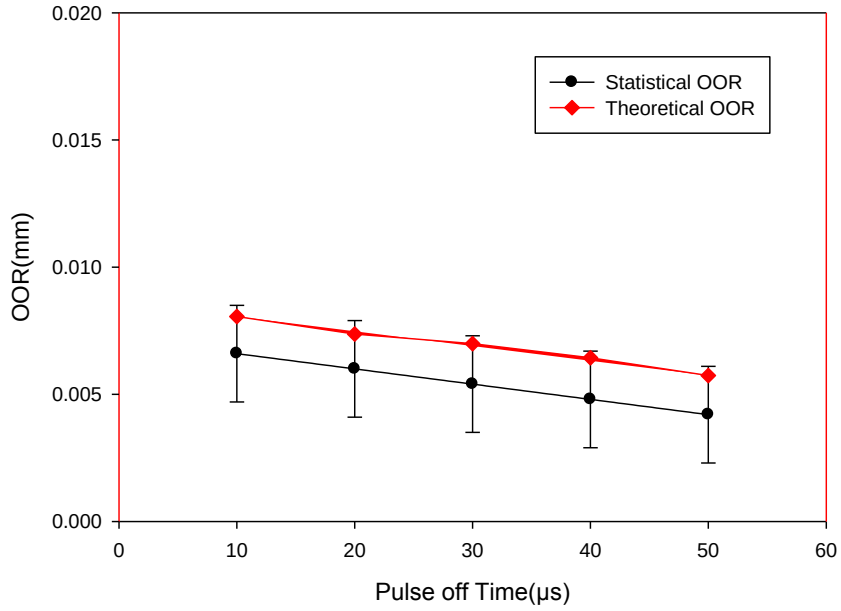

Figure 5.4 Comparison between statistical and theoretical values as
(a) OOR vs Ip, (b) OOR vs Ton, (c) OOR vs Toff

This plotted graph explore that OOR increases with discharge current because of increasing of impulse force and discharge energy density leads to the generation of larger and deeper craters which results in distortion of shape of tool tip. The graph also shows very minutely increment of SR with increase in pulse-on time. It has also been studied that as the pulse-off time is increased, OOR is slightly decreased. This is because of getting time to flush out the molten metal away from the workpiece which leads to the prevention of shape of tool tip to distort less.

5.4. CONCLUSION

A mathematical model of the material removal rate, tool wear rate, surface roughness and out of roundness has been figured utilizing dimensional analysis by distinguishing both the physical and the electrical parameters that influence the procedure of material expulsion in a die-sinking electrical discharge machining (EDM). The dimensionless constant and types have been controlled by nonlinear estimation of exploratory information. It is discovered that the material removal rate, tool wear rate, surface roughness and out of roundness are relative to the Discharge Current , Pulse-Off Time , pulse-on time, thermal conductivity, density, linear coefficient of expansion, electrical resistivity and hardness of the material. Ascertained outcomes from the model show great understanding when contrasted with the exploratory discoveries. The model would thus be able to be utilized to anticipate the material expulsion for a die-sinking electrical discharge machine.

CHAPTER 6

SUMMARY, CONCLUSIONS AND SCOPE FOR FURTURE WORK

The main unavoidable problem of high tool wear rate during the EDM process is required to be solved by manufacturing of different numbers of tool electrode for machining a job. The current study is focused upon mainly the reduction of tool wear rate, surface roughness and distortion of tool shape and increment of the material removal rate. So, further attempt has been made to overcome the problem of improper surface finish. This chapter discusses about summary, conclusions and future scope of the work.

6.1 SUMMARY

In this current research work, the tool materials have been decided according to past survey. The main motive was to decrease tool wear rate. EDM has been used for machining H13 tool steel workpiece by two electrode tools i.e. Copper (Cu) and Copper Titanium Carbide (Cu-TiC). The statistical models have been evaluated for the prediction of the response parameters i.e. tool wear rate, material removal rate, out of roundness and surface roughness in EDM process by utilizing the process parameters i.e. discharge current, pulse-on time, and pulse-off time. Different measurements have been taken with the help of various instruments are weighing machine, surface roughness machine and co-ordinate measurement machine. For justifying significance of the model, ANOVA has been used. Some of the process parameters i.e. discharge current has been found to be significantly affecting majorly the response parameters. It has been observed that TWR increases as the discharge current increases but it decreases slightly when the pulse duration increases. Same trend has been shown by OOR. It has also been observed that MRR increases as the discharge current increases and it also increases but slightly when pulse duration increases. Further, it has been seen that MRR increases when the discharge current increases but when pulse duration increases, MRR increases slightly upto certain limits then decreases.

These process parameters have been used in regression analysis for the generation of the statistical equations which are also called statistical model. Statistical models have been developed for both the tools machining and compared. Then optimization of the model has been performed for its validation. Further, the surface morphology has been investigated by testing the samples of workpieces in Scanning Electron Microscope. Then the statistical models have been generated by the help of experimental data and further checked it adequacy. Theoretical error has been checked by comparing the predicting model values with the theoretical model values. Then, the statistical and theoretical models have been compared.

6.2 CONCLUSION

Based on the current research work represented in last five chapters and the above summarize part, the following conclusions have been concluded from current work of research.

- Cu-TiC ceramic tool machining has been found statistically better than Cu tool machining in case of TWR and MRR but found not good in case of SR and OOR. This is because of increase in hardness of ceramic tool fabricated.
- MRR, TWR, SR, and OOR are found to be higher in case of higher discharge current and lower at low value of discharge current.
- Confirmation of the experiments were conducted under some test conditions represented that models which were developed can do prediction of the TWR, MRR, SR and OOR within an accuracy of confidence level of 99%.
- As per surface morphological studies, the surface integrity and the machining characteristics of the workpiece machined by the Copper tool and the Copper Titanium Carbide ceramic tool have been studied.
- The surface deformities which are cracks, pores, debris, recast layers, white cast layers per unit area on the workpiece specimen surface have been found less in machining by Cu too in comparison to machining by Cu-TiC ceramic tool.
- The theoretical model of the response parameters resulted by machining with Cu-TiC ceramic tool is found in a range of the error generated by the statistical model for the same tool.
- The prediction errors have found to be upto 5% for TWR, 3.7% for MRR, 2.9% for SR and 6.9% for OOR.

6.3 SCOPE FOR THE FUTURE WORK

The represented research work in this thesis can be extended further in the given points as follows:-

1. More fabrication of the tool electrode is required for increasing the hardness so that MRR can be increase with the decrement in TWR.
2. Factor of Surface roughness has to be taken under consideration while selecting the material of the tool.
3. Make use of other technique to develop model for studying the effect of response parameters.
4. More harder workpiece can be tried to machine by same material tools.

REFERENCES

[1] Boothroyd G, Knight WA, *Fundamentals of Machining and Machine Tools*, Taylor & Francis, Florida, 2006.

[2] Ho KH and Newman ST (2003). State of the art electrical discharge machining (EDM). *International Journal of Machine Tools and Manufacture*, *43*(13), 1287-1300.

[3] Hassan HF, *Advanced Machining Process,* McGraw-Hill, 2005.

[4] Abbas NM, Solomon DG, and Bahari MF (2007). A review on current research trends in electrical discharge machining (EDM). *International Journal of Machine Tools and Manufacture*, *47*(7-8), 1214-1228.

[5] Mishra PK, *Non-Conventional Machining*, Narosa Publishing House, 2007

[6] Pandey PC, Shan HS, *Morden Machining Processes*, Tata McGraw-Hill Publishing Company Limited, 1998

[7] Fonda P *et al.* (2008). A fundamental study on Ti–6Al–4V's thermal and electrical properties and their relation to EDM productivity. *Journal of Materials Processing Technology*, *202*(1-3), 583-589.

[8] Li L *et al.* (2001). EDM performance of TiC/copper-based sintered electrodes. *Materials & Design*, *22*(8), 669-678.

[9] Kumar BM *et al.* (2007). Electro-discharge machining performance of TiCN-based cermets. *International Journal of Refractory Metals and Hard Materials*, *25*(4), 293-299.

[10] Monzón M *et al.* (2008). Validation of electrical discharge machining electrodes made with rapid tooling technologies. *Journal of Materials Processing Technology*, *196*(1-3), 109-114.

[11] Singh H (2012). Investigating the effect of copper chromium and aluminium electrodes on EN-31 Die steel on electric discharge machine using positive polarity. *Proceedings of the World Congress on Engineering*, 3, 4-6.

[12] Satyarthi MK and Pandey PM (2013). Surface and Subsurface Study on EDG and EDM Processing of Advanced Ceramic Composite Material. In *ASME 2013 International Mechanical Engineering Congress and Exposition* (pp. V02BT02A062-V02BT02A062). American Society of Mechanical Engineers.

[13] Islak S, Kır D and Buytoz S (2014). Effect of sintering temperature on electrical and microstructure properties of hot pressed Cu-TiC composites. *Science of Sintering*, *46*(1), 15-21.

[14] Ahmed A (2016). Deposition and analysis of composite coating on aluminium using

Ti–B4C powder metallurgy tools in EDM. *Materials and Manufacturing Processes*, *31*(4), 467-474.

[15] Younis MA *et al.* (2015). Effect of electrode material on electrical discharge machining of tool steel surface. *Ain Shams Engineering Journal*, *6*(3), 977-986.

[16] Gadow R, Landfried R and Kern F (2016). Electrical Discharge Machining (EDM) of High-Performance Ceramics. *Proceedings of the III Advanced Ceramics and Applications Conference,* Atlantis Press, Paris, pp. 25-32.

[17] Liu Z *et al.* (2017). Densification of high-strength B4C–TiB2 composites fabricated by pulsed electric current sintering of TiC–B mixture. *Scripta Materialia*, *135*, 15-18.

[18] Ozgedik A and Cogun C (2006). An experimental investigation of tool wear in electric discharge machining. *The International Journal of Advanced Manufacturing Technology*, *27*(5-6), 488-500.

[19] Jaharah AG *et al.* (2008). Performance of copper electrode in electical discharge machining (EDM) of AISI H13 harden steel. *International Journal of Mechanical and Materials Engineering*, *3*(1), 25-29.

[20] Pellicer N, Ciurana J and Delgado J (2011). Tool electrode geometry and process parameters influence on different feature geometry and surface quality in electrical discharge machining of AISI H13 steel. *Journal of Intelligent Manufacturing*, *22*(4), 575-584.

[21] Rajesha S, Sharma AK and Kumar P (2012). On electro discharge machining of Inconel 718 with hollow tool. *Journal of Materials Engineering and Performance*, *21*(6), 882-891.

[22] Singh B, Kumar J and Kumar S (2015). Influences of process parameters on MRR improvement in simple and powder-mixed EDM of AA6061/10% SiC composite. *Materials and Manufacturing Processes*, *30*(3), 303-312.

[23] Sahani OP, Kumar R and Vashista M (2014). Effect of Electro Discharge Machining Process Parameters on Material Removal Rate. *Journal of Basic and Applied Engineering Research*, *1*(2), 17-20.

[24] Balasubramanian P and Senthilvelan T (2014). Optimization of machining parameters in EDM process using cast and sintered copper electrodes. *Procedia Materials Science*, *6*, 1292-1302.

[25] Mandaloi G *et al.* (2016). Effect on crystalline structure of AISI M2 steel using tungsten–thorium electrode through MRR, EWR, and surface finish. *Measurement*, *90*, 74-84.

[26] Niamat M *et al.* (2017). Effect of Different Dielectrics on Material Removal Rate,

Electrode Wear Rate and Microstructures in EDM. *Procedia CIRP, 60,* 2-7.

[27] Wang P J and Tsai KM (2001). Semi-empirical model on work removal and tool wear in electrical discharge machining. *Journal of Materials Processing Technology*, *114*(1), 1-17.

[28] Tsai KM and Wang PJ (2001). Semi-empirical model of surface finish on electrical discharge machining. *International Journal of Machine Tools and Manufacture*, *41*(10), 1455-1477.

[29] Yahya A and Manning CD (2004). Determination of material removal rate of an electro-discharge machine using dimensional analysis. *Journal of Physics D: Applied Physics*, *37*(10), 1467.

[30] Ekmekci B, Tekkaya AE and Erden A (2006). A semi-empirical approach for residual stresses in electric discharge machining (EDM). *International Journal of Machine Tools and Manufacture*, *46*(7-8), 858-868.

[31] Poroś D and Zaborski S (2009). Semi-empirical model of efficiency of wire electrical discharge machining of hard-to-machine materials. *Journal of Materials Processing Technology*, *209*(3), 1247-1253.

[32] Patil NG and Brahmankar PK (2010). Determination of material removal rate in wire electro-discharge machining of metal matrix composites using dimensional analysis. *The International Journal of Advanced Manufacturing Technology*, *51*(5-8), 599-610.

[33] Kumar S *et al.* (2017). Modeling the tool wear rate in powder mixed electro-discharge machining of titanium alloys using dimensional analysis of cryogenically treated electrodes and workpiece. *Proceedings of the Institution of Mechanical Engineers, Part E: Journal of Process Mechanical Engineering*, *231*(2), 271-282.

[34] Bhaumik M, Maity K and Mohapatra KD (2016). Determination of Material Removal Rate and Radial Overcut in Electro Discharge Machining of AISI 304 Using Dimensional Analysis. *Applied Mechanics and Materials*, 852, 160-165.

[35] Wu KL *et al.* (2005). Improvement of surface finish on SKD steel using electro-discharge machining with aluminum and surfactant added dielectric. *International Journal of Machine Tools and Manufacture*, *45*(10), 1195-1201.

[36] Montgomery DC, *Design and Analysis of Experiments*, John Willey & Sons Inc., Singapore, 1991.

[37] Khuri AI nad Cornell JA, *Response Surfaces: Designs and Analyses*, Marcel Dekker Inc., New York, USA, 1996

[38] Myres RH and Montgomery DC, *Response Surface Methodology: Process and*

Product Optimization using Designed Experiments, John Willey & Sons Inc., New York, USA, 2002.

[39] Kiran MB, Ramamoorthy B and Radhakrishnan V (1998). Evaluation of surface roughness by vision system. *International Journal of Machine Tools and Manufacture*, *38*(5-6), 685-690.

[40] Mathew N and Kumar D (2014). Study of tool wear rate of different tool materials during electric discharge machining of H11 steel at reverse polarity. *International Journal of Mechanical Engineering and Robotics Research*, *3*(3), 53.

[41] Patel KM, Pandey PM and Rao PV (2011). Study on machinabilty of Al2O3 ceramic composite in EDM using response surface methodology. *Journal of Engineering Materials and Technology*, *133*(2), 021004.

[42] Khuri AI and Cornell JA, *Response Surfaces: Designs and Analyses*, Marcel Dekker Inc., New York, USA, 1996.

[43] Lin YC *et al.* (2006). Machining characteristics and optimization of machining parameters of SKH 57 high-speed steel using electrical-discharge machining based on Taguchi method. *Materials and Manufacturing Processes*, 21(8), 922-929.

[44] Chen Y and Mahdavian SM (1999). Parametric study into erosion wear in a computer numerical controlled electro-discharge machining process. *Wear*, *236*(1-2), 350-354.

[45] Pandey PC and Jilani ST (1986). Plasma channel growth and the resolidified layer in EDM. *Precision Engineering*, *8*(2), 104-110.

[46] Lee HT and Tai TY (2003). Relationship between EDM parameters and surface crack formation. *Journal of Materials Processing Technology*, *142*(3), 676-683.

[47] Zeid OA (1995). On the effect of electrodischarge machining parameters on the fatigue life of AISI d6 tool steel. In *Current Advances in Mechanical Design and Production*, 6, 81-89.

[48] Lee LC *et al.* (1988). Quantification of surface damage of tool steels after EDM. *International Journal of Machine Tools and Manufacture*, *28*(4), 359-372.

[49] Chiang KT (2008). Modeling and analysis of the effects of machining parameters on the performance characteristics in the EDM process of Al 2 O 3+ TiC mixed ceramic. *The International Journal of Advanced Manufacturing Technology*, *37*(5-6), 523-533.

[50] Patel KM, Pandey PM and Rao PV (2009). Surface integrity and material removal mechanisms associated with the EDM of Al2O3 ceramic composite. *International Journal of Refractory Metals and Hard Materials*, *27*(5), 892-899.

[51] Ramasawmy H and Blunt L (2004). Effect of EDM process parameters on 3D surface

topography. *Journal of Materials Processing Technology*, *148*(2), 155-164.

[52] Puri AB and Bhattacharyya B (2005). Modeling and analysis of white layer depth in a wire-cut EDM process through response surface methodology. *The International Journal of Advanced Manufacturing Technology*, *25*(3-4), 301-307.

[53] Bhattacharyya B, Gangopadhyay S and Sarkar BR (2007). Modelling and analysis of EDMed job surface integrity. *Journal of Materials Processing Technology*, *189*(1-3), 169-177.

[54] Van Dijck FS and Dutre WL (1974). Heat conduction model for the calculation of the volume of molten metal in electric discharges. *Journal of Physics D: Applied Physics*, *7*(6), 899.

[55] Roethel F, Kosec L and Garbajs V (1976). *Contribution to the Micro-Analysis of the Spark Eroded Surfaces,* Annals of the CIRP, 25 (1) (1976) 135–140.

[56] Mamalis AG *et al.* (1987). Macroscopic and microscopic phenomena of electro-discharge machined steel surfaces: an experimental investigation. *Journal of Mechanical Working Technology*, *15*(3), 335-356.

[57] Patel KM, Pandey PM and Rao PV (2009). Determination of an optimum parametric combination using a surface roughness prediction model for EDM of Al2O3/SiCw/TiC ceramic composite. *Materials and Manufacturing Processes*, *24*(6), 675-682.

[58] Langhaar HL (1980). *Dimensional Analysis and Theory of Models*. Robert E. Krieger publishing company, 1980

[59] Buckingham E (1914). On physically similar systems; illustrations of the use of dimensional equations. *Physical Review*, *4*(4), 345.

[60] Winzemer AM (1947). Dimensional Analysis of Electromagnetic Equations. *Proceedings of the IRE*, *35*(11), 1383-1384.

LIST OF PUBLICATIONS FROM THE RESEARCH

1. Arminder Singh Walia, Vineet Srivastava, Vivek Jain, Mayank Garg, "Modelling and Analysis of Change in Shape of Sintered Cu-TiC Tool Tip during Electrical Discharge Machining Process", All India Manufacturing Technology Design and Research (AIMTDR) Conference-2018, December 13^{th}-15^{th} 2018, College of Engineering Guindy, Anna University, Chennai, India. (UNDER REVIEW)

Mayank Thesis

ORIGINALITY REPORT

18%	5%	16%	7%
SIMILARITY INDEX	INTERNET SOURCES	PUBLICATIONS	STUDENT PAPERS

PRIMARY SOURCES

1	Vineet Srivastava, Pulak M. Pandey. "Effect of process parameters on the performance of EDM process with ultrasonic assisted cryogenically cooled electrode", Journal of Manufacturing Processes, 2012 Publication	2%
2	Rahul Mulik. "Experimental Investigations and Modeling of Temperature in the Work-Brush Interface during Ultrasonic Assisted Magnetic Abrasive Finishing Process", Materials and Manufacturing Processes, 2011 Publication	2%
3	Submitted to Thapar University, Patiala Student Paper	2%
4	Vineet Srivastava, Pulak M Pandey. "Experimental investigation on electrical discharge machining process with ultrasonic-assisted cryogenically cooled electrode", Proceedings of the Institution of Mechanical Engineers, Part B: Journal of Engineering	1%